KONINKLIJKE NEDERLANDSCHE AKADEMIE VAN WETENSCHAPPEN

PROCEEDINGS

VOLUME LII

No. 5

President: A. J. KLUYVER
Secretary: M. W. WOERDEMAN

1949
NORTH-HOLLAND PUBLISHING COMPANY
(N.V. Noord-Hollandsche Uitgevers Mij.)
AMSTERDAM

CONTENTS

Biochemistry. — *Elastic viscous oleate systems containing KCl.* VI [1]. *a) The elastic properties as a function of the KCl concentration. b) Influence of some alcohols and fatty acid anions on the elastic behaviour.* By H. G. BUNGENBERG DE JONG, H. J. VAN DEN BERG and D. VREUGDENHIL.

(Communicated at the meeting of April 23, 1949.)

1) *Introduction, and the measuring technique with half filled spheres.*

Having kept in the preceding Parts of this Series the KCl concentration constant (viz. at or very near to that concentration at which the damping of the elastic oscillation is a minimum), we will in the present communication investigate the dependence of the elastic properties on the KCl concentration (section 2).

The knowledge of this dependence is, of course, of importance for a future theory of the elastic viscous oleate systems, it is so too for studying the influence of organic substances on the elastic behaviour. A broader survey of the influence of an organic substance can indeed be obtained if its action is investigated not only at the KCl concentration of minimum damping (of the blank), but also at lower and higher KCl concentrations (section 2).

In the next sections, 3 and 4, in which the influence of a number of terms of the *n*. primary alcohols and of the fatty acid anions is studied, we were compelled (see section 3) to restrict ourselves to the KCl concentration of minimum damping. The points of view obtained in section 2 will, however, guide us in interpreting the results and will heed us from making erroneous generalizations.

For the methods (rotational oscillation in spherical vessels of known capacity at 15°) we refer to Parts I, II and III of this series, with the only exception that instead of using completely filled spherical vessels we used exactly half filled vessels. We know from the experiments in Part I (cf. ibid. section 2) that the period depends on the degree of filling of the vessel and that at 50 % degree of filling (by volume) the period is practically the same as in the completely filled sphere. According to not published previous work this practical equality also holds for the damping ratio b_1/b_3, which is used for calculating Λ, the logarithmic decrement.

Half filled vessels of nominally 500 cc capacity (provided with ground in glass-stoppers) highly serve the purpose of investigating the influence of added organic substances. We first measure the elastic properties of the blank, add a small known quantity of the organic substance into the vessel (e.g. drops from a suitable micropipette, which delivers drops of known weight), shake vigorously (e.g. 5 minutes or more) and put the vessel in the thermostate (15°) till the next morning (to get rid of the

[1]) Part I has appeared in these Proceedings **51**, 1197 (1948), Part II—V in these Proceedings **52**, 15, 99, 363, 377 (1949).

enclosed air) and measure the elastic properties anew. We continue in this way with alternately adding more substance and measuring the next morning until a sufficient number of experimental points has been obtained to characterize the action of the added substance.

This method has the advantage of economizing oleate, KCl and organic substance [2]), its disadvantage is that its takes many days. This disadvantage is compensated however by running a number of half filled vessels simultaneously.

The reliability of the method depends of course on the assumption that during the whole process no changes take place in the oleate system when no organic substance is added. To control this, we take a half filled sphere and treat it in the same way as the other spheres (measuring, opening the glass stopper for a short time, closing it again, vigorously shaking of the vessel, placing it in the thermostate and so on repeating this for several days). With 500 cc stoppered vessels and oleate systems containing the usual small quantity of KOH we found no changes which obviously surpassed the experimental errors.

The method described above is very convenient for added substances which exert their full influence in small concentrations already. The quantity of substance added is very small then (e.g. n. hexyl-, n. amyl-, n. butyl alcohol) and no corrections are necessary.

If the substance exerts its full influence at concentrations which correspond to additions of one to several percent, of the oleate system (e.g. methanol, ethanol), corrections are necessitated by the increase in the degree of filling and its consequences, viz. decrease of the oleate concentration and of the KCl concentration and change in the density.

The addition of one percent by volume changes the degree of filling from 50 % to 50.5 %. From Table I in Part I we calculate for this increase an increase of 0.35 % of the period. Later, more accurate measurements gave the somewhat smaller value of 0.25 %. The addition decreases also the oleate concentration by one percent, which gives an increase in the period of approximately 1 % (see Part III, where we found that ν ($= 1/T$), is roughly speaking, proportional to the oleate concentration).

The two changes considered result therefore already in an increase of 1.25 % in the period, and as the shear modulus G is proportional to ν^2, the addition of one percent to the volume will lead, if not corrected, to a value of G which is 2.5 % too low. The two other changes above mentioned will, in general, have only a slight influence when compared to the two considered here.

To come to a practical limit for the volume of an added substance, below which no corrections are needed, it is necessary to know the reproducibility of G, calculated from measurements on a number of exactly half filled vessels, using an identical oleate system.

The next survey gives the results of the measurements on the eight vessels half filled with the blank oleate system which were used for the experiments in section 3.

R (cm)	5.00	5.01	5.01	5.01	5.03	5.04	5.04	5.05
n	48.0	48.2	47.9	48.0	48.1	47.9	48.2	47.8
Λ	0.222	0.222	0.222	0.223	0.219	0.224	0.219	0.222
λ (sec)	2.57	2.56	2.57	2.57	2.60	2.54	2.60	2.60
G (dynes/cm^2)	40.4	40.7	40.4	40.3	41.2	41.1	41.0	40.8

[2]) It would of course also be economical to use spherical vessels of much smaller capacity than 500 cc, for instance 100 cc vessels, but experience taught us that it is not advisable to use them as the experimental errors are greater then. This is partly due to the more difficult measurement of the period and especially of the damping ratio (in 1.2 % oleate systems T and Λ are proportional to the radius, see Part II, and are therefore much smaller in 100 cc vessels than in 500 cc vessels). This may also be due to the fact that smaller vessels do not approximate the ideal spherical form so well.

We see from this example that in practice differences up to 2 % in the G value may occur. Therefore we may content ourselves not to object to the introduction of an error in the order of 1 %; and corrections may be neglected, if the volume of the added substance does not exceed 0.5 % of that of the oleate system.

For methanol and ethanol larger quantities must be added to characterize their influence on the oleate system and therefore corrections are necessary.

By measuring the influence of known quantities of distilled water on a vessel half filled with the blank system we determined in section 3 experimentally the correction to be applied in order to account for three of the four changes mentioned above (viz. the increase in the degree of filling, decrease in the oleate concentration and decrease in the KCl concentration. The correction for the fourth change (decrease of the density) was applied separately.

In the ethanol series in section 2, the necessity of applying corrections for the changes in the degree of filling and in the oleate concentration was made redundant by adding a volume b of ethanol and a volume $b/_2$ of the oleate stocksol and, after mixing the contents of the vessel, by removing a volume of 1.5 b with a pipette. After the addition the oleate concentration is not changed (the stock solution having a threefold larger oleate concentration) and after the removal the original degree of filling is restored. Only a slight change in the KCl concentration remains which can be calculated. For this reason the corresponding points on the curves A, B and C of fig. 4 do not longer lie at precisely the same abscis-values (as in fig. 2).

2) *The elastic behaviour as a function of the KCl concentration and the influence of n. hexylalcohol and aethanol thereon.*

Starting from a stock solution (36 g. Na oleinicum medicinale pur. pulv. Merck + 820 cc H_2O + 180 cc KOH 2 N) we made 11 mixtures according to the formula 100 cc stock solution + a cc KCl 3.8 N + (200—a) cc H_2O.

In these mixtures the oleate concentration (1.2 g. p. 100 cc) and the KOH concentration (0.12 N) are constant and the KCl concentration increases by degrees from 0.57 N to 1.90 N. The highest concentration used closely approaches the coacervation limit (slightly above 2 N KCl).

Eleven "500 cc" spherical vessels of known real capacity, the radius of which (R) had been calculated, were each exactly half filled with one of the above mixtures and put in the thermostate of 15°. The next morning the elastic behaviour was measured, and afterwards the same small quantity of *n*. Hexylalcohol was added to each vessel.

The mixtures were thoroughly shaken, put in the thermostate and once more measured the following morning. Two further additions of hexylalcohol were measured in the same way. Table I gives the results of these measurements [3]).

---

[3]) From experiments in Part II of this series it appeared that for the 1.2 % oleate system at or near to the KCl concentration of minimum damping $\Lambda \sim R$, which enables us to calculate λ, the relaxation time. This proportionality characteristic in the 1.2 % oleate system is not lost if by various causes Λ is increased very considerably (e.g. with increase of temperature, see Part II, or the addition of hexylalcohol, see Part V). We have therefore assumed that this proportionality is still present in the 1.2 % oleate system if Λ is increased considerably by changing the KCl concentration to other values than that of minimum damping, or by adding the various substances used in section 3 and 4, others than hexylalcohol. As this assumption is not entirely safe of course, we give in

TABLE I.

The elastic behaviour as a function of the KCl concentration and the influence of *n* hexylalcohol thereon.

KCl concentration mol/*l*	G (dynes/cm^2)				λ (sec.)			
	Hexylalcohol concentr. mol/*l*				Hexylalcohol concentr. mol/*l*			
	blank	0.0016	0.0042	0.0094	blank	0.0016	0.0042	0.0094
0.57	—	—	13.2	28.7	—	—	0.32	0.61
0.76	17.4	21.9	30.4	44.2	0.32	0.47	0.74	0.64
0.95	30.4	32.2	38.1	80.5	0.90	1.14	1.02	0.15
1.14	35.0	37.5	46.9	— *	1.58	2.00	0.88	— *
1.235	37.7	40.9	51.0	—	2.12	1.93	0.69	—
1.33	38.9	43.1	56.7	—	2.52	1.40	0.41	—
1.425	40.2	48.7	67.8	—	2.68	0.90	0.23	—
1.52	42.2	52.5	—	—	2.47	0.76	—	—
1.615	45.5	54.9	— *	—	1.32	0.63	— *	—
1.71	51.5	62.4	—	—	0.90	0.29	—	—
1.90	63.1	— *	—	—	0.30	— *	—	—

KCl concentration mol/*l*	$1/\Lambda$				n			
	Hexylalcohol concentr. mol/*l*				Hexylalcohol concentr. mol/*l*			
	blank	0.0016	0.0042	0.0094	blank	0.0016	0.0042	0.0094
0.57	—	—	0.33	0.93	0	0	4.0	13.1
0.76	0.38	0.63	1.17	1.21	5.1	10.7	17.8	17.0
0.95	1.40	1.84	1.78	0.37	18.6	29.3	31.4	4.0
1.14	2.65	3.45	1.70	— *	39.8	41.4	27.2	— *
1.235	3.60	3.40	1.36	—	45.1	40.5	21.0	—
1.33	4.33	2.53	0.86	—	48.1	38.5	14.9	—
1.425	4.69	1.74	0.52	—	49.4	31.8	7.0	—
1.52	4.42	1.51	—	—	48.5	24.7	1.0	—
1.615	2.46	1.29	— *	—	38.3	18.9	— *	—
1.71	1.75	0.62	—	—	29.5	9.5	—	—
1.90	0.66	— *	—	—	12.2	— *	—	—

* First mixture in each column which shows coacervation.

We will first discuss the blank series (see fig. 1). The curves for λ (time of relaxation in sec.), $1/\Lambda$ (the reciprocal value of the logarithmic decrement Λ), n (the number of oscillations visible through the telescope of the kathetometer) show a maximum at approximately 1.43 N KCl, and at this concentration the curve for G (shear modulus in dynes/cm^2) shows an inflexion point (compare the vertical, dotted line B at 1.43 N KCl). On either side of this concentration the λ, $1/\Lambda$ and n curves descend and, if extrapolated further downwards, reach the abscis axis at approximately

the following tables and figures besides the calculated values of λ the values for $1/\Lambda$ as well to characterize the damping in every case. We also give n, i.e. the maximum number of observable oscillations, which, as will be discussed in section 5, gives an approximate measure of $1/\Lambda$.

the two same KCl concentrations (0.63 and 2.05 N) indicated by the vertical, dotted lines *A* and *C*.

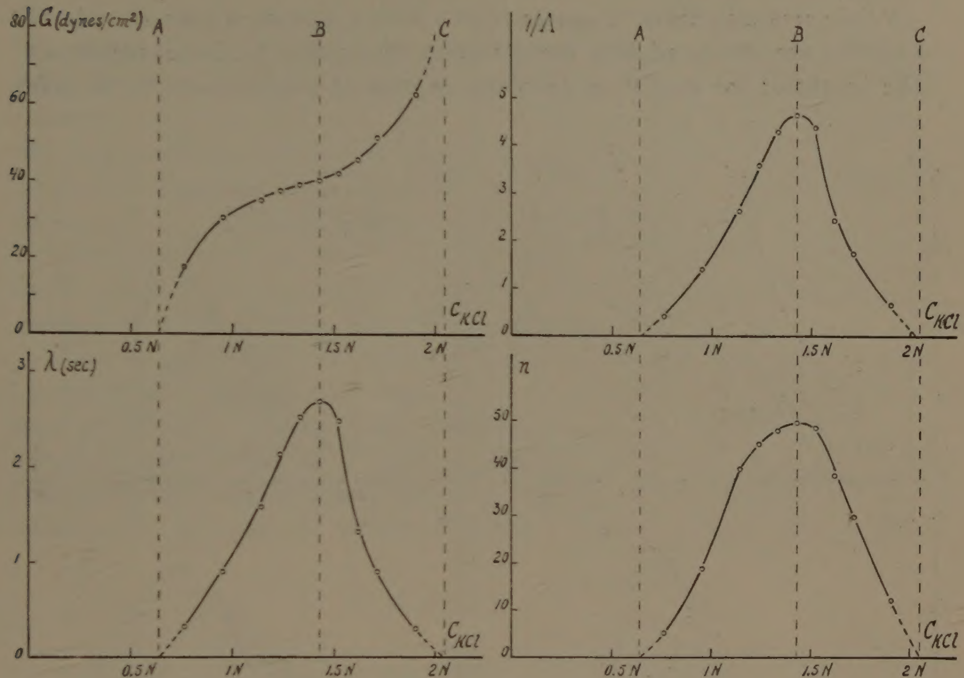

Fig. 1.

The latter of these KCl concentrations lies very near to the coacervation limit (at 2.00 N KCl not yet coacervation, at 2.09 N KCl coacervation). In the case of *n* we know from previous experiments that it indeed reaches the value zero just before the separation into two liquid phases (coacervate and equilibrium liquid) sets in (i.e. at slightly further increase of the KCl concentration). We may therefore say that the vertical, dotted line *C* indicates practically the coacervation limit.

If we now direct our attention to the *G* curve, we notice that it has quite another character than the λ, $1/\Lambda$ or *n* curves. By increasing the KCl concentration *G* always increases, though transitorily at a slower rate when nearing the KCl concentration of minimum damping (inflexion point of the *G* curve).

It seems further probable that the *G* curve begins with the value zero at the KCl concentration, indicated by the dotted vertical line *A* and that the *G* curve still continues sloping upwards if the KCl concentration approaches the coacervation limit *C*. Any future theory of the elastic viscous oleate systems must be able to explain the characteristic shapes of the curves in fig. 1 as discussed above. For the present we do not yet wish to speculate on this matter, as we are convinced, that more facts should be known as described hitherto in this series of communications.

We now come to the influence of added hexylalcohol. Fig. 2 shows that *n* hexylalcohol displaces the G, λ, $1/\Lambda$ and n curves. Let us consider this displacement more closely:

While retaining their character (curve with a maximum) the λ, $1/\Lambda$ and n curves are displaced into the direction of smaller KCl concentrations. The height of the maximum decreases in case of displacement to the left,

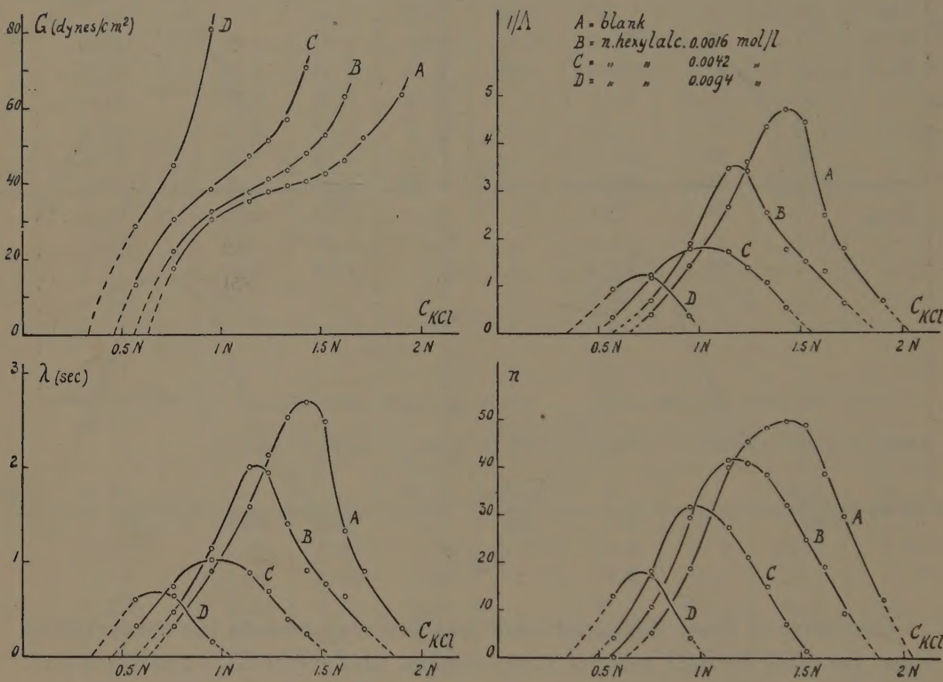

Fig. 2.

and the distance of the footpoints of these curves on the abscis axis grows smaller [4]).

When we consider the displacement of a characteristic point of these curves, viz. the maximum point, we see that it is displaced downwards to the left, which may be looked upon as to consist of a horizontal and vertical component (see fig. 3 scheme *A*, lower graph.)

The G curve (see fig. 2) while retaining its character of having an inflexion point is also displaced towards smaller KCl concentrations; besides it becomes steeper, in consequence of which the inflexion point becomes less marked.

When we consider the displacement of a characteristic point of this curve, viz. the inflexion point, (in practice determined by reading G at the KCl concentration of the maxima of the λ, $1/\Lambda$ or n curves) we obtain

[4]) The coacervation limit, which still practically coincides with the right footpoint of these curves, is therefore shifted to smaller KCl concentrations. See asterisks in Table I.

only a displacement in a horizontal direction [5]) (see fig. 3 scheme A, upper graph.).

The above induces one to attribute a twofold action to the added hexylalcohol. In its presence smaller KCl concentrations are needed to set up the typical elastic viscous system (horizontal displacement of the inflexion point on the G curve and horizontal component of the displacement of the maximum point on the λ, $1/\Lambda$ and n curves), i.e. hexylalcohol facilitates the large scale associations of the soap molecules which we assume to be present in the elastic viscous system. The existence of a vertical component downwards in the displacement of the maximum point of the λ, $1/\Lambda$ and n curves, however, indicates that hexylalcohol at the same time influences these elastic structures in such a way that the damping is generally increased (without altering the shear modulus).

If for the two above actions of hexylalcohol different points of attack on the elastic structure are supposed, it may be conceived that there also exist substances, which, when added to the oleate system, share with hexylalcohol the general increasing influence on the damping, but which counteract KCl in setting up the elastic viscous system (compare fig. 3 scheme C). In between the two extreme schemes A and C of fig. 3 a

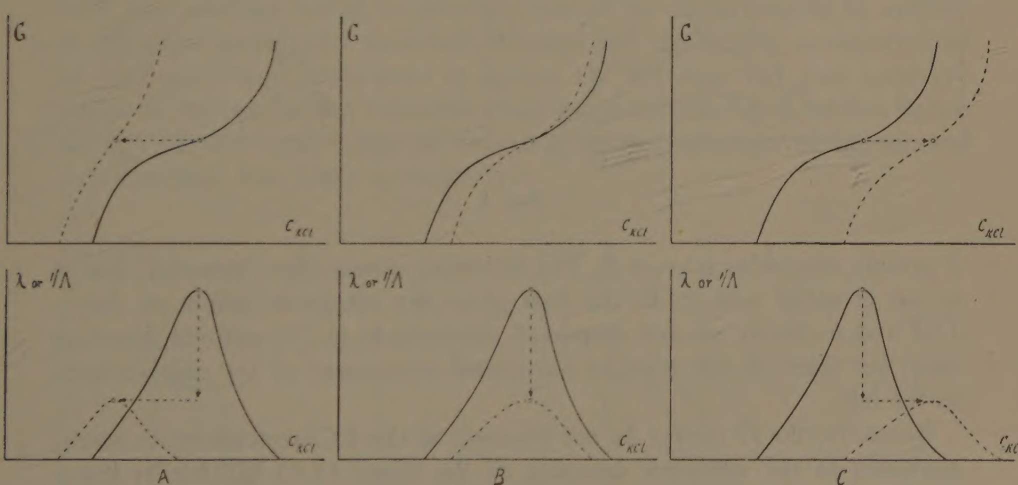

Fig. 3.

whole series of intermediate schemes may be conceived and half way it the scheme, indicated by B in fig. 3, represents a substance which neither helps nor counteracts KCl in setting up the elastic system. In the discussion of further experiments in this and following sections the schemes of fig. 3 will play a helpful rôle.

---

[5]) At the KCl concentrations corresponding with the maxima of the λ, $1/\Lambda$ and n curves A, B, C and D, we read of the following values of G on the corresponding G curves A, B, C and D: 40.5, 39, 40 and 38 dynes/cm^2, which cannot with certainty be considered as really different.

We also investigated the influence of ethanol on G, λ, $1/\Lambda$ and n in an analogous way as described above for the influence of n hexylalcohol. We shall not give elaborate tables of the results but represent them graphically in fig. 4. When we compare this figure with fig. 3 we see that

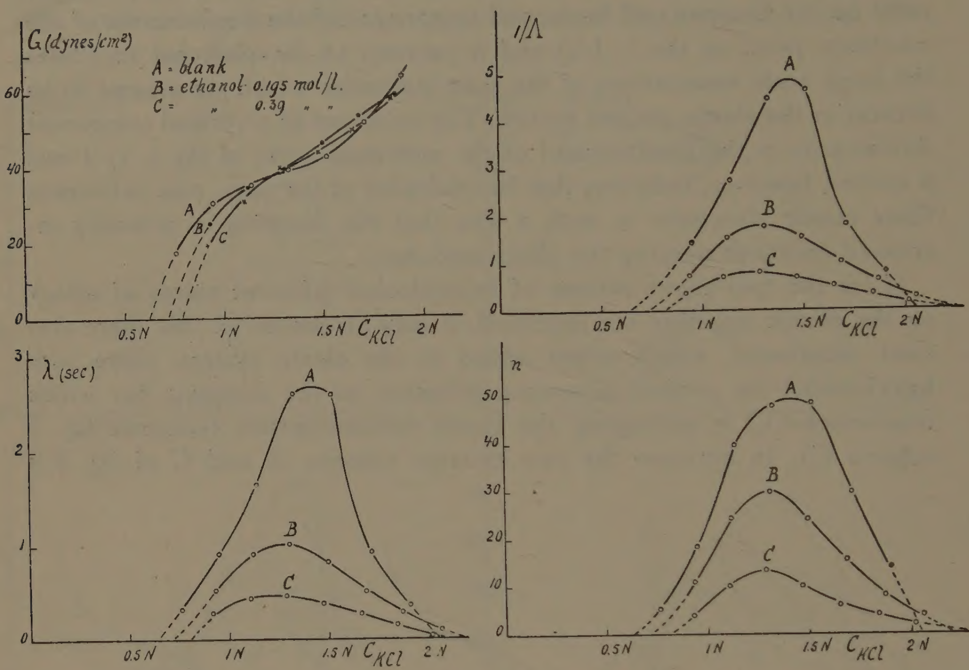

Fig. 4.

it greatly resembles scheme B. The following points show however, that it is not identical with it. In the first place the maximum points on the λ, $1/\Lambda$ and n curves are not displaced downwards in the vertical direction only, but there is still a slight horizontal component of the displacement to the left.

Secondly, the G curves do not intersect at the KCl concentration corresponding to the minimum damping of the blank (1.43 N) but at lower concentrations ($\pm$ 1.25 N).

Ethanol therefore corresponds to a case intermediate between the schemes A and B, which stands much closer to B than to A on account of the slight horizontal displacement to the left relative to the vertical displacement downwards.

We must further remark that ethanol shows another complication, which cannot be predicted from the simple schemes of fig. 3. If we direct our attention to the course of the λ, $1/\Lambda$ and n curves at KCl concentrations above approximately 1.7 N, we perceive that those in the presence of ethanol cut the blank curve. Here the coacervation limit is shifted not to smaller KCl concentrations but to higher. A similar phenomenon is present in the course of the G curves above 1.7 N KCl. Those corresponding to systems to which ethanol has been added, tend now to cut the G curve of the blank. Both facts seem to

indicate that the action of ethanol still depends on the absolute value of the KCl concentrations. With concentrations up to ± 1.7 N ethanol is a substance which slightly helps KCl in building up the elastic system, with concentrations higher than ± 1.7 N it counteracts KCl slightly.

3) *Influence of the first six terms of the n. primary alcohols on the elastic behaviour of the 1.2 % oleate system at the KCl concentration of minimum damping.*

As our stock of Na oleinicum medicinale pur. pulv. Merck was nearly exhausted and could not possibly be replenished, we decided to use for the experiments in this and the following section the large volume of oleate system, which had already served in previous experiments (on the dependence of T and Λ on R, see Part II of this series). It had the composition 1.2 g. oleate per 100 cc 1.52 N KCl + 0.08 N KOH, which electrolyte composition lies near to the minimum damping of the elastic oscillations. Eight spherical vessels of nominally 500 cc capacity (with radii varying from 5.01—5.04 cm) were exactly half filled with this system, put in the thermostate (15°) and measured the next morning.

Six of these vessels were used to determine the influence of the six alcohols, the seventh to control that the blank does not alter its properties with time and the eighth to ascertain part of the corrections to be applied to the experiments with methanol, ethanol and the highest concentrations of n propanol (cf. small print in section 1). We shall not give elaborate tables of the results, but represent them graphically in fig. 5. In this figure G, λ, $1/\Lambda$ and n are given as functions of the logarithm of the alcohol concentration (the latter in moles/l).

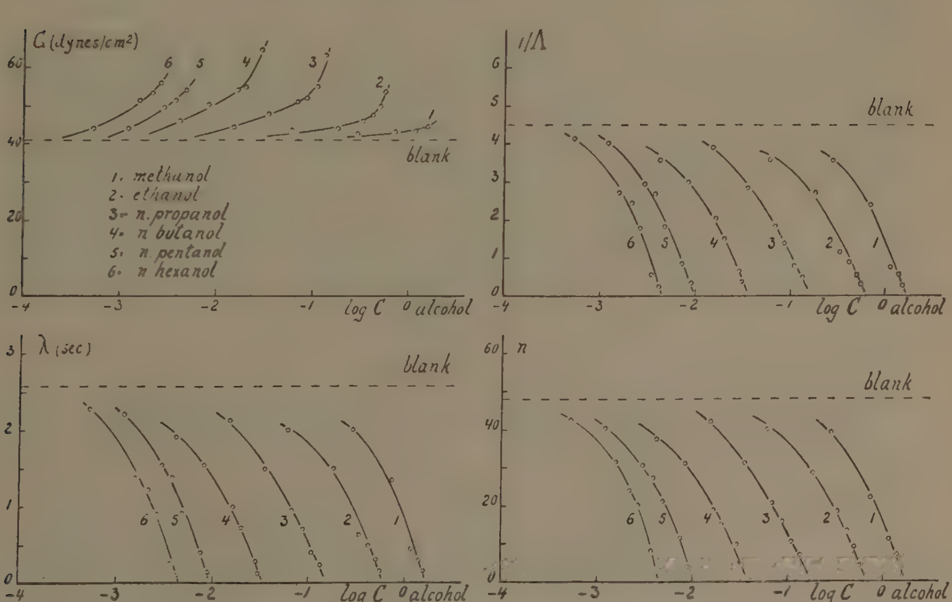

Fig. 5.

We see that all alcohols decrease λ, $1/\Lambda$ and n, and increase G. In the case of methanol the increase of G is so slight however, that one may doubt if it surpasses the experimental errors (taking into account that here the greatest correction had to be applied, which of course diminishes the reliability of the actual augmentation of the G curve above the blank level).

In connection with what was said in section 2, we come to the conclusion that the shift to the left in horizontal direction of the inflection point on the G curve in fig. 1 diminishes in the order $6 > 5 > 4 > 3 > 2 > 1$, by which it is perhaps not excluded that $1 =$ methanol shows already a very slight shift to the right.

As we have investigated here (fig. 5) the action of the alcohols at the KCl concentration of minimum damping, λ, $1/\Lambda$ and n can only decrease of course. Here too we have the same order of the curves as we had for G.

For a future theory of the action of n primary alcohols it is important that their action increases very considerably every time the alcohol is lenghtened with one carbon atom. Below we give for instance the logarithms of the alcohol concentration corresponding to a decrease of λ, $1/\Lambda$ and n to 50 % of its original value.

	n hexyl alcohol	*n* amyl alcohol	*n* butyl alcohol	*n* propyl alcohol	ethanol	methanol
λ	0.27—3	0.58—3	0.06—2	0.67—2	0.32—1	0.84—1
$1/\Lambda$	0.32—3	0.63—3	0.15—2	0.74—2	0.34—1	0.85—1
n	0.35—3	0.64—3	0.12—2	0.73—2	0.37—1	0.84—1
mean logarithmic difference	0.31	0.49	0.60	0.63	0.50	

The differences in the logarithms correspond (at least when going from methanol to amylalcohol) to ratios of approximately 3 or 4 (the logarithmic differences of two succeeding G curves is of the same order or even greater). This reminds us of the ratios occurring in TRAUBE's rule and suggests that the alcohol molecules exert their influence in the adsorbed state, and that in the latter state the carbon chain of the alcohol lies flat against certain either external or internal surfaces of the elastic soap structures.

4) *Influence of the fatty acid anions C_8—C_{14} on the elastic behaviour of the 1.2 % oleate system at the KCl concentration of minimum damping.*

Preliminary experiments showed that the viscous and elastic properties of the oleate systems containing KCl are not only sensitive to alcohols, but to a great many classes of organic non electrolytes as well, hydrocarbons included.

This sensitivity to organic non electrolytes of all kinds is also found in

the two phase (coacervate/equilibrium liquid) oleate systems, which are formed from the one phase elastic viscous oleate systems at a somewhat higher KCl concentration. The characteristic influence of organic non electrolytes manifests itself here in the change of the partial solubility of the two phases (at constant KCl concentration) and can be conveniently studied by measuring the shift of the coacervation limit (i.e. the KCl concentration which is just needed for the separation into two phases) [6].

So far as our experience reaches and speaking very generally it appears that as regards the connection between constitution and action of organic non electrolytes analogous rules hold for both the one phase elastic viscous oleate systems and the two phase (coacervate/equilibrium liquid) oleate systems.

It was recently shown in our laboratory by H. L. BOOIJ that oleate coacervates are also sensitive to organic anions and that in the case of the fatty acid anions, the action of the same bound quantity depended in an unexpected way on the number of carbon atoms of the fatty acid anion [7]. From C_7 onward the coacervation limit is shifted to higher KCl concentrations, but this shift reaches a maximum value for undecylic acid (C_{11}) and diminishes thereafter very considerably (at C_{14}—C_{16}), to increase one more to approximately the level as reached with C_{11} if the hydrocarbon chain of the fatty acid anion is sufficiently lenghtened (C_{20}—C_{22}).

To see if now again a parallel could be drawn between elastic oleate systems and oleate coacervates, we decided also to include in the present investigation the influence of a number of fatty acid anions (from C_8—C_{14}) on the elastic properties of the 1.2 % oleate system at the KCl concentration of minimum damping. The method we followed was the same as in section 3 (half filled vessels of nominally 500 cc capacity 15°) and because a sufficient amount of KOH is present in the oleate system, we added known amounts of the fatty acids themselves (the terms with m.p. below room temperature as drops of known weight, the solid terms weighed amounts of the crystals). To accelerate the dissolution of the added acids, the vessels were agitated for 5 min. while immersed in a waterbath of 52°, the contents were thoroughly shaken then and the vessels replaced in the thermostate of 15° and the measurements made the next morning.

In order to check if this warming up of the oleate system has in itself no influence on the elastic behaviour after cooling down to 15° (though at the temperature of ± 45° as was reached during the heat treatment the oleate system is no longer elastic) a spherical vessel half filled with a blank system was subjected to the same treatment for three consecutive

---

6) H. G. BUNGENBERG DE JONG and G. W. H. M. VAN ALPHEN, these Proceedings **50**, 1011 (1947).

7) H. L. BOOIJ and H. G. BUNGENBERG DE JONG, Biochimica Acta, in press.

days. It was found that an influence exceeding the experimental errors could not be detected [8]).

The results of these measurements are represented in fig. 6. In connection with the discussion in section 2 (c.f. fig. 3) it is easy to see that the results are compatible with the assumption that the lower fatty acid anions (C_8—C_{11}) shift the G, the λ, the $1/\Lambda$ and n curves of the blank in the reverse directions as hexylalcohol did in fig. 2. This assumption [9]) explains why in fig. 6 the G curves for C_8, C_9, C_{10} and C_{11} bend downwards (in contrast to the G curves for the higher terms of the alcohols in fig. 5, which bend upwards). With the alcohols (fig. 5) any contrast in the course of the λ, $1/\Lambda$ and n curves, which here (fig. 6) too only [10]) bend downwards, is, however, not to be expected, since here too we started with a blank oleate system at the KCl concentration of minimum damping (see scheme C of fig. 3).

In the four diagrams of fig. 6 we notice that the action of the fatty acid anions increases in the order $C_8 < C_9 < C_{10}$.

We see, however, that C_{11} is slightly less or very slightly more active than C_{10} (c.f. 100 G/G_0 diagram and the remaining ones, respectively). The next term C_{12} is decidedly less active than C_{11}.

All this means, that for a same concentration of the fatty acid anions, the above mentioned shifts of various curves (G. λ etc. in fig. 3, scheme C) towards higher KCl concentrations do not increase indefinitely with the length of the carbon chain of the fatty acid anion, but that these shifts reach a maximum value at about C_{10} or C_{11}. A further lengthening diminishes this shift rapidly (C_{12}) and the characteristic property of the lower fatty acid anions is already lost at C_{14}. Obviously this anion (myristate-) resembles the oleate anion that much already, that it no longer counteracts the elastic structures built up by the KCl in the oleate system, but even positively contributes to the elastic properties of the oleate system. This positive contribution reveals from the strong increase of G, λ, $1/\Lambda$ and n above the blank values, just as a further increase of the oleate concentration of the blank will also bring about.

---

[8]) In the survey below four numbers are placed each time behind the symbols $10 \times \frac{T}{2}$, b_1/b_3 and n. They give the values found before the heat treatment, and after the first, the second and third heat treatment:

$10 \times \frac{T}{2}$: 5.60; 5.59; 5.59 and 5.59 sec.
b_1/b_3 : 1.248; 1.250; 1.247 and 1.250
n : 46.5; 46.6; 46.6 and 46.8

[9]) For the undecylate ion subsequent work has confirmed this assumption.

[10]) We neglect here that the curves mentioned, first run in fig. 6 in the opposite direction and after reaching a maximum located some 6—10 percent above the blank value take the course discussed in the text. This curve form is to be expected if the KCl concentration in the blank oleate system (here 1.52 N) does not exactly correspond with the KCl concentration of the minimum damping (according to table I = 1.43 N) but is slightly higher.

When we summarize the result of the above measurements it appears that there is really a parallel with the action of the fatty acid anions on

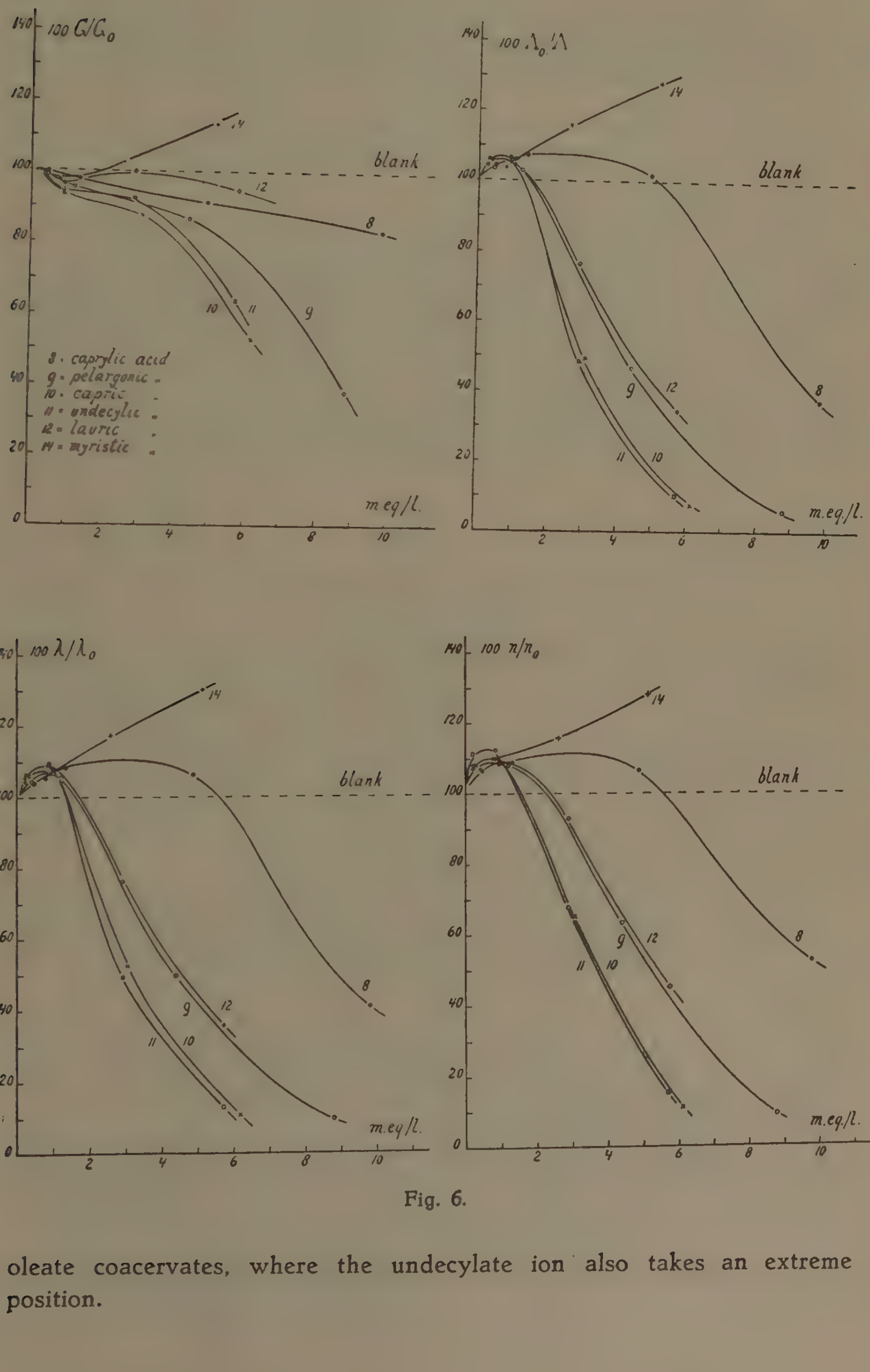

Fig. 6.

oleate coacervates, where the undecylate ion also takes an extreme position.

5) *Correlation between n and Λ.*

In the preceding Parts of this series, we have also inserted in many Tables referring to elastic measurements the values for n, i.e. the maximum number of observable oscillations (cf. already Part I, section 7, 9 and 10). An inspection of the above mentioned Tables will reveal that n decreases whenever Λ increases and reversely, but in none is the correlation between n and Λ a very simple one. In these Tables we considered the influence of the type of oscillation, the radius of the vessel, the temperature and the concentration of the oleate.

In the present communication, these four data are held constant while the KCl concentration is varied or when held constant small amounts of organic substances are added. Now the correlation between n and Λ is far much simpler and can be expressed very roughly speaking by $n.\,\Lambda$ = constant.

To show this, we have inserted in the figures of this communication graphs in which the ordinates are n and $1/\Lambda$ or $100\,n/n_0$ and $100\,\Lambda_0/\Lambda$.

It is true $n\,.\,\Lambda$ is not really constant so that the graphs for n/n_0 give a deformed picture of the graphs for Λ_0/Λ (see eg. fig. 1 and 2, and 4). Nevertheless the former give qualitatively the same details as the latter. Compare fig. 5 and especially fig. 6.

The above may be of practical importance, as it is not always easy to find an observer who is able to perform the difficult measurement of the decrement. In such a case the determination of the period and of the maximum number of observable oscillations can help to continue investigations of the type given in section 3 and 4, viz. those on the connection between the action of an organic substance and its structure.

Summary.

1) If the KCl concentration is increased the values of G, λ, $1/\Lambda$ and n are very low (presumably zero) at the first appearance of elastic phenomena. The last three increase to a maximum and then decrease to zero just before the coacervation limit is reached. G increases in this whole tract of KCl concentrations. The G curve shows an inflexion point at the KCl concentration corresponding to the maxima of the λ, $1/\Lambda$ and n curves.

2) The influence on the elastic behaviour of a number of n primary alcohols and of fatty acid anions has been studied and it appeared that the former (C_1—C_6) help the KCl in setting up the typical elastic viscous systems, the latter (C_8—C_{11}) counteract KCl in doing so.

3) The action of the alcohols increases considerably with increasing length of the carbon chain, each following term of the homologous series requiring for the same effect a 3—4 fold lower concentration than the preceding one.

4) The action of the fatty acid anions increases with the length of the carbon chain but this holds only up to C_{11} (undecylate), the action diminishes rapidly by further lengthening the carbon chain (C_{12}) and it has wholly disappeared in C_{14}.

5) For a certain type of work and under conditions described, the maximum number n of observable oscillations, may in emergency cases be used as an approximate measure of $1/\Lambda$.

Department of Medical Chemistry
University of Leiden.

Mathematics. — *Een iteratieproces voor de oplossing van een randwaardeprobleem bij een lineaire partiële differentiaalvergelijking van de tweede orde.* II. By J. J. DRONKERS. (Communicated by Prof. W. VAN DER WOUDE.)

(Communicated at the meeting of February 26, 1949.)

§ 4.

Bij de bepaling van z_1 (zie (11)) moet één keer naar x geïntegreerd worden. De integrand bestaat uit drie termen, ieder met twee factoren, bijv. α en $u_0^{(1)}$ en één term met één factor nl. δ. Verder bestaat u_1 uit twee termen met twee factoren, terwijl ook één keer naar x geïntegreerd moet worden.

De integrand van de functie z_2 bestaat vóór de eliminatie van u_1 en z_1 ook weer uit drie termen met twee factoren; zij bevat echter geen term met één factor.

Worden u_1 en z_1 geëlimineerd, dan zal, als de integraties buiten beschouwing gelaten worden, z_2 onder meer uit termen met drie factoren bestaan, waaronder δ niet voorkomt. Eén dier termen heeft bijv. de vorm:

$$z_0^{(2)} \int \alpha \int \beta_2 \, d x^2.$$

Zodra echter in een term δ of één van haar partiële afgeleiden naar y voorkomt, bevat zij twee factoren.

Bij de berekening van z_n moet na de eliminaties, in iedere term n keer naar x geïntegreerd worden, terwijl zij $n+1$ of n factoren bevat. Iedere term is dan een n voudige integraal van de vorm:

$$z_0^{(k)} \int \alpha^{(l_1)} \int \gamma_1^{(l_2)} \ldots \int \gamma_2^{(l_n)} d x^n. \quad \ldots \ldots \ldots \quad (16)$$

waarbij dan $z_0^{(k)}$ ook door $u_0^{(k)}$ vervangen kan zijn.

Zoals gemakkelijk uit (11) en (12) blijkt, geldt dan dat

$$k + l_1 + l_2 + \ldots + l_n \leqslant n.$$

Dan kunnen een aantal grootheden l, of k, gelijk aan nul zijn.

Evenzo bestaat u_n uit overeenkomstige termen met $n+1$ of n factoren.

Nu wordt door $A_{nk} z_0^{(k)}$ de som van alle termen van z_n aangeduid, die dezelfde factor $z_0^{(k)}$ bevatten. Evenzo is $u_0^{(k)} B_{n,k}$ de som van alle termen met dezelfde factor $u_0^{(k)}$, enz.

Bij de achtereenvolgende eliminaties van z_i en u_i wordt gevonden, dat de hoogste afgeleiden naar y van z_0 en u_0, die in z_n voorkomen, $z_0^{(n)}$ en $u_0^{(n)}$ zijn. Tevens komen ook alle andere afgeleiden $z_0^{(k)}$ en $u_0^{(k)}$ voor ($k = 1$,

...... n). Dan kunnen z_n en u_n in de volgende vorm geschreven worden:

$$\left.\begin{array}{ll}(a) & z_n = \sum_{k=1}^{n} z_0^{(k)} A_{n,k} + z_0 A_{n,0} + V_n + \sum_{k=1}^{n} u_0^{(k)} B_{n,k} \quad \text{en} \\ (b) & u_n = \sum_{k=1}^{n} z_0^{(k)} C_{n,k} + z_0 C_{n,0} + W_n + \sum_{k=1}^{n} u_0^{(k)} D_{n,k}. \end{array}\right\} \quad . \quad (17)$$

Eveneens kan voor z_{n+1} geschreven worden:

$$z_{n+1} = \sum_{k=1}^{n+1} z_0^{(k)} A_{n+1,k} + z_0 A_{n+1,0} + V_{n+1} + \sum_{k=1}^{n+1} u_0^{(k)} B_{n+1,k},$$

terwijl ook:

$$z_{n+1} = \int (\alpha u_n^{(1)} + \beta_1 z_n^{(1)} + \gamma_1 z_n)\, dx.$$

Door (17) in dit rechterlid te substituëren wordt het verband gevonden, dat bestaat tussen de coëfficiënten $A_{n+1,k}$ enz. van z_{n+1} en $A_{n,k}$ enz. van z_n en u_n.

Dan blijkt voor $k = 1, 2, \ldots, n+1$.

$$\left.\begin{array}{l} A_{n+1,k} = \int [\alpha (C_{n,k-1} + C_{n,k}^{(1)}) + \beta_1 (A_{n,k-1} + A_{n,k}^{(1)}) + \gamma_1 A_{n,k}]\, dx, \\ B_{n+1,k} = \int [\alpha (D_{n,k-1} + D_{n,k}^{(1)}) + \beta_1 (B_{n,k-1} + B_{n,k}^{(1)}) + \gamma_1 B_{n,k}]\, dx, \\ A_{n+1,0} = \int (\alpha C_{n,0}^{(1)} + \beta_1 A_{n,0}^{(1)} + \gamma_1 A_{n,0})\, dx \quad \text{en} \\ V_{n+1} = \int (\alpha W_n^{(1)} + \beta_1 V_n^{(1)} + \gamma_1 V_n)\, dx. \end{array}\right\} (18a)$$

Hierbij moet worden opgemerkt, dat

$$C_{n,n+1} = A_{n,n+1} = D_{n,n+1} = B_{n,n+1} = 0.$$

Evenzo wordt voor de coëfficiënten $C_{n+1,k}$ enz. van u_{n+1} gevonden:

$$\left.\begin{array}{l} C_{n+1,k} = \int [\beta_2 (A_{n,k-1} + A_{n,k}^{(1)}) + \gamma_2 A_{n,k}]\, dx; \\ C_{n+1,0} = \int (\beta_2 A_{n,0}^{(1)} + \gamma_2 A_{n,0})\, dx; \; W_{n+1} = \int (\beta_2 V_n^{(1)} + \gamma_2 V_n)\, dx; \\ D_{n+1,k} = \int [\beta_2 (B_{n,k-1} + B_{n,k}^{(1)}) + \gamma_2 B_{n,k}]\, dx. \end{array}\right\} (18b)$$

In de formule (17a) kunnen daarna de functies $u_0^{(k)}$ worden vervangen, immers volgens (9) kan $u_0^{(1)}$ lineair uitgedrukt worden in:

$$\left(\frac{\delta z}{\delta x}\right)_{x=0}, \quad z^{(1)}(0, y) \quad \text{en} \quad z(0, y).$$

Achtereenvolgens kunnen dan ook de afgeleiden $u_0^{(k)}$ lineair worden uitgedrukt in de afgeleiden naar y van de zojuist genoemde functies.

Na substitutie in (17a) wordt dan gevonden:

$$z_n = \sum_{k=1}^{n} z_0^{(k)} \bar{A}_{n,k} + z_0 \bar{A}_{n,0} + \bar{V}_n + \sum_{k=1}^{n-1} \left(\frac{\delta z}{\delta x}\right)_{x=0}^{(k)} \bar{B}_{n,k} + \left(\frac{\delta z}{\delta x}\right)_{x=0} B_{n,0}.$$

Ten slotte is dan voor de integraal $z(x, y)$ te schrijven:

$$
\left.\begin{aligned}
z(x,y) = \sum_{m=1}^{\infty} z^{(m)}(0,y)\, A_m(x,y) + z(0,y)\, A_0(x,y) + V_0(x,y) + \\
+ \sum_{m=1}^{\infty} \left(\frac{\delta z}{\delta x}\right)^{(m)}_{x=0} B_m(x,y) + \left(\frac{\delta z}{\delta x}\right)_{x=0} B_0(x,y).
\end{aligned}\right\} \qquad (19)
$$

Daar de randwaarden volgens (2) bekend zijn, zijn van het rechterlid alle functies gegeven.

§ 5.

De functies z_n en u_n bestaan uit termen van de vorm (16). Om een overzicht te krijgen, wordt in deze paragraaf het aantal termen (16) tussen grenzen gesloten.

In het vervolg geven wij het aantal termen van z_n en u_n, die uit $n+1$ factoren bestaan, resp. door (z_n) en (u_n) aan. Zo bestaat z_1 uit drie termen met twee factoren en 1 term met 1 factor, terwijl u_1 uit twee termen met twee factoren bestaat.

Volgens (11) is het aantal termen van z_2 en u_2 met 3 factoren resp. gelijk aan:

$$
\begin{aligned}
&(z_2) = (u_1^{(1)}) + (z_1^{(1)}) + (z_1) = 2(u_1) + 3(z_1) \quad \text{en} \\
&(u_2) = (z_1^{(1)}) + (z_1) = 3(z_1).
\end{aligned}
$$

In het algemeen is:

$$
\left.\begin{aligned}
&(z_n) = n\,(u_{n-1}) + (n+1)\,(z_{n-1}) \quad \text{en} \\
&(u_n) = (n+1)\,(z_{n-1}).
\end{aligned}\right\} \quad \ldots\ldots \quad (20)
$$

Met behulp van de betrekkingen (20) kan het aantal termen van z_n en u_n met $n+1$ factoren achtereenvolgens worden berekend. In het vervolg worden echter (z_n) en (u_n) benaderd, door deze tussen twee grenzen in te sluiten.

Voor $n \geqq 3$ geldt nl.:

$$
2\tfrac{3}{5}\, n^2 (z_{n-2}) < (z_n) < 3\, n^2 (z_{n-2}). \quad \ldots\ldots \quad (21)
$$

Bewijs: Uit (20) wordt eerst de volgende betrekking afgeleid voor $n \geqq 4$:

$$
(z_n) = (3\,n^2 + n - 1)\,(z_{n-2}) - (n-2)^2\,(n^2 - 1)\,(z_{n-4}). \quad \ldots \quad (22)
$$

Uit (20) volgt nl.:

$$
\begin{aligned}
&(z_n) = n^2 (z_{n-2}) + (n+1)\,(z_{n-1}) \quad \text{dus:} \\
&(z_{n-2}) = (n-2)^2 (z_{n-4}) + (n-1)\,(z_{n-3}) \quad \text{en} \\
&(z_{n-1}) = (n-1)^2 (z_{n-3}) + n\,(z_{n-2}).
\end{aligned}
$$

Door (z_{n-1}) en (z_{n-3}) te elimineren wordt (22) afgeleid.
Het tweede deel van (21) wordt eerst aangetoond:

Immers uit $(z_n) < (3n^2 + n-1)\,(z_{n-2})$ is af te leiden:

$$(z_{n-4}) > \frac{(z_{n-2})}{3n^2-11n+9} > \frac{(z_{n-2})}{3\,(n-2)\,(n-1)} \text{ voor } n \geqq 4.$$

Dus is volgens (22):

$$(z_n) < (2\tfrac{2}{3}n^2 + 1\tfrac{1}{3}n)\,(z_{n-2}) \leqq 3n^2\,(z_{n-2}) \text{ als } n \geqq 4.$$

Voor de laatste ongelijkheid kan vanzelfsprekend nog een scherpere benadering worden aangegeven.

De ongelijkheid $(z_n) < 3\,n^2(z_{n-2})$ geldt ook nog voor $n = 3$.

Wij zullen verder bewijzen dat $(z_n) > 2\tfrac{3}{5}\,n^2(z_{n-2})$.

Daar $(z_0) = 1$; $(z_1) = 3$; $(z_2) = 13$; $(z_3) = 79$; $(z_4) = 603$, is aan deze ongelijkheid voldaan voor $n = 3$, 4 enz.

Laat ze gelden tot $n-2$ toe, zodat:

$$(z_{n-2}) > 2\tfrac{3}{5}\,(n-2)^2\,(z_{n-4}).$$

Dan is volgens (22):

$$(z_n) > (2\tfrac{8}{13}\,n^2 + n - \tfrac{8}{13})\,(z_{n-2}) > 2\tfrac{3}{5}\,n^2(z_{n-2});\ n \geqq 3.$$

Het voorgaande is nog uit te breiden. Er bestaat een getal n_l, zodat voor $n > n_l$:

$$(z_n) < 3\,(n-l)\,(n-l-1)\,(z_{n-2}). \quad \ldots\ldots \quad (23)$$

B e w ij s: Uit (21) volgt:

$$(z_{n-4}) > \frac{(z_{n-2})}{3\,(n-2)^2}.$$

Dus volgens (22):

$$(z_n) < (z_{n-2})\,[3\,n^2 - (\tfrac{1}{3}n^2 - n + \tfrac{2}{3})].$$

Wij bepalen nu het gehele getal n_l, zodat:

$$\tfrac{1}{3}\,n_l^2 - n_l \geqq (6\,l+3)\,n_l - 3\,l^2 - 3\,l \text{ of } n_l \geqq 6 + 9\,l + 3\sqrt{4 + 11\,l + 8\,l^2} \quad (23a)$$

Kiezen wij n groter dan dit getal n_l, dan zal in ieder geval (23) gelden. Zo wordt gevonden voor $l = 0$; $n_l \geqq 12$.

Uit (23) volgt verder, dat voor $n > n_l$:

$$(z_n) < \frac{(z_{n_l+1})}{(n_l+1-l)\,!}\,3^{\frac{n-n_l}{2}}\,(n-l)\,! \quad \ldots\ldots \quad (24)$$

Dan kan n of n_l zowel even als oneven zijn.

Bij de afleiding van deze ongelijkheid moet dan voor het geval n en n_l beiden even of oneven zijn, rekening gehouden worden met het feit, dat

$$\frac{(z_{n_l+1})}{(n_l+1-l)\,!} > \frac{(z_{n_l})}{(n_l-l)\,!}$$

Deze ongelijkheid is direct met behulp van (20) aan te tonen.

Voor (u_n) kan een overeenkomstige schatting worden gemaakt, terwijl dit eveneens kan geschieden voor het aantal termen van (z_n) en (u_n) met n factoren. Dit aantal termen is vanzelfsprekend kleiner dan het aantal met $n+1$ factoren.

§ 6.

In deze paragraaf wordt aangetoond, dat de reeksen:

$$z = \sum_{k=0}^{\infty} z_k \text{ en } u = \sum_{k=0}^{\infty} u_k \quad \ldots \ldots \quad (25)$$

die in § 3 zijn opgesteld [zie (11) en (12)], oplossingen zijn van de partiële differentiaalvergelijkingen (4*a*) en (4*b*) en de gestelde randwaarden.

De functie $z(x, y)$, die wordt verkregen door de daarin voorkomende functies u_0, u_1, u_2 ...... u_n uit te drukken in de randwaarden $z(0, y)$ en $\left(\frac{\partial z}{\partial x}\right)_{x=0}$ en haar afgeleiden naar y, zal dan aan (1) en de randwaarden (2) voldoen.

Wij bewijzen nu de volgende stelling:

Laat de functies a, b, c, d, e en f van de partiële differentiaalvergelijking (1), benevens de randwaarden $z(0, y)$ en $\left(\frac{\delta z}{\delta x}\right)_{x=0}$, voldoen aan de voorwaarden in § 1 genoemd.

Dan geldt:

1e. De reeksen (25) convergeren gelijkmatig voor de intervallen:

$$0 \leqq y \leqq B; \quad 0 \leqq x < \frac{1}{4 M \varrho} \leqq A$$

(zie voor de bepaling van M het hiernavolgende bewijs).

2e. Voor dit interval zullen de functies z en u voldoen aan de partiële differentiaalvergelijkingen (4*a*) en (4*b*), terwijl voor $x = 0$, $z(x, y)$ in de gegeven functie $z(0, y)$ en $u(x, y)$ in $u(0, y)$ zal overgaan.

3e. Worden de functies u_0, u_1, u_2 enz., die in de functie $z(x, y)$ als som van de reeks (25) voorkomen, in de gegeven randwaarden van $z(x, y)$ en haar afgeleiden uitgedrukt, dan wordt de oplossing verkregen, die aan (1) en de gestelde randwaarden voldoet.

Bewijs:

1e. Als de coëfficiënten a, b, c, d, e en f aan de gestelde eisen voldoen, zullen de partiële differentiaalvergelijkingen (6) waarin de genoemde functies a, b enz. als bekenden voorkomen, oplossingen voor α, β_1, γ_1, β_2, γ_2 en δ geven, waarvoor analoge voorwaarden gelden als voor a, b enz. Zo bestaat er een getallenwaarde M, die de absolute waarden van deze functies α enz. en haar partiële afgeleiden naar y van de k^e orde, na deling door $k!$ en ϱ^k voor de genoemde intervallen overschrijdt.

Deze partiële afgeleiden van de functies α, β_1 enz. kunnen uit (6) worden berekend, waarna een grootste waarde kan worden aangegeven (zie hiervoor § 2).

Wij zullen nu bewijzen, dat de reeks $z = \sum_{k=0}^{\infty} z_k$ gelijkmatig convergeert voor $0 \leqslant x < \frac{1}{4 M \varrho}$.

Volgens de formule voor z_1 is (zie § 3):

$|z_1| < 3\varrho M^2 x + Mx < 4\varrho Mx$, als $M < 1$; of $< 4\varrho M^2 x$, als $M \geqslant 1$,

terwijl

$|u_1| < 2\varrho M^2 x$.

Hierbij is verondersteld, dat $\varrho \geq 1$. Dit zullen we in het vervolg ook steeds aannemen. Indien $\varrho < 1$ kunnen analoge schattingen worden uitgevoerd. Het is duidelijk, dat als de convergentie is aangetoond voor $\varrho \geq 1$, de convergentie ook zal gelden voor $\varrho < 1$ als $0 \leq x \leq \frac{1}{4M}$. Het blijkt echter, dat ook voor $\varrho < 1$, gelijkmatige convergentie voor $0 \leq x \leq \frac{1}{4 M \varrho}$ zal optreden.

Nu bestaat z_2 uit de som van een aantal termen van de vorm:

$$z_0^{(k)} \int \alpha^{(l_1)} \int \beta_1^{(l_2)}\, dx^2, \text{ waarbij } k + l_1 + l_2 \leqslant 2.$$

Ook kan $z_0^{(k)}$ door $u_0^{(k)}$ vervangen zijn, terwijl een dergelijke factor ook kan ontbreken. Door het aantal termen van z_2 te bepalen, blijkt dat in ieder geval:

$$|z_2| < 4^2 \varrho^2 M^3 x^2 \text{ als } M \geqslant 1; \text{ of } < 4^2 \varrho^2 M^2 x^2, \text{ als } M < 1.$$

Bij nauwkeuriger schatting blijkt zelfs $|z_2| < 9\varrho^2 M^3 x^2$ als $M \geq 1$ enz. Zowel voor $M \geq 1$, als $M < 1$ is dus zeker:

$$|z_2| < 4\varrho M x \cdot \text{majorant van } |z_1|.$$

In het algemeen bestaat z_n uit een som van n voudige integralen van de vorm (16) (zie § 3):

$$\Sigma z_0^{(k)} \int \alpha^{(l_1)} \int \alpha^{(l_2)} \ldots \int \gamma_2^{(l_n)}\, dx^n.$$

Verder geldt:

$$k + l_1 + \ldots + l_n \leqslant n.$$

Volgens het gegeven dat $|\alpha^{(l_1)}| < M l_1! \varrho^{l_1}$ enz., is dus

$$|z_n| < M^{n+1} \varrho^n \frac{x^n}{n!} \Sigma k!\, l_1!\, l_2! \ldots l_n!$$

Hierin is M groter dan 1 verondersteld; indien $M < 1$, moet M^{n+1} vervangen worden door M^n.

Wij beschouwen nu:

$$z_{n+1} = \Sigma z_0^{(k')} \int \alpha^{(l'_1)} \int \ldots \int \gamma_2^{(l'_{n+1})}\, dx^{n+1}$$
$$k' + l'_1 + l'_2 + \ldots + l'_{n+1} \leqslant n + 1.$$

Anderzijds is echter:

$$z_{n+1} = \int_0^x (\alpha\, u_n^{(1)} + \beta_1\, z_n^{(1)} + \gamma_1\, z_n)\, dx.$$

Hierin worden u_n en z_n gesubstitueerd, die respectievelijk bestaan uit een som van termen van de vorm (16). Door de differentiaties uit te voeren en daarna de termen te schatten, wordt gevonden:

$$|z_{n+1}| < \frac{x^{n+1}}{(n+1)!}\,\varrho^{n+1}\,M^{n+2}\,\{\Sigma\, 2\,[(k+1)!\,l_1!\ldots l_n! +$$

$$+ k!\,(l_1+1)!\,l_2!\ldots l_n! + \ldots + k!\,l_1!\ldots(l_n+1)!] + \Sigma\, k!\,l_1!\ldots l_n!\} <$$

$$< \frac{x^{n+1}}{(n+1)!}\,\varrho^{n+1}\,M^{n+2}\,\Sigma\, k!\,l_1!\ldots l_n!\,[2\,(k+1+l_1+1+\ldots+l_n+1)+1] <$$

$$< \frac{x^{n+1}}{(n+1)!}\,\varrho^{n+1}\,M^{n+2}\,(4n+3)\,\Sigma\, k!\,l_1!\ldots l_n! < 4\,\frac{x^{n+1}}{n!}\,\varrho^{n+1}\,M^{n+2}\,\Sigma\, k!\,l_1!\ldots l_n!.$$

$$(k + l_1 + l_2 + \ldots + l_n \leq n).$$

Uiteindelijk wordt dus gevonden, dat:

$$|z_{n+1}| < 4\,\varrho\, M x\,.\ \text{majorant}\, |z_n|.$$

Dit geldt zowel voor $M \geq 1$ als $M < 1$. Dus:

$$z_0 + |z_1 + z_2| + \ldots + z_n < z_0 + 4\,\varrho\, M^2 x + 4^2 \varrho^2 M^3 x^2 + 4^3 \varrho^3 M^4 x^3 +$$
$$+ \ldots + 4^n \varrho^n M^{n+1} x^n + \ldots\}.$$

Hierbij is $M \geq 1$; als $M < 1$ moeten de exponenten van M met één verminderd worden. In het vervolg wordt $M \geq 1$ aangenomen.

De z reeks (zie (25)) zal dus gelijkmatig convergeren voor $x < \frac{1}{4\,M\varrho}$.

Wordt de reeks bij z_n afgebroken, dan is:

$$|R_{n+1}| < \sum_n^{\infty} 4^{n+1}\,\varrho^{n+1}\,M^{n+2}\,x^{n+1} = \frac{4^{n+1}\,\varrho^{n+1}\,M^{n+2}\,x^{n+1}}{1 - 4\,M\varrho x} \quad . \quad . \quad . \quad (26)$$

Op dezelfde wijze kunnen wij bewijzen, dat de u reeks in ieder geval gelijkmatig convergeert voor $x < \frac{1}{4\,M\varrho}$. Het aantal termen van u_n is o.a. kleiner dan dat van z_n.

2e. Wij bewijzen nu dat de functies z en u bepaald volgens (25), voldoen aan de partiële differentiaalvergelijkingen (4) en de bijbehorende randwaarden. Dit laatste is volgens (11) en (12) evident.

Wij substitueren in (4*a*) en (4*b*):

$$z = z_0 + z_1 + z_2 + \ldots + z_n + R_{n+1},$$
$$u = u_0 + u_1 + u_2 + \ldots + u_n + R_{n+1}^{+},$$

en vinden dan voor het verschil tussen de linker- en rechterleden, in verband met (11) en (12):

$$\left.\begin{aligned} &\frac{\partial R_{n+1}}{\partial x} - \alpha R_n^{+(1)} - \beta_1 R_n^{(1)} - \gamma_1 R_n = \overline{R}(x, y) \\ &\frac{\partial R_{n+1}^{+}}{\partial x} - \beta_2 R_n^{(1)} - \gamma_2 R_n = \overline{R}_2(x, y). \end{aligned}\right\} \quad . \; . \; . \quad (27)$$

Worden de termen van

$$\frac{\partial R_{n+1}}{\partial x} = \sum_{q=1}^{\infty} \frac{\partial z_{n+q}}{\partial x}$$

op overeenkomstige wijze geschat als in het voorgaande voor z_n enz. is geschiedt, dan wordt gevonden:

$$\left|\frac{\partial R_{n+1}}{\partial x}\right| < 4\varrho^{n+1} M^{n+2} \frac{x^n}{(n-1)!} \left[\sum_{p=0}^{\infty} (4\varrho M x)^p \left(1 + \frac{p+1}{n}\right)\right] \Sigma\, k!\, l_1! \ldots l_n!$$

Op analoge wijze wordt gevonden:

$$\left|\beta_1 \frac{\partial R_n}{\partial y}\right| < 2\varrho^{n+1} M^{n+2} \frac{x^n}{(n-1)!} \left[\sum_{p=0}^{\infty} (4\varrho M x)^p \left(1 + \frac{p+1}{n}\right)\right] \Sigma\, k!\, l_1! \ldots l_n!$$

Dan is $k + l_1 + \ldots\ldots + l_n \leq n$.

Dergelijke benaderingen kunnen ook worden opgesteld voor de overige termen in (27).

Er is dus een waarde N te bepalen, zodanig dat voor $n > N$ en $x < \dfrac{1}{4 M \varrho}$ de verschillende termen van de linkerleden van (27) kleiner zijn dan een willekeurig klein gekozen getal ε_1, terwijl dan $\overline{R}_1(x, y)$ en $\overline{R}_2(x, y)$ kleiner zijn dan $\bar{\varepsilon}$.

Hiermede is aangetoond, dat de functies $z(x, y)$ bepaald volgens (25), voldoen aan de partiële differentiaalvergelijkingen (4*a*) en (4*b*).

3e. Ten slotte is nog te bewijzen, dat de functie $z(x, y)$ nadat de functies u_0, u_1, u_2 enz. zijn uitgedrukt in $z(0, y)$, $\left(\dfrac{\partial z}{\partial x}\right)_{x=0}$ en haar afgeleiden naar y, eveneens aan (1) voldoet. De algemene term van de z reeks, die verkregen wordt door $u_{n-1}^{(1)}$ te elimineren, is door (13) aangegeven. Ook nu substitueren wij in (1):

$$z = z_0 + z_1 + z_2 + \ldots + z_n + R_{n+1}.$$

Bij de herleiding wordt dan gebruik gemaakt van (15) en (15*a*), terwijl

$$\frac{\partial z_0}{\partial x} = \frac{\partial^2 z_0}{\partial x^2} = \frac{\partial^2 z_0}{\partial x\, \partial y} = 0.$$

De formule (15) wordt dan toegepast voor $n = 2, 3,$ enz.

Na de herleiding wordt gevonden:

$$\left.\begin{aligned}&\frac{\partial^2 R_{n+1}}{\partial x^2}+b\,\frac{\partial^2 R_n}{\partial x\,\partial y}+a\,\frac{\partial^2 R_{n-1}}{\partial y^2}+c\,\frac{\partial R_{n+1}}{\partial x}+d\,\frac{\partial R_n}{\partial y}+\\&+e\,R_n-\gamma_1\frac{\partial z_n}{\partial x}-\left(\alpha\,\frac{\partial\beta_2}{\partial y}+\alpha\gamma_2\right)\frac{\partial z_{n-1}}{\partial y}-\alpha\,\frac{\partial\gamma_2}{\partial y}\,z_{n-1}=\overline{R}(x,y).\end{aligned}\right\}\quad(28)$$

Ook nu is weer gemakkelijk aan te tonen, dat een getal N te bepalen is, zodat voor $n>N$, $R(x,y)<\varepsilon$. Ieder der termen van het linkerlid van (28) is nl. willekeurig klein te maken.

Zo is bijvoorbeeld:

$$\left|\frac{\partial^2 R_{n+1}}{\partial x^2}\right|<\varrho^n M^{n+1}\frac{x^{n-2}}{(n-2)!}\left[\sum_{p=1}^{\infty}(4\varrho Mx)^p\left(1+\frac{p}{n}\right)\left(1+\frac{p}{n-1}\right)\right]\cdot$$
$$\cdot\,\Sigma\,k!\,l_1!\ldots l_n!$$

waarbij weer $k+l_1+\ldots\ldots+l_n\leq n$; terwijl voor

$$\left|a\,\frac{\partial^2 R_{n-1}}{\partial y^2}\right|\quad\text{en}\quad\left|b\,\frac{\partial^2 R_n}{\partial x\,\partial y}\right|$$

analoge uitdrukkingen gelden.

De functie $z(x,y)$ voldoet dus aan (1) en de gestelde randwaarden, hetgeen aangetoond moest worden.

Mathematics. — *Note on a certain class of Banach spaces.* By A. C. ZAANEN. (Communicated by Prof. W. VAN DER WOUDE.)

(Communicated at the meeting of April 23, 1949.)

1. *Introduction.* The abstract theory of Banach space is usually illustrated by examples from the functionspaces $L_p(\triangle)$, $1 \leqslant p \leqslant \infty$, where, for $1 \leqslant p < \infty$, $L_p(\triangle)$ is the class of all LEBESGUE-measurable, complex-valued functions $f(x)$ such that $|f(x)|^p$ is summable over the interval $\triangle$ (one- or more-dimensional, finite or infinite), and where $L_\infty(\triangle)$ is the class of all measurable, complex-valued functions $f(x)$ such that $|f(x)|$ is bounded almost everywhere in $\triangle$. ORLICZ [1] (cf. also [2]), in 1932, introduced the class of functionspaces $L_\Phi(\triangle)$, which contains the spaces $L_p(\triangle)$ as special cases for $1 < p < \infty$, but not for $p = 1$ and $p = \infty$. Shortly, the definition of the space $L_\Phi(\triangle)$ runs as follows: Let $\varphi(\bar{u})$, $\bar{u} \geqslant 0$, $\psi(\bar{v})$, $\bar{v} \geqslant 0$, be two continuous functions, vanishing at the origin, strictly increasing, tending to infinity, and inverse to each other. Then, for u and $v \geqslant 0$, we have YOUNG's inequality [3]

$$u v \leqslant \Phi(u) + \Psi(v), \text{ where } \Phi(u) = \int_0^u \varphi(\bar{u})\, d\bar{u},\ \Psi(v) = \int_0^v \psi(\bar{v})\, d\bar{v}.$$

By $L_\Phi^*(\triangle)$ we mean the class of all complex, measurable functions $f(x)$ in $\triangle$, for which $\Phi|f(x)|$ is summable over $\triangle$, and the class $L_\Psi^*(\triangle)$ is introduced similarly. The space $L_\Phi(\triangle)$ is now defined to consist of all complex, measurable functions $f(x)$ in $\triangle$, such that $f(x)\, g(x)$ is summable over $\triangle$ for every $g(x) \in L_\Psi^*(\triangle)$, and the norm $\|f\|_\Phi$ is defined by

$$\|f\|_\Phi = \text{l.u.b.} \left|\int_\triangle f(x)\, g(x)\, dx\right| \text{ for all } g(x) \text{ with } \int_\triangle \Psi|g|\, dx \leqslant 1.$$

The space $L_\Psi(\triangle)$ is introduced similarly. (The notations used here differ slightly from those in [1] and [2]). It is proved then that $L_\Phi(\triangle)$ and $L_\Psi(\triangle)$, thus defined, are Banach spaces, that is, normed complete vectorspaces. Obviously, by YOUNG's inequality, L_Φ^* is contained in L_Φ. The case that $\Phi(2u) \leqslant C\, \Phi(u)$ for all $u \geqslant 0$ and a fixed positive constant C deserves special attention, because in this case L_Φ and L_Φ^* (but not necessarily L_Ψ and L_Ψ^*) are identical. Recently the present author [4] has proved, under this additional condition, that L_Φ is separable and that every bounded linear functional $F(f)$ in L_Φ is of the form

$$F(f) = \int_\triangle f(x)\, g(x)\, dx,$$

where $g(x) \in L_\Psi$ and $\frac{1}{2}\|g\|_\Psi \leqslant \|F\| \leqslant \|g\|_\Psi$. It is easily verified that

for $\varphi(\bar{u}) = \bar{u}^{p-1}$ $(1 < p < \infty)$, hence $\Phi(u) = u^p/p$, the space $L_\Phi(\triangle)$ is identical with the space $L_p(\triangle)$, and that

$$\|f\|_\Phi = q^{1/q}\,\|f\|_p, \text{ where } 1/p + 1/q = 1, \quad \|f\|_p = (\int_\triangle |f|^p\,dx)^{1/p}.$$

It will be felt as a defect, both of aesthetical and practical nature, that the spaces $L_p(\triangle)$, $p = 1$ and $p = \infty$, are excluded in this way from the class of spaces $L_\Phi(\triangle)$, so that, to obtain completeness, these "boundarycases" would need a separate treatment. It is our purpose to show here that with some care, altering some of the mentioned definitions and revising or supplementing some proofs, these exceptional cases may be included into the general theory of spaces $L_\Phi(\triangle)$. The principal change is that we no longer suppose the function $\varphi(\bar{u})$ to be continuous, strictly increasing and tending to infinity, but merely to be non-decreasing.

2. YOUNG's *inequality*. Let $v = \varphi(u)$, $u \geq 0$, be non-decreasing, $\varphi(0) = 0$. Then, for every $u > 0$, the number $\varphi(u-)$ exists; the same is true, for every $u \geq 0$, of the number $\varphi(u+)$, and $\varphi(u-) \leq \varphi(u) \leq \varphi(u+)$, if we define $\varphi(0-) = \varphi(0) = 0$. At those values of u where $\varphi(u-) = \varphi(u+)$, the function $\varphi(u)$ is continuous; at those values of u where $\varphi(u-) < \varphi(u+)$, we say that $\varphi(u)$ has a jump from $\varphi(u-)$ to $\varphi(u+)$. It is well-known that for any $u_0 \geq 0$ the set of values $u \leq u_0$ at which $v = \varphi(u)$ has a jump is at most enumerably infinite.

We shall suppose now that $v = \varphi(u)$ is continuous from the left, hence $\varphi(u) = \varphi(u-)$ for every $u \geq 0$. (This is no loss of generality since we are ultimately interested in $\int_0^u \varphi(\bar{u})\,d\bar{u}$, and not in $\varphi(u)$ itself). By $u = \psi(v)$ the inverse function is defined, with this understanding that if $\varphi(u)$ makes a jump at $u = a$, then $\psi(v) = a$ for $\varphi(a-) < v \leq \varphi(a+)$, while, if $\varphi(u) = c$ for $a < u \leq b$ (but $\varphi(u) < c$ for $u < a$), then $\psi(c) = a$. Furthermore $\psi(0) = 0$ and, if $\lim\limits_{u \to \infty} \varphi(u) = l$ is finite, then $\psi(v) = +\infty$ for $v > l$. Thus defined, $u = \psi(v)$ is evidently a non-decreasing function of v for $v \geq 0$, and continuous from the left for those v for which $\psi(v) < \infty$. We observe that $v = \varphi(u)$ implies $u \geq \psi(v) = \psi(v-)$, and $u = \psi(v)$ implies $v \geq \varphi(u) = \varphi(u-)$ for finite u.

Lemma 1. *If* $v < \varphi(u)$ *for a point* (u, v) *in the* uv*-plane, then* $u > \psi(v)$. *If* $v > \varphi(u)$, *then* $u \leq \psi(v)$.

Proof. From $v < \varphi(u)$ follows $v + p = \varphi(u)$ for a positive p, hence $u \geq \psi(v + p) \geq \psi(v)$. But $u = \psi(v)$ is impossible, for then $v \geq \varphi(u)$ in contradiction with the hypothesis. Hence $u > \psi(v)$.

Let now $v > \varphi(u) = \varphi(u-)$. If $v \leq \varphi(u+)$, then $u = \psi(v)$ by definition. If $v > \varphi(u+)$, then $v - p = \varphi(u+)$ for a positive p, hence

$$u = \psi(v - p) \leq \psi(v).$$

This completes the proof.

On account of this lemma we may now divide the quadrant $u \geqslant 0$, $v \geqslant 0$ into four sets E_1, E_2', E_2'' and E_3, where

E_1 consists of all points (u, v) such that $v < \varphi(u)$, hence $u > \psi(v)$,
E_2' consists of all points (u, v) such that $v = \varphi(u)$,
E_2'' consists of all points (u, v) such that $v > \varphi(u)$ and $u = \psi(v)$,
E_3 consists of all points (u, v) such that $v > \varphi(u)$ and $u < \psi(v)$.

The set $E_2 = E_2' + E_2''$ consists therefore of all points (u, v) for which one at least of the relations $v = \varphi(u)$ and $u = \psi(v)$ is satisfied.

Lemma 2. *The sets E_1 and E_3 are open (relative to the quadrant $u \geqslant 0$, $v \geqslant 0$), so that the complementary set E_2 is closed.*

Proof. Suppose that $(u_0, v_0) \in E_1$, hence $v_0 < \varphi(u_0)$ or $v_0 = \varphi(u_0) - 2p$, where p is positive. Since $\varphi(u_0) = \varphi(u_0 -)$, there exists a positive number δ such that $\varphi(u) > \varphi(u_0) - p$ if only $u \geqslant u_0 - \delta$. In the rectangle $|u - u_0| \leqslant \delta$, $|v - v_0| \leqslant p$ (inasfar as this rectangle is contained in the quadrant $u \geqslant 0$, $v \geqslant 0$), we have now $v \leqslant v_0 + p = \varphi(u_0) - p < \varphi(u)$, which shows that this rectangle belongs to E_1. If $(u_0, v_0) \in E_3$, the proof is similar.

Lemma 3. *Let, for arbitrary $u_0 > 0$, $v_0 > 0$, the closed interval $[0, u_0;\ 0, v_0]$ be denoted by $\triangle$. Then the measure of the productset $\triangle \cdot E_2$ satisfies $m(\triangle \cdot E_2) = 0$.*

Proof. Since $\triangle \cdot E_2$ is bounded and closed, it is measurable. If $c(u, v)$ is its characteristic function, we have therefore by FUBINI's theorem

$$m(\triangle \cdot E_2) \int_{\triangle} c(u, v)\, du\, dv = \int_0^{u_0} du \int_0^{v_0} c(u, v)\, dv = 0,$$

because the inner integral can differ from zero only for those values of u at which $\varphi(u)$ has a jump, so that it vanishes almost everywhere in $[0, u_0]$.

Definition. *If the non-decreasing functions $v = \varphi(u)$ and $u = \psi(v)$, inverse to each other, satisfy the above conditions, then*

$$\Phi(u) = \int_0^u \varphi(\bar{u})\, d\bar{u}, \quad \Psi(v) = \int_0^v \psi(\bar{v})\, d\bar{v},$$

defined for $u \geqslant 0$, $v \geqslant 0$, are called complementary in the sense of YOUNG.

Theorem (YOUNG's *inequality*). *If $\Phi(u)$ and $\Psi(v)$ are complementary in the sense of* YOUNG, *then*

$$uv \leqslant \Phi(u) + \Psi(v)$$

for arbitrary $u, v \geqslant 0$, where equality holds if and only if one at least of the relations $v = \varphi(u)$ and $u = \psi(v)$ is satisfied.

Proof. The geometrical meaning of the theorem is evident, which does not mean that no proof is necessary.

Let $u_0 \geqq 0$, $v_0 \geqq 0$ be given, and denote the interval $[0, u_0; 0, v_0]$ by $\triangle$. Then, using the same notations as before, we have by Lemma 3

$$u_0 v_0 = m(\triangle) = m(\triangle \cdot E_1) + m(\triangle \cdot E_2) + m(\triangle \cdot E_3) =$$
$$m(\triangle \cdot E_1) + m(\triangle \cdot E_3) = \int_\triangle d(u, v)\, du\, dv + \int_\triangle e(u, v)\, du\, dv,$$

where $d(u, v)$ and $e(u, v)$ are the characteristic functions of the measurable sets $\triangle \cdot E_1$ and $\triangle \cdot E_3$. Now, by FUBINI's theorem,

$$\int_\triangle d(u, v)\, du\, dv = \int_0^{u_0} du \int_0^{v_0} d(u, v)\, dv = \int_0^{u_0} du \int_0^{m(u)} dv,$$

where $m(u) = \min[v_0, \varphi(u)]$; hence

$$\int_\triangle d(u, v)\, du\, dv \leqq \int_0^{u_0} du \int_0^{\varphi(u)} dv = \int_0^{u_0} \varphi(u)\, du = \Phi(u_0),$$

with equality if and only if $v_0 \geqq \varphi(u_0)$. In the same way

$$\int_\triangle e(u, v)\, du\, dv \leqq \Psi(v_0),$$

with equality if and only if $u_0 \geqq \psi(v_0)$. Hence

$$u_0 v_0 \leqq \Phi(u_0) + \Psi(v_0),$$

with equality if and only if $v_0 \geqq \varphi(u_0)$, $u_0 \geqq \psi(v_0)$ hold simultaneously. But, since $v_0 > \varphi(u_0)$, $u_0 > \psi(v_0)$ are incompatible by Lemma 1, this means that one at least of the relations $v = \varphi(u)$ and $u = \psi(v)$ must be satisfied in the case of equality.

Remark. If $v = \varphi(u) = u^{p-1}$ $(1 < p < \infty)$, $1/p + 1/q = 1$, YOUNG's inequality takes the form $u\, v \leqq u^p/p + v^q/q$, with equality if and only if $v = u^{p-1}$.

3. *The space L_Φ.* Let $\triangle$ be a finite or infinite interval in the m-dimensinal Euclidean space R_m $(m \geqq 1)$, and let $\Phi(u)$, $\Psi(v)$ be complementary in the sense of YOUNG, such that $\Phi(u)$ does not vanish identically (equivalent with assuming that $\varphi(u)$ does not vanish identically). It is easy to see that if $f(x)$ is measurable in $\triangle$, then $\varphi|f(x)|$ is also measurable in $\triangle$. Indeed, with every number $a \geqq 0$ corresponds a number $b \geqq 0$ such that $\varphi(u) \leqq a$ holds if and only if $u \leqq b$. In the same way it is seen that $\psi|f(x)|$, $\Phi|f(x)|$ and $\Psi|f(x)|$ are measurable in $\triangle$.

Definition. *By $L^*_\Phi(\triangle)$ we shall mean the class of all complex, measurable functions $f(x)$ on $\triangle$, for which $\Phi|f(x)|$ is summable over $\triangle$. The class $L^*_\Psi(\triangle)$ is defined similarly.*

Remark. If $\Phi(u) = c\, u^p$ $(c > 0,\ p \geqq 1)$, the class $L^*_\Phi(\triangle)$ is identical with $L_p(\triangle)$. For $p > 1$ the complementary class $L^*_\Psi(\triangle)$ is identical with

$L_q(\triangle)$, where $1/p+1/q=1$, and for $p=1$ the class $L^*_\Psi(\triangle)$ consists of all measurable functions for which $|f(x)|\leqslant c$ holds almost everywhere in $\triangle$ (since in this case $\Psi(v)=0$ in $0\leqslant v\leqslant c$, $\Psi(v)=\infty$ for $v>c$).

The classes $L^*_\Phi(\triangle)$ and $L^*_\Psi(\triangle)$ are, as a rule, not linear, that is, the summability of $\Phi|f_1|$ and $\Phi|f_2|$ does not necessarily imply the summability of $\Phi|f_1+f_2|$. For this reason, linear classes $L_\Phi(\triangle)$ and $L_\Psi(\triangle)$ are defined, containing $L^*_\Phi(\triangle)$ and $L^*_\Psi(\triangle)$ as subclasses.

Definition. *By $L_\Phi(\triangle)$ we shall mean the class of all complex, measurable functions $f(x)$ on $\triangle$, such that $f(x)\,g(x)$ is summable over $\triangle$ for every $g(x)\in L^*_\Psi(\triangle)$, and such that*

$$\|f\|_\Phi=\text{l.u.b.}\left|\int_\triangle f(x)\,g(x)\,dx\right| \text{ for all } g(x) \text{ with } \int_\triangle \Psi|g|\,dx\leqslant 1$$

is finite.

The complementary class $L_\Psi(\triangle)$ is defined similarly.

Remark. It will be seen in what follows (Theorem 5) that $\|f\|_\Phi<\infty$ is automatically satisfied if only $f(x)\,g(x)$ is summable for every $g\in L^*_\Psi$.

Theorem 1. *The class L_Φ is linear and contains L^*_Φ as a subclass. For $f_1, f_2\in L_\Phi$ the inequality $\|f_1+f_2\|_\Phi\leqslant\|f_1\|_\Phi+\|f_2\|_\Phi$ holds. For $f\in L^*_\Phi$ we have $\|f\|_\Phi\leqslant\int_\triangle\Phi|f|\,dx+1$. Furthermore $\|f\|_\Phi=0$ if and only if $f(x)=0$ almost everywhere in $\triangle$. A similar theorem holds for L_Ψ.*

Proof. The only statement which is not immediately evident is that $\|f\|_\Phi=0$ implies $f(x)=0$ almost everywhere in $\triangle$. We observe first that we might have defined $\|f\|_\Phi$ as well by

$$\|f\|_\Phi=\text{l.u.b.}\int_\triangle|fg|\,dx \text{ for all } g(x) \text{ with } \int_\triangle\Psi|g|\,dx\leqslant 1.$$

If $\|f\|_\Phi=0$, we have therefore $f(x)\,g(x)=0$ almost everywhere in $\triangle$ for every $g(x)$ with $\int_\triangle\Psi|g|\,dx\leqslant 1$. Since we have supposed that $\varphi(u)$ does not vanish identically, there exist positive u_0, v_0 such that $v_0=\varphi(u_0)$, hence $u_0\geqslant\psi(v_0)$, so that $\psi(v)\leqslant u_0$ for $v\leqslant v_0$. It follows that $\Psi(v)\leqslant u_0 v$ for $v\leqslant v_0$ or $\lim_{v\to 0}\Psi(v)=0$. If therefore $\triangle_1$ is an arbitrary finite subinterval of $\triangle$ with measure $m(\triangle_1)$, there exists a positive number p such that $\Psi(p)\leqslant 1/m(\triangle_1)$. Taking now $g(x)=p$ for $x\in\triangle_1$ and $g(x)=0$ elsewhere, we have $\int_\triangle\Psi|g|\,dx=\int_{\triangle_1}\Psi(p)\,dx\leqslant 1$, so that, on account of $f(x)\,g(x)=0$, also $f(x)=0$ almost everywhere in $\triangle_1$. Hence $f(x)=0$ almost everywhere in $\triangle$.

Theorem 2. *If $f(x)\in L_\Phi$, and $\|f\|_\Phi\neq 0$, then*

$$\int_\triangle\Phi\left[|f|/\|f\|_\Phi\right]dx\leqslant 1.$$

A similar theorem holds for any $g(x)\in L_\Psi$.

Proof. As in [2], we observe that $\Psi(qv) \geqslant q\,\Psi(v)$ or $\Psi(v) \leqslant \Psi(qv)/q$ for $q \geqslant 1$ and every $v \geqslant 0$, which is easily proved. Supposing now that $f \in L_\Phi$ and $g \in L_\Psi^*$, we have $\int_\triangle |fg|\,dx \leqslant \|f\|_\Phi$ if $\varrho(g) = \int_\triangle \Psi|g|\,dx \leqslant 1$. If $\varrho(g) > 1$, then $\int_\triangle \Psi|g/\varrho(g)|\,dx \leqslant \int_\triangle \Psi|g|/\varrho(g)\,dx = 1$, hence $\int_\triangle |fg|\,dx \leqslant \|f\|_\Phi \cdot \varrho(g)$. We conclude therefore that

$$\int_\triangle |fg|/\|f\|_\Phi\,dx \leqslant \varrho'(g) = \max[\varrho(g), 1].$$

In the case that $f(x)$ is bounded on $\triangle$ and $\triangle$ is finite, both functions $\Phi[|f|/\|f\|_\Phi]$ and $\Psi[\varphi\{|f|/\|f\|_\Phi\}]$ are bounded on $\triangle$ (observe in particular that this is also true in the case that $\lim\limits_{u\to\infty} \varphi(u)$ is finite), and therefore summable over $\triangle$; hence

$$\varrho'(g) \geqslant \int_\triangle |fg|/\|f\|_\Phi\,dx = \int_\triangle \Phi[|f|/\|f\|_\Phi]\,dx + \varrho(g),$$

where $g = \varphi\{|f|/\|f\|_\Phi\}$, so that YOUNG's inequality becomes an equality. The result follows now.

Supposing now $\triangle$ to be still finite but $f(x)$ no longer to be bounded, we put $f_n(x) = f(x)$ if $|f(x)| \leqslant n$ and $f_n(x) = 0$ elsewhere $(n = 1, 2, \ldots)$. Then the non-decreasing sequence of bounded functions $|f_n(x)|$ converges to $|f(x)|$. It is easily seen that $\|f_n\|_\Phi \leqslant \|f\|_\Phi$ for every n, hence $\int_\triangle \Phi[|f_n|/\|f\|_\Phi]\,dx \leqslant 1$ for every n, so that

$$\int_\triangle \Phi[|f|/\|f\|_\Phi]\,dx = \lim \int_\triangle \Phi[|f_n|/\|f\|_\Phi]\,dx \leqslant 1.$$

The extension to infinite $\triangle$ is similar.

Let us suppose now that $g \in L_\Psi$. If $\Psi(v) < \infty$ for all $v < \infty$ (which is equivalent with $\lim\limits_{u\to\infty} \varphi(u) = \infty$), the proof of $\int_\triangle \Psi[|g|/\|g\|_\Psi]\,dx \leqslant 1$ offers no new aspects. If however $\lim\limits_{u\to\infty} \varphi(u) = l < \infty$, we observe first that $|g(x)|/\|g\|_\Psi \leqslant l$ almost everywhere in $\triangle$. Indeed, if $|g(x)| > l\,\|g\|_\Psi$ on a set $E \subset \triangle$ of positive measure $m(E)$, we may put $f(x) = [l \cdot m(E)]^{-1}$ in E and $f(x) = 0$ elsewhere. Then, on account of $\Phi(u) \leqslant l\,u$,

$$\int_\triangle \Phi|f|\,dx = \Phi[l \cdot m(E)]^{-1} \cdot m(E) \leqslant 1,$$

but

$$\int_\triangle |fg|\,dx = \int_E |g|\,dx/[l \cdot m(E)] > \|g\|_\Psi,$$

which is a contradiction. Supposing now $\triangle$ to be finite, and choosing the arbitrary but fixed number δ such that $0 < \delta < 1$, we see that both $\Psi[\delta|g|/\|g\|_\Psi]$ and $\Phi|f|$, where $f = \psi\{\delta|g|/\|g\|_\Psi\}$, are bounded and therefore summable over $\triangle$. Hence, if $\varrho(f) = \int_\triangle \Phi|f|\,dx$ and $\varrho'(f) = \max\,[\varrho(f), 1]$, $\delta\varrho'(f) \geqslant \int_\triangle |\delta g f|/\|g\|_\Psi\,dx = \int_\triangle \Psi[\delta|g|/\|g\|_\Psi]\,dx + \varrho(f)$,

so that, since $\varrho'(f)=1$ on account of $\varrho(f)\leqslant\delta\varrho'(f)<\varrho'(f)$, we have $\int\limits_{\triangle}\Psi[\delta|g|/\|g\|_{\Psi}]\,dx\leqslant\delta<1$. Making δ tend to 1, we obtain the desired result. The extension to an infinite interval is now evident.

Corollary. *If there exists a constant* $C>0$ *such that* $\Phi(2u)\leqslant C\,\Phi(u)$ *for all* $u\geqslant 0$, *the classes* L_{Φ}^{*} *and* L_{Φ} *are identical.*

Theorem 3. *If* $L_{\Phi}(\triangle)$ *and* $L_{\Psi}(\triangle)$ *are complementary,* $f\in L_{\Phi}$, $g\in L_{\Psi}$, *then* fg *is summable over* $\triangle$ *and*

$$\Big|\int\limits_{\triangle} fg\,dx\Big|\leqslant\int\limits_{\triangle}|fg|\,dx\leqslant\|f\|_{\Phi}\cdot\|g\|_{\Psi}.$$

Proof. If $\|g\|_{\Psi}=0$, then $|\int\limits_{\triangle} fg\,dx|=0$; we may suppose therefore that $\|g\|_{\Psi}\neq 0$. If $f\in L_{\Phi}$, then fg is summable over $\triangle$ for every $g\in L_{\Phi}^{*}$ by definition, so that $fg/\|g\|_{\Psi}$ is summable for every $g\in L_{\Psi}$. But then fg is summable as well. Furthermore

$$\Big|\int\limits_{\triangle} fg\,dx\Big|\leqslant\int\limits_{\triangle}|fg|\,dx=\int\limits_{\triangle}|fg|/\|g\|_{\Psi}\,dx\cdot\|g\|_{\Psi}\leqslant\|f\|_{\Phi}\cdot\|g\|_{\Psi},$$

since $\int\limits_{\triangle}\Psi[|g|/\|g\|_{\Psi}]\,dx\leqslant 1$.

Remark. If $\Phi(u)=c\,u^{p}$ $(c>0,\ 1\leqslant p<\infty)$, then $\Phi(2u)=2^{p}\,\Phi(u)$ for every $u\geqslant 0$, hence $L_{\Phi}(\triangle)\equiv L_{\Phi}^{*}(\triangle)\equiv L_{p}(\triangle)$. For $1<p<\infty$ the complementary class $L_{\Psi}(\triangle)$ is indentical with $L_{q}(\triangle)$, where $1/p+1/q=1$. For $p=1$, $L_{\Psi}(\triangle)\equiv L_{\infty}(\triangle)$, the class of all measurable functions bounded almost everywhere in $\triangle$. Indeed, if $g\in L_{\Psi}(\triangle)$, we have already seen in the proof of Theorem 2 that $|g(x)|/\|g\|_{\Psi}\leqslant c$ almost everywhere in $\triangle$, hence $g\in L_{\infty}(\triangle)$. Conversely, if $g\in L_{\infty}(\triangle)$, we have $|p\,g(x)|\leqslant c$ almost everywhere in $\triangle$ for some suitable positive p, hence $p\,g(x)\in L_{\Psi}^{*}(\triangle)$ or $g\in L_{\Psi}(\triangle)$.

Considering the particular case that $\Phi(u)=u^{p}/p\ (1<p<\infty)$, so that $\Psi(v)=v^{q}/q$, where $1/p+1/q=1$, we have

$$\|f\|_{\Phi}=\text{l.u.b.}\Big|\int\limits_{\triangle} fg\,dx\Big|\ \text{ for all } g(x) \text{ with } \int\limits_{\triangle}|g|^{q}\,dx\leqslant q,$$

$$\|f\|_{p}=\Big(\int\limits_{\triangle}|f|^{p}\,dx\Big)^{1/p}=\max\Big|\int\limits_{\triangle} fg\,dx\Big|\ \text{ for all } g(x) \text{ with } \int\limits_{\triangle}|g|^{q}\,dx\leqslant 1,$$

hence $\|f\|_{\Phi}=q^{1/q}\,\|f\|_{p}$. For $p=1$ we find in a similar way

$$\|f\|_{\Phi}=\|f\|_{1}=\int\limits_{\triangle}|f|\,dx \ \text{ and } \ \|f\|_{\Psi}=\|f\|_{\infty},$$

where $\|f\|_{\infty}$ is the number uniquely determined by $|f(x)|\leqslant\|f\|_{\infty}$ almost everywhere in $\triangle$ and $|f(x)|>\|f\|_{\infty}-\varepsilon$ for every $\varepsilon>0$ on a set of positive measure.

Theorem 4. *The functionspaces* $L_{\Phi}(\triangle)$ *and* $L_{\Psi}(\triangle)$ *are complete; in other words, pronounced for* L_{Φ}, *if* $f_{n}(x)\in L_{\Phi}\ (n=1,2,\ldots)$ *and* $\lim\|f_{n}-f_{m}\|_{\Phi}=0$ *as* $m,n\to\infty$, *there exists a function* $f(x)\in L_{\Phi}$ *such*

that $\lim \|f_n - f\|_\Phi = 0$. *This function* $f(x)$ *is uniquely determined apart from sets of measure zero.*

Proof. As in [2].

Theorem 5. *If the complex, measurable function* $f(x)$, *defined on the finite or infinite interval* $\triangle$, *has the property that* $f(x)\,g(x)$ *is summable over* $\triangle$ *for every* $g(x) \in L^*_\Psi(\triangle)$, *then* $f(x) \in L_\Phi(\triangle)$. *In the same way* $g(x) \in L_\Psi(\triangle)$ *if only* $f(x)\,g(x)$ *is summable for every* $f(x) \in L^*_\Phi(\triangle)$.

Proof. We have to show that $\|f\|_\Phi = \text{l.u.b.}\,|\int\limits_\triangle fg\,dx|$ for all $g(x)$ with $\int\limits_\triangle \Psi\,|g|\,dx \leqq 1$, is finite. We observe first that $f(x)\,g(x)$ is also summable over $\triangle$ for every $g(x) \in L_\Psi$. Putting now $f_n(x) = f(x)$ $(n = 1, 2, \ldots)$ whenever $|f(x)| \leqq n$ and $x \in \triangle \cdot \triangle_n$, where $\triangle_n$ is the interval $[-n, n; \ldots; -n, n]$, while $f_n(x) = 0$ elsewhere, we have $f_n(x) \in L_\Phi(\triangle)$ and $\lim f_n(x) = f(x)$. The functional $T_n(g) = \int\limits_\triangle f_n(x)\,g(x)\,dx$ is therefore a bounded linear functional in $L_\Psi(\triangle)$ as may be seen from $|T_n(g)| \leqq \|f_n\|_\Phi \cdot \|g\|_\Psi$. Furthermore the sequence $T_n(g)$ $(n = 1, 2, \ldots)$ is bounded for every $g \in L_\Psi$, as follows from $\lim \int\limits_\triangle f_n\,g\,dx = \int\limits_\triangle fg\,dx$, since $\lim f_n\,g = fg$, $|f_n\,g| \leqq |fg|$ and $|fg|$ is summable. Hence, by the BANACH—STEINHAUS theorem, $|T_n(g)| \leqq M\,\|g\|_\Psi$ for a fixed M. Taking now $g(x)$ such that $\int\limits_\triangle \Psi\,|g|\,dx \leqq 1$, so that $\|g\|_\Psi \leqq 2$, we have therefore $|\int\limits_\triangle f_n(x)\,g(x)\,dx| = |T_n(g)| \leqq 2\,M$, hence also $|\int\limits_\triangle f(x)\,g(x)\,dx| \leqq 2\,M$. This shows that $\|f\|_\Phi \leqq 2\,M$.

The proof that $g \in L_\Psi$ if only fg is summable for every $f \in L^*_\Phi$, is similar. The crucial part is that the functions $g_n(x)$, equal to $g(x)$ for $|g(x)| \leqq n$ and $x \in \triangle \cdot \triangle_n$, and zero elsewhere, all belong to $L_\Psi(\triangle)$, even if $\lim\limits_{u \to \infty} \varphi(u) = l < \infty$.

4. *Concluding remarks.* If $\Phi(2\,u) \leqq C\,\Phi(u)$ for every $u \geqq 0$ and a fixed $C > 0$, the space $L_\Phi(\triangle)$ is separable and every bounded linear functional $F(f)$ in $L_\Phi \triangle$ is of the form $F(f) = \int\limits_\triangle f(x)\,g(x)\,dx$, where $g(x) \in L_\Psi(\triangle)$ and $\frac{1}{2}\,\|g\|_\Psi \leqq \|F\| \leqq \|g\|_\Psi$. For the proofs we refer to [4], as well as for the application of these facts to integral equations in L_Φ. (We permit ourselves however one remark. In the cited paper the interval $\triangle$ is the linear interval $[a, b]$, and, if $F(f)$ is a bounded linear functional in $L_\Phi(\triangle)$, it is proved first that $F(\xi_x) = G(x)$ is an absolutely continuous function, where ξ_x is the characteristic function of $[a, x]$. The derivative $G'(x) = g(x)$ exists therefore almost everywhere in $[a, b]$ and $F(\xi_x) = G(x) = \int\limits_a^x g(u)\,du = \int\limits_a^b \xi_x(u)\,g(u)\,du$. The analogous fact in the case of a moredimensional, possibly infinite interval $\triangle$ is

proved as follows: Letting $f(x)$ run through the characteristic functions of all measurable sets X contained in a finite interval $\triangle_1 \subset \triangle$, it is proved that $F(f)$ is an additive, absolutely continuous function of a set X on $\triangle_1$, so that, by the RADON—NIKODYM theorem (cf. [5], Ch. I, § 14), there exists a summable function $g(x)$ in $\triangle_1$ such that

$$F(f) = \int_X g(x)\,dx = \int_{\triangle_1} f(x)\,g(x)\,dx.$$

Since $\triangle$ may be considered as a sum of finite intervals, $g(x)$ may be extended to the whole of $\triangle$ and $F(f) = \int_{\triangle} f(x)\,g(x)\,dx$ holds for the characteristic function of any finite measurable set contained in $\triangle$).

We finally mention some other applications (variations upon examples from [6], Ch. 12).

1. If $f_n(x)$ $(n = 1, 2, \ldots)$ is measurable on the finite interval $\triangle$, and $|f_n(x)| \leqslant C$, $f(x) = \lim f_n(x)$ for $x \in \triangle$, then $\lim \int_{\triangle} \Phi |f - f_n|\,dx = 0$. The same holds with Φ replaced by Ψ, provided $\Psi(v) < \infty$ for $v \leqslant 2C$.

2. If $f_n(x) \in L_\Phi(\triangle)$, $f(x) \in L_\Phi(\triangle)$, $\lim \|f - f_n\|_\Phi = 0$, and $g(x) = \lim f_n(x)$ almost everywhere in $\triangle$, then $f(x) = g(x)$ almost everywhere in $\triangle$. A similar statement is true if Φ is replaced by Ψ.

(Observe that $\lim \|f - f_n\|_\Phi = 0$ implies the existence of a subsequence, tending almost everywhere in $\triangle$ to $f(x)$).

3. If $f_n(x)$, $f(x) \in L_\Phi(\triangle)$; $g_n(x)$, $g(x) \in L_\Psi(\triangle)$; $\lim \|f - f_n\|_\Phi = 0$, $\lim \|g - g_n\|_\Psi = 0$, then $\int_{\triangle} fg\,dx = \lim \int_{\triangle} f_n g_n\,dx$.

4. If $\Phi(2u) \leqslant C\,\Phi(u)$ for $u \geqslant 0$, $f(x) \in L_\Phi(\triangle)$ and $\varepsilon > 0$ is given, there is a continuous function $g(x)$ such that $\|f - g\|_\Phi < \varepsilon$.

(There is a stepfunction $h(x)$ such that $\|f - h\|_\Phi < \varepsilon/2$ (cf. [4]), and it is obvious that there is a continuous $g(x)$ such that $\|h - g\|_\Phi < \varepsilon/2$).

5. If $\Phi(2u) \leqslant C\,\Phi(u)$ for $u \geqslant 0$, $f(x) \in L_\Phi(\triangle_1)$ and $\triangle$ is a finite interval contained in the interior of $\triangle_1$, then

$$\lim_{h \to 0} (\|f(x+h) - f(x)\|_\Phi \text{ over } \triangle) = 0.$$

(For continuous $f(x)$ the statement is easy to prove. For non-continuous $f(x)$ we make use of the previous example).

6. If $f(x) \in L_\Phi(R_m)$, where R_m is the whole m-dimensional Euclidean space, and $\triangle_i = [-i, i; \ldots; -i, i]$ $(i = 1, 2, \ldots)$, then $\|f\|_\Phi$ over $R_m = \lim_{i \to \infty} (\|f\|_\Phi$ over $\triangle_i)$.

(Obviously $\|f\|$ over $\triangle_i \leqslant \|f\|$ over R_m. Furthermore, if $\varepsilon > 0$ is given, there exists a function $g(x)$ such that $\int_{R_m} \Psi |g|\,dx \leqslant 1$ and

$\|f\|-\varepsilon<\int_{R_m}|fg|\,dx$. Hence, for i sufficiently large, $\|f\|-\varepsilon<\int_{\Delta_i}|fg|\,dx\leqslant\|f\|$ over Δ_i).

7. It is evident, if E is a measurable set, what $f(x)\in L_\Phi(E)$ means. If E_1 and E_2 are measurable sets having no common points, and $f\in L_\Phi(E_1+E_2)$, then

$$\|f\| \text{ (over } E_1+E_2)\leqslant\|f\| \text{ (over } E_1)+\|f\|$$

(over E_2).

(Put $f=f_1+f_2$, where $f_1=f$ on E_1 and $f_1=0$ on E_2).

8. If $\Phi(2u)\leqslant C\,\Phi(u)$ for $u\geqslant 0$, $f(x)\in L_\Phi(R_m)$ and

$$\Delta_i=[-i,i;\ldots;-i,i]\ (i=1,2,\ldots),$$

then

$$\lim_{i\to\infty}(\|f(x+h)\|_\Phi \text{ over } R_m-\Delta_i)=0,$$

uniformly for all points h having distance $\leqslant 1$ from the origin.

(Denoting $\|f(x)\|$ (over R_m) $=\|f(x+h\|$ (over R_m) simply by $\|f\|$, we have $\int_{R_m}\Phi[|f(x+h)|/\|f\|]\,dx\leqslant 1$; hence, if $\varepsilon>0$ is given,

$$\int_{R_m-\Delta_i}\Phi[|f(x+h)|/\|f\|]\,dx<\varepsilon \text{ for } i\geqslant i_0(\varepsilon),$$

uniformly for all h having distance $\leqslant 1$ from the origin. The result follows now from the fact that $\lim\int_{R_m}\Phi|f_i|\,dx=0$ implies $\lim\|f_i\|_\Phi=0$).

9. If $\Phi(2u)\leqslant C\,\Phi(u)$ for $u\geqslant 0$ and $f(x)\in L_\Phi(R_m)$, then

$$\lim_{h\to 0}\|f(x+h)-f(x)\|_\Phi=0.$$

($\|f(x+h)-f(x)\|\leqslant\|f(x+h)-f(x)\|$ (over Δ_i) $+\|f(x+h)\|$ (over $R_m-\Delta_i$) $+\|f(x)\|$ (over $R_m-\Delta_i$)).

10. If $\Phi(u)$ and $\Psi(v)$ are complementary, $\Phi(2u)\leqslant C\,\Phi(u)$ for $u\geqslant 0$, $f\in L_\Phi(R_m)$, $g\in L_\Psi(R_m)$, then

$$F(t)=\int_{R_m}f(x+t)\,g(x)\,dx$$

is a continuous function of t.

$$(|F(t+h)-F(t)|\leqslant\|f(x+t+h)-f(x+t)\|_\Phi\cdot\|g\|_\Psi).$$

11. If, with the notations of the previous example, also $\Psi(2v)\leqslant C\,\Psi(v)$ for $v\geqslant 0$, the function $F(t)$ satisfies $\lim F(t)=0$ as t tends to infinity.

(In linear space R_1 we may write

$$|F(t)|\leqslant\int_{-\infty}^{-t/2}|f(x+t)g(x)|\,dx+\int_{t/2}^{\infty}|f(x)g(x-t)|\,dx\leqslant A\,\|f\|_\Phi+B\,\|g\|_\Psi,$$

where $\lim A = \lim B = 0$ as $t \to +\infty$. For $t \to -\infty$ the proof is similar. In a space of more dimensions t tends to infinity if and only if one at least of its coordinates tends to $\pm\infty$. If e.g. the first coordinate t_1 tends to $+\infty$, we split $\int_{-\infty}^{\infty} dx_1$ up into $\int_{-\infty}^{-t_1/2} + \int_{-t_1/2}^{\infty}$).

12. If $\Phi(2u) \leqslant C\,\Phi(u)$ for $u \geqslant 0$ and $f(x) \in L_\Phi(-\infty, \infty)$, then

$$F(t) = \int_{-\infty}^{\infty} \frac{f(x)}{1+(x-t)^2}\, dx$$

is a continuous function of t.

(In the proof of Theorem 1 we have seen that there exist positive numbers u_0, v_0 such that $\Psi(v) \leqslant u_0 v$ for $v \leqslant v_0$, hence

$$\int_{-\infty}^{\infty} \Psi[v_0/(1+x^2)]\, dx \leqslant u_0 v_0 \int_{-\infty}^{\infty} dx/(1+x^2),$$

which shows that $1/(1+x^2) \in L_\Psi(-\infty, \infty)$. Hence

$$|F(t+h) - F(t)| \leqslant \int_{-\infty}^{\infty} |f(x+h) - f(x)| / \{1 + (x-t)^2\}\, dx \leqslant$$
$$\leqslant \| f(x+h) - f(x) \|_\Phi \cdot \| 1/(1+x^2) \|_\Psi).$$

REFERENCES.

1. W. ORLICZ, Über eine gewisse Klasse von Räumen vom Typus B, Bull. d, l'Acad. Polonaise, classe A (1932), pp. 207—220.
2. A. ZYGMUND, Trigonometrical Series, 4. 541, Warsaw (1935).
3. W. H. YOUNG, On classes of summable functions and their Fourier series, Proc. of the Royal Soc. (A), vol. 87 (1912), pp. 225—229.
4. A. C. ZAANEN, On a certain class of Banach spaces, Annals of Math., vol. 47 (1946), pp. 654—666.
5. S. SAKS, Theory of the integral, Warsaw (1937).
6. E. C. TITCHMARSH, The theory of functions, Oxford (1932).

University of Indonesia, Bandoeng (Java).

Mathematics. — *A property of a* DIRICHLET *series, representing a function satisfying an algebraic difference-differential equation.* By J. POPKEN. (Communicated by Prof. J. G. VAN DER CORPUT.)

(Communicated at the meeting of April 23, 1949.)

By definition a function $f(s)$ satisfies an algebraic difference-differential equation if there exists a polynomial $F(x_0, x_1, \ldots, x_t) \not\equiv 0$, a set of t real numbers $u_1, u_2, \ldots, u_t$ and a set of t non-negative integers $n_1, n_2, \ldots, n_t$, such that the t systems $(u_1, n_1), (u_2, n_2), \ldots, (u_t, n_t)$ are different and

$$F(s, f^{(n_1)}(s+u_1), \ldots, f^{(n_t)}(s+u_t)) = 0.$$

In this paper we will deduce the following

Theorem: *Let the convergent* DIRICHLET *series* $\sum_{h=1}^{\infty} a_h e^{-\lambda_h s}$, *with non-vanishing coefficients* a_h, *represent a function* $f(s)$ *satisfying an algebraic difference-differential equation. Then there exists a positive number* c, *such that*

$$\lambda_h > h^c \quad \ldots \ldots \ldots \ldots \quad (1)$$

is valid for all but a finite number of values of h.

This theorem can be used to derive the transcendental-transcendency of certain functions. Let us take for example

$$\zeta(s) = \sum_{h=1}^{\infty} e^{-s \log h},$$

then it is clear, that the exponents $\lambda_h = \log h$ in this series do not have the property (1), hence $\zeta(s)$ cannot satisfy an algebraic difference-differential equation; it follows in particular that $\zeta(s)$ is transcendental-transcendent [1]).

In this paper we confine ourselves to DIRICHLET series $\sum_{h=1}^{\infty} a_h e^{-\lambda_h s}$, where the "exponents" λ_h are real numbers with

$$\lambda_1 < \lambda_2 < \lambda_3 < \ldots, \ \lambda_h \to +\infty \ \textit{for} \ h \to \infty.$$

An "empty" sum, i.e. a formal sum with no terms at all, will be equal to zero by definition.

---

[1]) However this proof for HILBERT's theorem on the transcendental-transcendency of the ζ-function is not essentially new, but closely related to OSTROWSKI's proof in the paper cited below.

A well-known theorem of OSTROWSKI [2]) states: Let the convergent DIRICHLET series $\sum_{h=1}^{\infty} a_h e^{-\lambda_h s}$ with non-vanishing coefficients a_h, represent a function, satisfying an algebraic difference-differential equation. Then there exists for the set of all exponents λ_h a finite linear integral basis.

In the same paper of OSTROWSKI we find another result, connected with the foregoing theorem, which will serve us as a basis for the proof of our own theorem:

Lemma 1 [3]): *Let the convergent* DIRICHLET *series* $\sum_{h=1}^{\infty} a_h e^{-\lambda_h s}$, *with all coefficients* a_h *different from zero, represent a function, satisfying an algebraic difference-differential equation. Then there exists a real number* Λ *and a positive integer* N, *such that for sufficiently large values of* h *every number* $\lambda_h + \Lambda$ *is a sum of* N *exponents at most, taken from the sequence* $\lambda_1, \lambda_2, \ldots, \lambda_{h-1}$.

Now for sufficiently large values of h the number $\lambda_h + \Lambda$ is positive, hence the sum mentioned in the lemma is not empty. Putting $\lambda_0 = -\Lambda$ we can give this lemma the following form: *There exists a positive integer* r, *such that*

$$\lambda_h = \lambda_{h_1} + \lambda_{h_2} + \ldots + \lambda_{h_n} + \lambda_0 \text{ for } h \geqq r, \quad \ldots \ldots \quad (2)$$

where $n = n(h)$ *denotes a positive integer* $\leqq N$ *and* $h_1 \geqq h_2 \geqq \ldots \geqq h_n$ *represent positive integers* $< h$.

Evidently

$$\lambda_h > \lambda_{h_1} \geqq \lambda_{h_2} \geqq \ldots \geqq \lambda_{h_n} \geqq \lambda_1.$$

We can take r so large, that

$$\lambda_h \neq 0 \text{ for } h \geqq r. \quad \ldots \ldots \ldots \ldots \quad (3)$$

In order to prove our theorem we first deduce the following

Lemma 2: *Let the conditions of lemma 1 be fulfilled, so that* (2) *holds. Then there exists a positive integer* $H \geqq r$, *such that*

$$\lambda_h^2 \geqq \lambda_{h_1}^2 + \lambda_{h_2}^2 + \ldots + \lambda_{h_n}^2 + \lambda_0^2 \text{ for } h \geqq H.$$

P r o o f. We put

$$|\lambda_0| + N|\lambda_1| = c_1,$$

then it follows $c_1 \geqq 0$ and

$$\lambda_0^2 + N\lambda_1^2 \leqq c_1^2.$$

Let h take the values $r, r+1, r+2, \ldots$, so that

$$\lambda_h = \lambda_{h_1} + \lambda_{h_2} + \ldots + \lambda_{h_n} + \lambda_0.$$

---

[2]) A. OSTROWSKI, Über Dirichletsche Reihen und algebraische Differentialgleichungen. Mathem. Zeitschrift 8, 241—298 (1921), Satz 6, p. 260.

[3]) A. OSTROWSKI, loc. cit. p. 261—262; compare the proof of "Satz 7". OSTROWSKI's notations for h, N and Λ are respectively l, n and Λ_1.

Now we distinguish the following two cases:

1⁰. $n=1$ or $n \geqq 2$, $\lambda_{h_2} \leqq 3c_1$,

2⁰. $n \geqq 2$, $\lambda_{h_2} > 3c_1$.

In the first case the expression

$$\lambda_h - \lambda_{h_1} = \lambda_{h_2} + \lambda_{h_3} + \ldots + \lambda_{h_n} + \lambda_0$$

can take only a finite number of different values; for this is clear for $n=1$, and, if $n \geqq 2$, then the positive integers $n, h_2, h_3, \ldots, h_n$ satisfy

$$n \leqq N, h_n \leqq h_{n-1} \leqq \ldots \leqq h_2,$$

where h_2 is bounded on account of $\lambda_{h_2} \leqq 3c_1$, $\lambda_h \to +\infty$ for $h \to \infty$. Hence the numbers $\lambda_h - \lambda_{h_1}$, being positive, have a positive minimum. It follows the existence of a positive integer $H \geqq r$, such that

$$\lambda_h^2 - \lambda_{h_1}^2 = (\lambda_h + \lambda_{h_1})(\lambda_h - \lambda_{h_1}) > 9Nc_1^2 \text{ if } h \geqq H. \quad . \quad . \quad . \quad (4)$$

Now

$$\lambda_{h_2}^2 + \lambda_{h_3}^2 + \ldots + \lambda_{h_n}^2 \leqq (N-1)(\lambda_1^2 + \lambda_{h_2}^2),$$

on account of

$\lambda_1 \leqq \lambda_{h_n} \leqq \lambda_{h_{n-1}} \leqq \ldots \leqq \lambda_{h_3} \leqq \lambda_{h_2}$; also $\lambda_1 \leqq \lambda_{h_2} \leqq 3c_1$, $\lambda_1^2 \leqq c_1^2$, hence $\lambda_{h_2}^2 \leqq 9c_1^2$,

so that

$$\begin{aligned}\lambda_{h_1}^2 + \lambda_{h_2}^2 + \ldots + \lambda_{h_n}^2 + \lambda_0^2 &\leqq \lambda_{h_1}^2 + \lambda_0^2 + (N-1)\lambda_1^2 + (N-1)\lambda_{h_2}^2 \\ &\leqq \lambda_{h_1}^2 + c_1^2 + 9(N-1)c_1^2 \\ &\leqq \lambda_{h_1}^2 + 9Nc_1^2.\end{aligned}$$

From (4) it follows for $h \geqq H$

$$\lambda_{h_1}^2 + \lambda_{h_2}^2 + \ldots + \lambda_{h_n}^2 + \lambda_0^2 < \lambda_{h_1}^2 + \lambda_h^2 - \lambda_{h_1}^2 = \lambda_h^2,$$

and the assertion of our lemma is true in the considered case.

If, on the other hand, $n \geqq 2$, $\lambda_{h_2} > 3c_1$, then we denote the positive exponents in the right-hand member of $\lambda_h = \lambda_{h_1} + \lambda_{h_2} + \ldots + \lambda_{h_n} + \lambda_0$ by $\lambda_{h_1}, \lambda_{h_2}, \ldots, \lambda_{h_m}$ $(m \geqq 2)$ and we write

$$\lambda_h = \lambda_{h_1} + \lambda_{h_2} + \ldots + \lambda_{h_m} + \delta_h,$$

where

$$|\delta_h| \leqq (n-m)|\lambda_1| + |\lambda_0| \leqq N|\lambda_1| + |\lambda_0| = c_1.$$

Now

$$\begin{aligned}\lambda_h^2 &\geqq \left(\sum_{\mu=1}^{m} \lambda_{h_\mu}\right)^2 + 2\delta_h \sum_{\mu=1}^{m} \lambda_{h_\mu} \\ &\geqq \sum_{\mu=1}^{m} \lambda_{h_\mu}^2 + 2\lambda_{h_1} \sum_{\mu=2}^{m} \lambda_{h_\mu} - 2c_1 \sum_{\mu=1}^{m} \lambda_{h_\mu} \\ &= \sum_{\mu=1}^{m} \lambda_{h_\mu}^2 + (2\lambda_{h_1} - 2c_1) \sum_{\mu=3}^{m} \lambda_{h_\mu} + \lambda_{h_1}(\lambda_{h_2} - 2c_1) + \lambda_{h_2}(\lambda_{h_1} - 2c_1).\end{aligned}$$

We have $\lambda_{h_2}-2c_1>c_1$, hence $\lambda_{h_1}-2c_1>0$, $2\lambda_{h_1}-2c_1>0$; it follows

$$\lambda_h^2 \geqq \sum_{\mu=1}^{m} \lambda_{h_\mu}^2 + \lambda_{h_1} c_1 \geqq \sum_{\mu=1}^{m} \lambda_{h_\mu}^2 + 3c_1^2.$$

The exponents $\lambda_{h_{m+1}}, \lambda_{h_{m+2}}, \ldots, \lambda_{h_n}$ are negative or zero, hence

$$\lambda_0^2 + \sum_{\nu=m+1}^{n} \lambda_{h_\nu}^2 \leqq \lambda_0^2 + N\lambda_1^2 \leqq c_1^2.$$

It follows

$$\lambda_h^2 \geqq \sum_{\mu=1}^{m} \lambda_{h_\mu}^2 + \sum_{\nu=m+1}^{n} \lambda_{h_\nu}^2 + \lambda_0^2.$$

This proves the lemma.

P r o o f o f t h e t h e o r e m: On account of lemma 1 we have

$$\lambda_h = \lambda_{h_1} + \lambda_{h_2} + \ldots + \lambda_{h_n} + \lambda_0 \text{ for } h \geqq r,$$

with $1 \leqq n \leqq N$, $h_n \leqq h_{n-1} \leqq \ldots \leqq h_1 < h$.

Now we consider r arbitrary numbers $x_0, x_1, \ldots, x_{r-1}$ and the infinite sequence $x_0, x_1, \ldots, x_{r-1}, x_r, x_{r+1}, \ldots$, defined by the recurrent relations

$$x_h = x_{h_1} + x_{h_2} + \ldots + x_{h_n} + x_0 \text{ for } h = r, r+1, r+2, \ldots, \quad (5)$$

where $n, h_1, h_2, \ldots, h_n$ are the same integers as in the foregoing formula. It follows that the sequence $x_0, x_1, x_2, \ldots$ has an integral linear basis consisting of the numbers $x_0, x_1, \ldots, x_{r-1}$; we even have

$$x_h = p_{h0}\, x_0 + p_{h1}\, x_1 + \ldots + p_{h,r-1}\, x_{r-1} \qquad (h = 0, 1, 2, \ldots), \quad (6)$$

where $p_{h0}, p_{h1}, \ldots, p_{h,r-1}$ denote integers $\geqq 0$.

In particular

$$\lambda_h = p_{h0}\,\lambda_0 + p_{h1}\,\lambda_1 + \ldots + p_{h,r-1}\,\lambda_{r-1} \qquad (h = 0, 1, 2, \ldots).$$

Let

$$X_\varrho = \begin{cases} 1 \text{ if } \lambda_\varrho \neq 0 \\ 0 \text{ if } \lambda_\varrho = 0 \end{cases} \text{ for } \varrho = 0, 1, \ldots, r-1 \quad . \quad . \quad . \quad . \quad (7)$$

(so that at most two of the numbers $X_0, X_1, \ldots, X_{r-1}$ are zero, the others being equal to unity). Hence

$$X_0\,\lambda_0 = \lambda_0,\ X_1\,\lambda_1 = \lambda_1, \ldots, X_{r-1}\,\lambda_{r-1} = \lambda_{r-1},$$

so that

$$\lambda_h = p_{h0}\,X_0\,\lambda_0 + p_{h1}\,X_1\,\lambda_1 + \ldots + p_{h,r-1}\,X_{r-1}\,\lambda_{r-1} \qquad (h = 0, 1, 2, \ldots).$$

Now all exponents $\lambda_1, \lambda_2, \lambda_3, \ldots$ are different; it follows that all systems

$$(p_{h0}\,X_0, p_{h1}\,X_1, \ldots, p_{h,r-1}\,X_{r-1}) \text{ for } h = 1, 2, 3, \ldots$$

are different.

Let P denote an arbitrary positive integer. The total number of different systems

$$(p_0 X_0, p_1 X_1, \ldots, p_{r-1} X_{r-1}),$$

where $p_0, p_1, \ldots, p_{r-1}$ are integers with $0 \leqq p_\varrho \leqq P-1$ $(\varrho = 0, 1, \ldots, r-1)$ is $P^{r-\tau}$, τ denoting the number of zeros in the sequence $X_0, X_1, \ldots, X_{r-1}$. Hence there exists in the sequence $1, 2, \ldots, P^r + 1$ at least one number k, such that the system

$$(p_{k0} X_0, p_{k1} X_1, \ldots, p_{k,r-1} X_{r-1})$$

contains at least one integer $p_{k\varrho} X_\varrho \geqq P$, and therefore

$$p_{k0} X_0 + p_{k1} X_1 + \ldots + p_{k,r-1} X_{r-1} \geqq P.$$

We introduced already the numbers $X_0, X_1, \ldots, X_{r-1}$ in (7); let $X_r, X_{r+1}, \ldots$ satisfy the recurrent relations (5) with X_h in stead of x_h. It follows from (6)

$$X_h = p_{h0} X_0 + p_{h1} X_1 + \ldots + p_{h,r-1} X_{r-1} \qquad (h = 0, 1, \ldots).$$

Hence the sequence $1, 2, \ldots, P^r + 1$ contains at least one number k, such that

$$X_k \geqq P. \quad . \quad . \quad . \quad . \quad . \quad . \quad . \quad . \quad . \quad . \quad . \quad . \quad (8)$$

Let H be the integer of lemma 2. By (3) we know $\lambda_h \neq 0$ for $h \geqq r$; it follows from (7) that $\lambda_h = 0$ implies $X_h = 0$ $(h = 0, 1, 2, \ldots)$. Hence there exists a positive number c_2, such that

$$X_h \leqq c_2 \lambda_h^2 \text{ for } h = 0, 1, \ldots, H-1.$$

We shall show by induction that this inequality also holds for $h \geqq H$.

Let $h \geqq H$ and let

$$X_l \leqq c_2 \lambda_l^2 \text{ for } l = 0, 1, \ldots, h-1.$$

We have $h \geqq H \geqq r$, hence

$$X_h = X_{h_1} + X_{h_2} + \ldots + X_{h_n} + X_0,$$

where $1 \leqq h_\nu \leqq h-1$ $(\nu = 1, 2, \ldots, n)$, so that

$$X_h \leqq c_2 \lambda_{h_1}^2 + c_2 \lambda_{h_2}^2 + \ldots + c_2 \lambda_{h_n}^2 + c_2 \lambda_0^2.$$

Applying lemma 2 we find, on account of $h \geqq H$,

$$\lambda_{h_1}^2 + \lambda_{h_2}^2 + \ldots + \lambda_{h_n}^2 + \lambda_0^2 \leqq \lambda_h^2,$$

hence

$$X_h \leqq c_2 \lambda_h^2$$

holds for any number $h = 0, 1, 2, \ldots$.

Taking $h = k$, where k is the integer in formula (8), we deduce $c_2 \lambda_k^2 \geqq P$, so that every sequence $1, 2, \ldots, P^r + 1$ contains at least one number k, such that $c_2 \lambda_k^2 \geqq P$.

Now it is easy to prove the assertion of our theorem. Let h be an arbitrary integer $\geqq 4^r$, hence $h^{\frac{1}{r}} \geqq 4$; put $P = \left[h^{\frac{1}{r}}\right] - 1$, then

$$P > h^{\frac{1}{r}} - 2 \geqq \tfrac{1}{2} h^{\frac{1}{r}} \text{ and } P + 1 \leqq h^{\frac{1}{r}};$$

hence $P^r + 1 \leqq h$. It follows, that every sequence $1, 2, \ldots, h$ contains at least one number k, such that $c_2 \lambda_k^2 \geqq P > \frac{1}{2} h^{\frac{1}{r}}$. For sufficiently large h clearly $\lambda_k^2 > \lambda_1^2$, hence λ_k is positive and it follows $\lambda_k > c_3 h^{\frac{1}{2r}}$, where $c_3 = \frac{1}{\sqrt{2c_2}}$. Now $h \geqq k$, hence $\lambda_h \geqq \lambda_k > c_3 h^{\frac{1}{2r}}$. If we take for c a positive number $< \frac{1}{2r}$, then

$$\lambda_h > h^c$$

for all but a finite number of values of h.

Mathematics. — *Remark on my paper „On* LAMBERT's *proof for the irrationality of* π". By J. POPKEN.

In these Proceedings [1]) I have given an elementary proof for the irrationality of π. However Dr M. VAN VLAARDINGEN kindly informed me, that the method I used nearly is the same as that applied by HERMITE in the fourth edition of "Cours de la faculté des Sciences" (1891), p. 74—75 [2]).

---

[1]) Vol. XLIII (1940) p. 712—714.

[2]) See also: A. PRINGSHEIM, Vorlesungen über Zahlen- und Functionenlehre II, 1, p. 471—474; p. 613.

Mathematics. — *Affine embedding theory I: Affine normal spaces.* By V. HLAVATÝ. (Communicated by Prof. J. A. SCHOUTEN.)

(Communicated at the meeting of February 26, 1949.)

Synopsis. In a sequence of papers we shall establish an embedding theory of a X_m in a A_n $(1 \leqq m < n, n \geqq 3)$. In this first paper some fundamental transformation laws are found which enable us a construction of a connection (which stamps our X_m to an A_m) as well as of higher connections which lead to a well defined set of affine normal spaces of the A_m.

1. Introduction.

a) Let A_n be an affine space of n dimensions $(n \geqq 3)$ referred to a coördinate system ξ^{ν} [1]. $\Gamma^{\gamma}_{\alpha\beta} = \Gamma^{\gamma}_{\beta\alpha}$ its connection coefficients and ∇_{μ} by the corresponding covariant derivative operator. Any scalar or tensor defined by means of the usual transformation formula (with respect to a system of transformations $\xi^{\nu} \longleftrightarrow \xi^{\nu'}$) will be referred to as a *ξ-scalar* or *ξ-tensor.*

b) Let X_m be defined in A_n $(1 \leqq m < n)$ by parametric equations

$$\xi^{\nu} = \xi^{\nu}(\eta^1, \ldots, \eta^m), \quad \ldots \ldots \ldots \quad (1.1)$$

where the rank of the JACOBIAN matrix $\left(\left(\frac{\partial \xi}{\partial \eta}\right)\right)$ is m. Any scalar or tensor defined by means of the usual transformation formula (with respect to a system of transformations $\eta^a \longleftrightarrow \eta^{a'}$) will be referred to as a *η-scalar* or *η-tensor.* A *$(\xi\eta)$-scalar* (or *$(\xi\eta)$-tensor*) is a ξ-scalar (ξ-tensor) as well as η-scalar (η-tensor). Thus for instance

$$T^{\nu}_a \equiv \frac{\partial \xi^{\nu}}{\partial \eta^a} \quad \ldots \ldots \ldots \quad (1,2\,a)$$

is a $(\xi\eta)$-tensor because of its transformation law

$$T^{\nu'}_{a'} = \frac{\partial \xi^{\nu'}}{\partial \xi^{\nu}} \frac{\partial \eta^a}{\partial \eta^{a'}} T^{\nu}_a. \quad \ldots \ldots \ldots \quad (1,2\,b)$$

Consequently this $(\xi\eta)$-tensor is independent of a choice of coördinate system ξ^{ν} as well as of a choice of a parameter system η^a. On the other hand $T^{\nu}_1, T^{\nu}_2, \ldots, T^{\nu}_m$ may be thought of as a set of m linearly independent ξ-vectors which depend on the choice of parameter systems.

---

[1]) It is understood that small greek (latin) indices run from 1 to n (from 1 to m unless otherwise stated).

c) Introducing the operator $\nabla_a \equiv T^\mu_a \nabla_\mu$ we define an infinite set of ξ-vectors

$$\left. \begin{aligned} T^\nu_{a_x \dots a_1} = \nabla_{a_x} T^\nu_{a_{x-1} \dots a_1} = \partial_{a_x} T^\nu_{a_{x-1} \dots a_1} + \Gamma^\nu_{\lambda\mu} T^\mu_{a_x} T^\lambda_{a_{x-1} \dots a_1} = \\ = T^\nu_{a_x \dots a_3 a_1 a_2}. \end{aligned} \right\} \quad (1,3)$$

$(x = 2, 3, \dots)$.

each of them being dependent on the choice of a parameter system η^a. Because n is a finite integer, a least integer N may be found for which any ξ-vector $T^\nu_{a_M \dots a_1}$ (for $M > N$) is a linear combination of the ξ-vectors $T^\nu_{a_x \dots a_1}$, $x = 1, 2, \dots, N$. *Throughout this paper we shall assume* $N > 1$.

The linear space $\overset{y}{E}_{m_y}(P)$ spanned by the ξ-vectors

$$T^\nu_{a_1}(P),\ T^\nu_{a_2 a_1}(P), \dots,\quad T^\nu_{a_y \dots a_1}(P),\quad y = 1, 2, \dots, N. \quad . \quad (1,4)$$

will be referred to as the *y-th osculating space* of our X_m at its generator point P. Any of these spaces is obviously $(\xi\eta)$-invariant and moreover we have

$$\overset{1}{E}_{m_1} \subset \overset{2}{E}_{m_2} \subset \overset{3}{E}_{m_3} \subset \dots \subset \overset{N}{E}_{m_N}.$$

The ξ-vectors T^ν_a being linearly independent we have

$$m_1 = m, \quad . \quad . \quad . \quad . \quad . \quad . \quad . \quad . \quad . \quad (1,5\,a)$$

and because of (1, 3) we obtain

$$m_x \leqq m + \sum_1^{x-1} {}_z \frac{m^z (m+1)}{2}, \qquad x = 2, 3, \dots N \quad . \quad . \quad (1,5\,b)$$

If the equality sign holds our space X_m will be called a *maximal* X_m, the remaining case being termed a *restricted* X_m.

2. *Fundamental transformation formulae.*

Our starting point will be the analytic expression of the statement (contained in 1c)) on the integer N, namely

$$F^\nu_{a_{N+1} \dots a_1} \equiv T^\nu_{a_{N+1} \dots a_1} - \sum_1^N {}_x \Phi_{a_{N+1} \dots a_x \dots a_1}{}^{b_x \dots b_1} T^\nu_{b_x \dots b_1} = 0 \quad . \quad (2,1)$$

where the Φ's are some functions of the η's. If we are dealing with a maximal X_m, all ξ-vectors (1, 4) are linearly independent and consequently (2, 1) admits *only one solution for the* Φ's. This solution is obviously

of the ξ-order $N+1$ [2]). On the other hand if our X_m is a restricted X_m, the Φ's are not uniquely determined by (2, 1) unless this equation be a *given* one with an *unique given* set of Φ's. *We shall confine ourselves to this case if dealing with a restricted* X_m. [3]). Hence the Φ's are of the ξ-order $N+1$, (0) [4]). Later on we shall see that the η-order of $\Phi_{a_{N-1}\dots a_x \dots a_1}^{b_x \dots b_1}$ is $N+2-x$ $(N+2-x)$.

Let us now find the transformation law for the Φ's. If we introduce the abbreviations

$$\left.\begin{aligned} &P_b^{a'} = \frac{\partial \eta^{a'}}{\partial \eta^b}, \qquad P_{b_x \dots b_1}^{a'_x \dots a'_1} = P_{b_x}^{a'_x} P_{b_{x-1}}^{a'_{x-1}} \dots P_{b_1}^{a'_1} \\ &P_{b'}^{a} = \frac{\partial \eta^a}{\partial \eta^{b'}}, \qquad P_{b'_x \dots b'_1}^{a_x \dots a_1} = P_{b'_x}^{a_x} P_{b'_{x-1}}^{a_{x-1}} \dots P_{b'_1}^{a_1} \\ &P_{b'_x \dots b'_1}^{\;a} = \frac{\partial^x \eta^a}{\partial y^{b'_x} \dots \partial y^{b'_1}}, \qquad x = 1, 2, 3, \dots, \end{aligned}\right\} \quad . \quad . \quad (2, 2)$$

we may write the transformation law for the $T_{a_x \dots a_1}^{\nu}$ in the following way

$$\left.\begin{aligned} T_{a'_x \dots a'_1}^{\nu'} = {} & P_{a'_x \dots a'_1}^{a_x \dots a_1} T_{a_x \dots a_1}^{\nu} \\ & + \sum_{2}^{x-1} r \Big[\Big\{ P_{a'_x \dots a'_r}^{\;a_r} P_{a'_{r-1} \dots a_1}^{a_{r-1} \dots a_1} \Big\} + p_{a'_x \dots a'_r \dots a'_1}^{\;a_r \dots a_1} \Big] T_{a_r \dots a_1}^{\nu} \\ & + P_{a'_x \dots a'_1}^{a} T_a^{\nu}, \qquad x = 2, 3, \dots \end{aligned}\right\} \quad . \quad . \quad (2, 3)$$

Here $\Big\{ P_{a'_x \dots a'_r}^{\;a_r} P_{a'_{r-1} \dots a'_1}^{a_{r-1} \dots a_1} \Big\}$ symmetric in $a_2\,a_1$, stands for a sum of products of the type as introduced in the braces $\{\}$ with a conveniently chosen permutation of the upper as well as lower indices,

$$p_{a'_x\, a'_{x-1} \dots a'_1}^{\;a_{x-1} \dots a_1} = 0 = p_{a'_x \dots a'_1}^{\;a_1}$$

---

[2]) An object is said to be of the ξ-order (η-order) r if its construction in any coördinate system (parameter system) requires the derivatives of the ξ ($\eta^{a'}$) with respect to the η^a up to the r-th order only.

[3]) In other words: If dealing with a maximal case we start with (1, 1) and build up the equations (2, 1) which admit only one solution for the Φ's. If our X_m is a restricted one *we do not start with* (1, 1) and we consider (2, 1) *as an à priori given* set of partial differential equations with uniquely given coefficients Φ's.

[4]) The first number refers always to the *maximal* case, the number in parenthesis refers to the *restricted* case.

and $p_{a'_x \dots a'_r \dots a'_1}^{\;a_r \dots a_1}$ (symmetric in $a_2 a_1$) represents for $r = x-2,\ x-3, \dots, 2$ a sum of products of at least two of the expressions

$$P_{a'_2 a'_1}^{\;a},\ P_{a'_3 a'_2 a'_1}^{\;a}, \dots, P_{a'_{x-r} \dots a'_1}^{\;a} \quad \dots \dots \quad (2,4)$$

and eventually of some $P_{a'}^{a}$. 5)

The equation (2, 1) has to be $(\xi\eta)$-invariant. Hence

$$F_{a'_{N+1} \dots a'_1}^{\nu} = \varrho\, P_{a'_{N+1} \dots a'_1}^{\;a_{N+1} \dots a_1} F_{a_{N+1} \dots a_1}^{\nu} \quad \dots \dots \quad (2,5)$$

Comparing this equation with (2, 3) for $x = N+1$ we get an once

$$\varrho = 1 \quad \dots \dots \dots \quad (2,6)$$

---

5) A straightforward computation leads to

a)
$$\{P_{c'}^{b}{}_{b'} P_{a'}^{a}\} = P_{c'}^{(b}{}_{b'} P_{a'}^{a)} + P_{b'}^{(a}{}_{a'} P_{c'}^{b)} + P_{a'}^{(b}{}_{c'} P_{b'}^{a)},$$
$$p_{d'\,c'\,b'\,a'}^{\;\;\;\;\;\;b\;\;a} = P_{d'}^{(b}{}_{c'} P_{b'}^{a)}{}_{a'} + P_{d'}^{(b}{}_{b'} P_{a'}^{a)}{}_{c'} + P_{d'}^{(a}{}_{a'} P_{c'}^{b)}{}_{b'}$$

and

b)
$$\left\{P_{a'_{x+1} \dots a'_2}^{\;a_2} P_{a'_1}^{a_1}\right\} = \left\{\left(\partial_{a'_{x+1}} P_{a'_x \dots a'_2}^{\;(a_2}\right) P_{a'_1}^{a_1)}\right\} + P_{a'_{x+1}}^{(a_1} P_{a'_x \dots a'_1}^{\;a_2)}$$

$$\left\{P_{a'_{x+1} \dots a'_s}^{\;a_s} P_{a'_{s-1} \dots a'_1}^{a_{s-1} \dots a_1}\right\} = \left\{\left(\partial_{a'_{x+1}} P_{a'_x \dots a'_s}^{\;a_s}\right) P_{a'_{s-1} \dots a'_1}^{a_{s-1} \dots a_1}\right\} +$$
$$+ P_{a'_{x+1}}^{a_s} \left\{P_{a'_x \dots a'_{s-1}}^{\;a_{s-1}} P_{a'_{s-2} \dots a'_1}^{a_{s-2} \dots a_1}\right\}, \qquad s = 3, \dots, x-1$$

$$\left\{P_{a'_{x+1} a'_x}^{\;a_x} P_{a'_{x-1} \dots a'_1}^{a_{x-1} \dots a_1}\right\} = \partial_{a'_{x+1}} P_{a'_x \dots \dots a'_1}^{a_x \dots (a_2 a_1)} + P_{a'_{x+1}}^{a_x} \left\{P_{a'_x a'_{x-1}}^{\;a_{x-1}} P_{a'_{x-2} \dots a'_1}^{a_{x-2} \dots a_1}\right\},$$

c)
$$p_{a'_{x+1} \dots a'_s \dots s'_1}^{\;a_s \dots a_1} = \left\{P_{a'_x \dots a'_s}^{\;a_s} \partial_{a'_{x+1}} P_{a'_{s-1} \dots a'_1}^{a_{s-1} \dots a_1}\right\} + \partial_{a'_{x+1}} p_{a'_x \dots a'_s \dots a'}^{\;a_s \dots a_1}$$
$$+ p_{a'_x \dots a'_{s-1} \dots a'_1}^{\;a_{s-1} \dots a_1} P_{a'_{x+1}}^{a_s}, \qquad s = 3, \dots, x-1$$

$$p_{a'_{x+1} \dots a'_2 a'_1}^{\;a_2 a_1} = \left\{P_{a'_{x+1} \dots a'_2}^{\;a_2} \partial_{a'_{x+1}} P_{a'_1}^{a_1}\right\} + \partial_{a'_{x+1}} p_{a'_x \dots a'_2 a'_1}^{\;a_2 a_1} \qquad x = 3, 4, \dots.$$

These formulas enable us to compute all the symbols { } as well as all the p's.

Theorem (2, 1). If our X_m is a maximal one then

$$\left.\begin{aligned}
&\text{(a)}\quad \Phi_{a_{N+1}a_N\ldots a_1}^{\;b_N\ldots b_1} = P_{a_{N+1}\ldots a_1}^{a'_{N+1}\ldots a'_1}\Big[P_{b'_N\ldots b'_1}^{b_N\ldots b_1}\Phi_{a'_{N+1}a'_N\ldots a'_1}^{\;b'_N\ldots b'_1} - \\
&\qquad\qquad - \Big\{P_{a'_{N+1}a'_N}^{\;b_N} P_{a'_{N-1}\ldots a'_1}^{b_{N-1}\ldots b_1}\Big\}\Big],\\
&b)\quad \Phi_{a_{N+1}\ldots a_r\ldots a_1}^{\;b_r\ldots b_1} = P_{a_{N+1}\ldots a_1}^{a'_{N+1}\ldots a'_1}\Big[P_{b'_r\ldots b'_1}^{b_r\ldots b_1}\Phi_{a'_{N+1}\ldots a'_r\ldots a'_1}^{\;b'_r\ldots b'_1} + \\
&\quad + \sum_{r+1}^{N}{}_q\, \Phi_{a'_{N+1}\ldots a'_q\ldots a'_1}^{\;b'_q\ldots b'_1}\Big(\Big\{P_{b'_q\ldots b'_r}^{\;b_r} P_{b'_{r-1}\ldots b'_1}^{b_{r-1}\ldots b_1}\Big\} + P_{b'_q\ldots b'_r\ldots b'_1}^{\;b_r\ldots b_1}\Big)\\
&\quad - \Big\{P_{a'_{N+1}\ldots a'_r}^{\;b_r} P_{a'_{r-1}\ldots a'_1}^{b_{r-1}\ldots b_1}\Big\} - P_{a'_{N+1}\ldots a'_r\ldots a'_1}^{\;b_r\ldots b_1}\Big],\qquad r=2,\ldots,N-1\\
&c)\quad \Phi_{a_{N+1}\ldots a_1}^{\;b_1} = P_{a_{N+1}\ldots a_1}^{a'_{N+1}\ldots a'_1}\Big[P_{b'_1}^{b_1}\Phi_{a'_{N+1}\ldots a'_1}^{\;b'_1} + \\
&\qquad\qquad + \sum_{2}^{N}{}_q\, \Phi_{a'\ldots a'_q\ldots a'_1}^{\;b'_q\ldots b'_1} P_{b'_q\ldots b'_1}^{\;b_1} - P_{a'_{N+1}\ldots a'_1}^{\;b_1}\Big].
\end{aligned}\right\}\quad (2,7)$$

In the case of a restricted X_m these equations represent one of the possible conclusions taken from (2, 5). According to (2, 7) the $\Phi_{a_{N+1}\ldots a_x\ldots a_1}^{\;b_x\ldots b_1}$ are of the η-order $N+2-x$ $\quad(N+2-x)$, $x=1,\ldots,N$.

Proof. Substituting from (2, 6) and (2, 3) in (2, 5), we get an equation of the form

$$\sum_{1}^{N}{}_u\, T^{\nu}_{b_u\ldots b_1} X_{a_{N+1}\ldots a_u\ldots a_1}^{\;b_u\ldots b_1} = 0. \quad \ldots\ldots \quad (2,8)$$

If our X_m is a maximal one, then all the ξ-vectors $T^{\nu}_{b_u\ldots b_1}$ are linearly independent and consequently (2, 8) leads to

$$X_{a_{N+1}\ldots a_u\ldots a_1}^{\;b_u\ldots b_1} = 0, \qquad u=1,\ldots,N. \quad \ldots\ldots \quad (2,9)$$

In the case of a restricted X_m the equations (2, 9) represent one of the possible conclusions taken from (2, 9). The equations (2, 9) are equivalent to (2, 7). — The last part of our theorem is obvious.

3. *The connection Γ^a_{cb} of X_m.*

Let us introduce the functions

$$\Pi_{a_{N+1}a_N\ldots a_1}^{\;b_N\ldots b_1} = \Phi_{(a_{N+1}a_N\ldots a_1)}^{\;b_N\ldots b_1},\quad \Pi_{a'_{N+1}a'_N\ldots a'_1}^{\;b'_N\ldots b'_1} = \Phi_{(a'_{N+1}a'_N\ldots a'_1)}^{\;b'_N\ldots b'_1} \qquad (3,1\,a)$$

and

$$\left.\begin{aligned} A^{a}_{cb} &= A^{a}_{bc} = \Pi^{a_N \dots a_2 a}_{c\, a_N \dots a_2 b}, \quad A_c = A^{a}_{ca} \\ A^{a'}_{c'b'} &= A^{a'}_{b'c'} = \Pi^{a'_N \dots a'_2 a'}_{c'\, a'_N \dots a'_2 b'}, \quad A_{c'} = A^{a'}_{c'a'}. \end{aligned}\right\} \quad . \; . \quad (3,1\,b)$$

which we shall need later on. According to the definition of the symbols in braces we have obviously

$$\left.\begin{aligned} \left\{ P^{\;\;e}_{b'e'}\, \delta^{a_{N-1}\dots a_2 a}_{(a_{N-1}\dots a_2 c}\, P^{b'e'}_{b\;\;e)} \right\} &= r_1\, P^{\;\;a}_{b'e'}\, P^{e'b'}_{c\;\;b} \\ &+ r_2 \left(P^{\;\;e}_{b'e'}\, P^{b'e'}_{b\;\;e}\, \delta^{a}_{c} + P^{\;\;e}_{b'e'}\, P^{b'e'}_{c\;\;e}\, \delta^{a}_{b} \right)^{6)} \end{aligned}\right\} \quad (3,2\,a)$$

where r_1, r_2 are suitably chosen integers different from zero. Consequently

$$\left\{ P^{\;\;e}_{b'e'}\, \delta^{a_{N-1}\dots a_1}_{(a_{N-1}\dots a_1}\, P^{b'e'}_{b\;\;e)} \right\} = [r_1 + r_2(m+1)]\, P^{\;\;e}_{b'e'}\, P^{b'e'}_{b\;\;e} \quad . \quad (3,2\,b)$$

Theorem (3, 1). The functions

$$\Gamma^{a}_{cb} = \Gamma^{a}_{bc} = \frac{1}{r_1}\left[A^{a}_{cb} - \frac{r_2}{r_1 + r_2(m+1)} \left(\delta^{a}_{c} A_b + \delta^{a}_{b} A_c \right) \right] \quad . \quad (3,3)$$

are coefficients of a connection in X_m which stamps our X_m to an A_m. This connection is of the $\left.\begin{matrix}\xi-\\ \eta-\end{matrix}\right\}$ *order* $\left\{\begin{matrix} N+1 & (0) \\ 2 & (2) \end{matrix}\right.$.

Proof. From the first of (2, 7) and from (3, 1) we have

$$\left.\begin{aligned} \text{a)} \quad A^{a}_{cb} &= P^{c'b'a}_{c\;b\;a'}\, A^{a'}_{c'b'} - \left\{ P^{\;\;e}_{b'e'}\, \delta^{a_{N-1}\dots a_2 a}_{(a_{N-1}\dots a_2 c}\, P^{b'e'}_{b\;\;e)} \right\} \\ \text{b)} \quad A_b &= P^{b'}_{b}\, A_{b'} - \left\{ P^{\;\;e}_{b'e'}\, \delta^{a_N\dots a_1}_{(a_N\dots a_1}\, P^{b'e'}_{b\;\;e)} \right\} \end{aligned}\right\} \quad . \; . \quad (3,4)$$

Consequently it follows from (3, 2)

$$\left.\begin{aligned} \left\{ P^{\;\;e}_{b'e'}\, \delta^{a_{N-1}\dots a_2 a}_{(a_{N-1}\dots a_2 c}\, P^{b'e'}_{b\;\;e)} \right\} &= r_1\, P^{\;\;a}_{b'e'}\, P^{e'b'}_{c\;\;b} + \\ &+ \frac{r_2}{r_1 + r_2(m+1)} \left[\delta^{a}_{c} \left(P^{b'}_{b} A_{b'} - A_b \right) + \delta^{a}_{b} \left(P^{c'}_{c} A_{c'} - A_c \right) \right]. \end{aligned}\right\} \quad (3,5)$$

Substituting from (3, 5) in (3, 4a) we get

$$\Gamma^{a}_{cb} = P^{c'b'a}_{c\;b\;a'}\, \Gamma^{a'}_{c'b'} - P^{c'b'}_{c\;b}\, P^{a}_{c'b'}, \quad . \; . \; . \; . \; . \quad (3,6\,a)$$

or

$$P^{a}_{c'b'} = P^{a}_{a'}\, \Gamma^{a'}_{c'b'} - P^{c\;b}_{c'b'}\, \Gamma^{a}_{cb}, \quad . \; . \; . \; . \; . \quad (3,6\,b)$$

---

6) δ^{a}_{c} is the Kronecker delta and $\delta^{b_r\dots b_1}_{a_r\dots a_1} = \delta^{b_r}_{a_r} \dots \delta^{b_1}_{a_1}$.

where the Γ^{a}_{cb} are defined by (3, 3) and the $\Gamma^{a'}_{c'b'}$ are defined by a similar equation to (3, 3). Hence Γ^{a}_{cb} are the coefficients of a connection which is obviously of the $\left.\begin{matrix}\xi-\\ \eta-\end{matrix}\right\}$ order mentioned in the theorem.

4. *Higher degree connections.*

The r-th covariant derivative (with respect to the connection (3, 3)) of an η-tensor contains the $(r-1)$-derivatives of Γ^{a}_{cb} which is of the ξ-order $N+r$ $(r-1)$. In this section we shall replace these derivatives by another set of functions which are of the same ξ-order $N+1$ (0).

Lemma (4, 1). $p_{a'_{N+1}\dots a'_{N-1}\dots a'_1}^{\;b_{N-1}\dots b_1}$ *may be put in the form*

$$\left.\begin{aligned} p_{a'_{N+1}a'_N a'_{N-1}\dots a'_1}^{\;b_{N-1}\dots b_1} = P^{b_{N-1}\dots b_1}_{b'_{N-1}\dots b'_1}\,\omega_{a'_{N+1}\dots a'_{N-1}\dots a'_1}^{\;b'_{N-1}\dots b'_1} + \xi_{a'_{N+1}\dots a'_{N-1}\dots a_1}^{\;b_{N-1}\dots b_1} \\ - P^{a_{N+1}\dots a_1}_{a'_{N+1}\dots a'_1}\,\gamma_{a_{N+1}\dots a_{N-1}\dots a_1}^{\;b_{N-1}\dots b_1} \end{aligned}\right\} \tag{4, 1}$$

where $\gamma_{a_{N+1}\dots a_{N-1}\dots a_1}^{\;b_{N-1}\dots b_1}\left(\omega_{a'_{N-1}\dots a'_{N-1}\dots a'_1}^{\;b'_{N-1}\dots b'_1}\right)$ *is a sum of products of the* $\Gamma^{a}_{cb}\left(\Gamma^{a'}_{c'b'}\right)$ *only and does not contain* $P^{a}_{b'}$, $P^{a'}_{b}$ *and* $\xi_{a'_{N+1}\dots a'_{N-1}\dots a'_1}^{\;b_{N-1}\dots b_1}$ *is a sum of products of at least one of the* Γ^{a}_{cb} *and some* $\Gamma^{a'}_{c'b'}$ *(and of some* $P^{a}_{b'}$, $P^{a'}_{b}$*).*

Proof. $p_{a'_{N+1}\dots a'_{N-1}\dots a'_1}^{\;b_{N-1}\dots b_1}$ is a sum of products of at least two $P^{a}_{c'b'}$ and eventually of some $P^{a}_{b'}$. If the expressions (3, 6*b*) the substituted in these products we have at once the equation (4, 1), were γ is a function of the Γ^{a}_{cb}'s and does not contain the $\Gamma^{a'}_{c'b'}$'s. Let us suppose that it contains at least one of the $P^{a'}_{b}$'s, say $P^{c'}_{d}$. Then in γ one accentuated index (namely c') has to occur which makes the index c' of the $P^{c'}_{d}$ a dummy index. Because γ does not contain the $\Gamma^{a'}_{c'b'}$'s the required index may appear only in some of the $P^{a}_{b'}$, say in $P^{e}_{c'}$. Then $P^{e}_{c'}\,P^{c'}_{d}=\delta^{e}_{d}$. Hence γ does not contain the $P^{a'}_{b}$'s and similary it does not contain the $P^{a}_{b'}$'s. The remaining statements of the lemma may be proved by a similar device.

Theorem (4, 1). The equation (2, 7b) for $r=N-1$ admits only one solution

$$P_{d'c'b'}{}^{a} = P^{a}_{a'}\,\Omega_{d'c'b'}{}^{a'} + P^{a}_{a'}\,\Xi_{d'c'b'}{}^{a'} - P^{d\,c\,b}_{d'c'b'}\,\Gamma_{dcb}{}^{a} \quad . \quad . \quad . \qquad (4,2)$$

where Ω, Ξ and Γ are symmetric in the lower indices and

a) $\Gamma_{dcb}{}^{a}\left(\Omega_{d'c'b'}{}^{a'}\right)$ is a function of the $\Phi_{a_{N+1}\dots a_r \dots a_1}{}^{b_r\dots b_1}$ and $\left(\Phi_{a'_{N+1}\dots a'_r\dots a'_1}{}^{b'_r\dots b'_1}\right)$ only $[r=N-1, N]$ and does not contain $P^{a}_{b'}$, $P^{a'}_{b}$,

b) $\Xi_{d'c'b'}{}^{a'}$ represents a sum of products of at least one $\Gamma_{cb}{}^{a}$ and some $\Phi_{a'_{N+1}\,a'_N\dots a'_1}{}^{b'_N\dots b'_1}$ $\left(\text{and eventually of some } P^{a'}_{b},\ P^{a}_{b'}\right)$.

The functions $\Gamma_{dcb}{}^{a}$ are of the $\left.\begin{matrix}\xi-\\ y-\end{matrix}\right\}$ *order* $\begin{matrix}N+1 & (0)\\ 3 & (3)\end{matrix}$. *No derivatives $\partial_e \Gamma_{fg}{}^{h}$, $\partial_{e'}\Gamma_{f'g'}{}^{h'}$ occur in* (4, 2).

Proof. Let us introduce the abbreviations

$$\left.\begin{aligned}
&\Pi_{a_{N+1}\dots a_{N-1}\dots a_1}{}^{b_{N-1}\dots b_1} = \Phi_{(a_{N+1}\dots a_{N-1}\dots a_1)}{}^{b_{N+1}\dots b_1}, \quad \Lambda_{dcb}{}^{a} = \Pi_{dca_{N-1}\dots a_2 b}{}^{a_{N-1}\dots a_2 a}\\
&\Pi_{a'_{N+1}\dots a'_{N-1}\dots a'_1}{}^{b_{N-1}\dots b_1} = \Phi_{(a'_{N+1}\dots a'_{N-1}\dots a'_1)}{}^{b'_{N-1}\dots b'_1}, \quad \Lambda_{d'c'a'}{}^{a'} = \Pi_{d'c'a'_{N-1}\dots a'_2 b'}{}^{a'_{N-1}\dots a'_2 a'}
\end{aligned}\right\} . \qquad (4,3)$$

From (2, 7*b*) for $r=N-1$, from (3, 6*b*) and from (4, 1) we obtain

$$\begin{aligned}
&\Lambda_{dcb}{}^{a} - \gamma_{(dca'_{N-1}\dots a_2 b)}{}^{a_{N-1}\dots a_2 a} =\\
&= P^{d'c'b'a}_{d\,c\,b\,a'}\left[\Lambda_{d'c'b'}{}^{a'} + \Pi_{d'c'a'_{N-1}\dots a'_2 b'}{}^{d'_N \dots d'_1}\left\{\Gamma_{d'_N d'_{N-1}}{}^{a'_{N-1}}\,\delta^{a'_{N-2}\dots a'_2 a'}_{d'_{N-2}\dots d'_1}\right\} - \omega_{(d'c'a'_{N-1}\dots a'_2 b')}{}^{a'_{N-1}\dots a'_2 a'}\right]\\
&- P^{d'c'b'}_{d\,c\,b}\left[\Pi_{d'c'a'_{N-1}\dots a'_2 b'}{}^{d'_N\dots d'_1}\,P^{a'_{N-1}}_{e}\,P^{f\,g\,a}_{d'_N d'_{N-1} a'}\left\{\Gamma_{fg}{}^{e}\,\delta^{a'_{N-2}\dots a'_2 a'}_{d'_{N-2}\dots d'_1}\right\} + P^{a'_{N-1}\dots a'_2}_{d_{N-1}\dots d_2}\,\xi_{(d'c'a'_{N-1}\dots a'_2 b')}{}^{d_{N-1}\dots d_2 a}\right]\\
&\qquad\qquad - \left\{P_{d'c'h'}{}^{h}\,\delta^{d_{N-2}\dots d_2 a}_{(d_{N-2}\dots d_2 b}\right\}P^{h'd'c'}_{h\,d\,c)} .
\end{aligned} \qquad (4,4)$$

Applying on (4, 4) the same device as before we obtain the statement of our theorem.

Note. If we put

$$\gamma_{dcb}{}^{a} = \gamma_{(dca_{N-1}\dots a_2 b)}{}^{a_{N-1}\dots a_2 a}, \quad \gamma_{dc} = \gamma_{dca}{}^{a}, \quad \Lambda_{dc} = \Lambda_{dca}{}^{a}$$

then we have

$$\Gamma_{dcb}^{\ \ \ a} = c_1\left(\Lambda_{dcb}^{\ \ \ a} - \gamma_{dcb}^{\ \ \ a}\right) - c_2\delta_{(d}^{a}\left(\Lambda_{cb)} - \gamma_{cb)}\right) \quad . \quad . \quad . \quad (4,5)$$

where c_1, c_2 are suitably chosen integers different from zero.

The theorem (4, 1) may be easily generalized:

Theorem (4, 2). *The equations* (2, 7*b*) *for* $r = 3, 4, \dots N-1$ *admit only one solution*

$$\left.\begin{array}{l} P_{b'_q \dots b'_1}^{\ \ \ \ \ \ \ \ a} = P_{a'}^{a}\,\Omega_{b'_q \dots b'_1}^{\ \ \ \ \ \ \ \ a'} + P_{a'}^{a}\,\Xi_{b'_q \dots b'_1}^{\ \ \ \ \ \ \ \ a'} - P_{b'_q \dots b'_1}^{b_q \dots b_1}\,\Gamma_{b_q \dots b_1}^{\ \ \ \ \ \ \ \ a} \\ \qquad\qquad\qquad\qquad q = 3, 4, \dots N. \end{array}\right\} \quad . \quad (4,6)$$

where Ω, Ξ *and* Γ *are symmetric in the lower indices and*

a) $\Gamma_{b_q \dots b_1}^{\ \ \ \ \ \ \ \ a}\left(\Omega_{b'_q \dots b'_1}^{\ \ \ \ \ \ \ \ a'}\right)$ *is a function of the* $\Phi_{a_{N+1} \dots a_s \dots a_1}^{\ \ \ \ \ \ \ \ \ \ \ \ \ \ b_s \dots b_1}\left(\Phi_{a'_{N+1} \dots a'_s \dots a'_1}^{\ \ \ \ \ \ \ \ \ \ \ \ \ \ b'_s \dots b'_1}\right)$ *only* $[s = N+2-q, \dots, N]$ *and does not contain* $P_{b'}^{a}$, $P_{b}^{a'}$.

b) $\Xi_{b'_q \dots b'_1}^{\ \ \ \ \ \ \ \ a'_1}$ *represents a sum of products of at least one* $\Gamma_{b_u \dots b_1}^{\ \ \ \ \ \ \ \ a}$, $(u = 2, \dots q-1)$, *and some* $\Phi_{a'_{N+1} \dots a'_p \dots a'_1}^{\ \ \ \ \ \ \ \ \ \ \ \ \ \ b'_p \dots b'_1}$, $[p = N+3-q, \dots, N]$ *and eventually of some* $P_{b}^{a'}$, $P_{b'}^{a}$. *The functions* $\Gamma_{b_q \dots b_1}^{\ \ \ \ \ \ \ \ a}$ *are of the* $\left.\begin{array}{l}\xi -\\ \eta -\end{array}\right\}$ *order* $\left\{\begin{array}{l} N+1\ (0) \\ q\ \ (0) \end{array}\right.$.

No derivatives of $\Gamma_{b_u \dots b_1}^{\ \ \ \ \ \ \ \ a}$, $\Omega_{b'_u \dots b'_1}^{\ \ \ \ \ \ \ \ a'}$, $\Xi_{b'_u \dots b'_1}^{\ \ \ \ \ \ \ \ a'}$, $(u = 2, 3, \dots q-1)$ *occur in* (4, 6).

The proof is similar to the previous one [7]).

Note. Let (T) be an η-tensor and L be the transformation law for its r-th derivatives (with respect to the η's). If we start with (3, 6*b*) we

[7]) Let us suppose we have already proved (4, 6) for $q = 3, 4, \dots, u < N$. Then the following lemma (whose proof is similar to that of the lemma (4, 1)) has to be used:

$$p_{a'_x \dots a'_r \dots a'_1}^{\ \ \ \ \ \ \ \ \ \ \ \ \ b_r \dots b_1} = P_{b'_r \dots b'_1}^{b_r \dots b_1}\,\omega_{a'_x \dots a'_r \dots a'_1}^{\ \ \ \ \ \ \ \ \ \ \ \ \ b'_r \dots b'_1} + \xi_{a'_x \dots a'_r \dots a'_1}^{\ \ \ \ \ \ \ \ \ \ \ \ \ b_r \dots b_1} - P_{a'_x \dots a'_1}^{a_x \dots a_1}\,\gamma_{a_x \dots a_r \dots a_1}^{\ \ \ \ \ \ \ \ \ \ \ \ \ b_r \dots b_1}$$

$$x \leqq N+1,\ x-r = 2, \dots, u$$

where γ is a sum of products of at least two of the $\Gamma_{a_s \dots a_1}^{\ \ \ \ \ \ \ \ b}$, $s = 2, \dots, x-r$ only and does not contain $P_{a'}^{a}$, $P_{a}^{a'}$, ω is a function of the $\Phi_{a' \dots}^{b' \dots}$ and does not contain $P_{a'}^{a}$, $P_{a}^{a'}$ and ξ is a sum of products of at least one of the $\Gamma_{a_s \dots b_1}^{\ \ \ \ \ \ \ \ b}$, $s = 2, \dots, x-r$ and some $\Phi_{a' \dots}^{b' \dots}$ (and some $P_{a'}^{a}$, $P_{a}^{a'}$).

could deduce by derivation an equation of the type (4, 6) (which we shall designate by (4, 6)′), where the $\Gamma_{b_q\ldots b_1}^{\;a}$ is now a function of the $\Gamma_{ab}^{\;c}$ and its first $q-2$ derivatives and consequently is of the ξ-order $N-1+q$ $(q-2)$. Eliminating the $P_{b'\ldots}^{\;a}$ from L and (4, 6)′, we obtain the transformation law for the r-th covariant derivative $\left(\text{with respect to } \Gamma_{cb}^{\;a}\right)$, say $(T)_{(r)}$, of (T). The tensor $(T)_{(r)}$ contains the $\Gamma_{cb}^{\;a}$ and the $\Gamma_{b_s\ldots b_1}^{\;a}$, $(s=3, 4, \ldots r+1)$ involved in (4, 6)′, which consequently are of the ξ-order $N-1+s$ $(s-2)$. If we replace these $\Gamma_{b_s\ldots b_1}^{\;a}$ in $(T)_{(r)}$ by the $\Gamma_{b_s\ldots b_1}^{\;a}$ involved in (4, 6), we obtain another tensor (cf. the next section) which is of the ξ-order $N+1$ (0) $\left(\text{as far as the } \Gamma_{b_s\ldots b_1}^{\;a} \text{ are concerned}\right)$, provided $r \leqq N-1$. For that reason the $\Gamma_{b_q\ldots b_1}^{\;a}$ involved in (4, 6) may be thought of as coefficients of a „*higher degree connection*".

In the next lemma (we shall need later on) we denote by $\eta^{a'}$ a given parameter system (so that the $\Phi_{a'\ldots}^{\;b'\ldots}$ are known functions of the $\eta^{a'}$), by $P_{b'}^{a}$ a given system of constants of the rank m and by P a generator point $\eta^{a'}=0$:

Lemma (4, 2). *The parameter system* y^{a} *defined by*

$$\left.\begin{array}{l} y^{a}=P_{a'}^{a}\left[y^{a'}+\sum_{2}^{N}{}_{q}\,\dfrac{1}{q!}\left(\Omega_{b'_q\ldots b'_1}^{\;a'}\right)_P \eta^{a'_q}\ldots\eta^{a'_1}\right. \\ \qquad\qquad\qquad\qquad \left(\Omega_{c'b'}^{\;a'}=\Gamma_{c'b'}^{\;a'}\right) \end{array}\right\} \quad . \quad . \quad . \quad (4, 7)$$

(the so called privileged parameter system at P) satisfies the following conditions at P

$$\left.\begin{array}{l} \text{a)}\;\; P_{b'_r\ldots b'_1}^{\;a}=\Omega_{b'_r\ldots b'_1}^{\;a'},\quad b)\;\; \Xi_{b'_r\ldots b'_1}^{\;a'}=0,\quad c)\;\; \Gamma_{b_r\ldots b_1}^{\;a}=0 \\ \qquad\qquad \left(r=2,\ldots N,\;\; \Omega_{c'b'}^{a'}=\Gamma_{c'b'}^{a'}\right). \end{array}\right\} \quad (4, 8)$$

Proof. Put

$$\eta^{a}=P_{a'}^{a}\left[\eta^{a'}+\sum_{2}^{N}{}_{q}\,\frac{1}{q!}X_{b'_q\ldots b'_1}^{\;a'}\eta^{b'_q}\ldots\eta^{b'_1}\right] \quad . \quad . \quad (4, 9)$$

where the constants X are to be found. If $X_{b'c'}^{\;a'}=\left(\Gamma_{b'c'}^{\;a'}\right)_P$, then we get by virtue of (3, 6*b*) the equations (4, 8*a*, *c*) for $r=2$ (while (4, 8*b*) for $r=2$ is identically satisfied). Consequently, owing to the property of $\Xi_{b'c'd'}^{\;a'}$ mentioned in the theorem (4, 1) we have (4, 8*b*) for $r=3$. Hence

if $X_{c'b'd}^{\;\;\;\;a'}=\left(\Omega_{c'b'd'}^{\;\;\;\;\;a'}\right)_P$, we have (4, 8a, c) for $r=3$ and owing to the property of $\Xi_{b'_4\ldots b'_1}^{\;\;\;\;\;\;a'}$ mentioned in the theorem (4, 2) for $q=4$ we have (4, 8b) for $q=4$. Proceeding in this way we finally obtain (4, 8) a) b) c) for $r=2,\ldots N$.

5. *Affine normal spaces.*

Theorem (5, 1). If we eliminate from (2,3) (for $x=2,\ldots N$), (3,6)b and (4, 2), (4, 6) the $P_{b'\ldots}^{\;\;\;\;a}$, we obtain the usual transformation law for a ($\xi\,\eta$)-tensor (which we denote by $\triangle_{a_x}\ldots\triangle_{a_2}T_{a_1}^{\nu}$ and call the (x—1)st covariant pseudoderivative of T_a^{ν} [8]*)) with x covariant indices*

$$\left.\begin{aligned}
&a)\qquad \triangle_{a_2}T_{a_1}^{\nu}=T_{a_2a_1}^{\nu}-\Gamma_{a_1a_2}^{\;\;\;\;\;b}T_b^{\nu}\ \text{ for } x=2,\\
&b)\quad \triangle_{a_x}\ldots\triangle_{a_2}T_{a_1}^{\nu}=\\
&=T_{a_x\ldots a_1}^{\nu}-\sum_{2}^{x-1}{}_{r}\,T_{b_r\ldots b_1}^{\nu}\left[\left\{\Gamma_{a_x\ldots a_r}^{\;\;\;\;\;\;\;\;b_r}\,\delta_{a_{r-1}\ldots a_1}^{b_{r-1}\ldots b_1}\right\}+\gamma_{a_x\ldots a_r\ldots a_1}^{\;\;\;\;\;\;\;\;\;\;\;\;\;b_r\ldots b_1}\right]-\\
&\qquad\qquad -T_b^{\nu}\,\Gamma_{a_x\ldots a_1}^{\;\;\;\;\;\;\;\;\;b}\qquad (x=3,\ldots N).
\end{aligned}\right\}\ (5,1)$$

Proof. The equation (5, 1a) is obvious. If $N\geqq x>2$, then the elimination mentioned in the theorem leads to

$$\left.\begin{aligned}
&P_{a'_x\ldots a'_1}^{a_x\ldots a_1}\triangle_{a_x}\ldots\triangle_{a_2}T_{a_1}^{\nu}=-\sum_{1}^{x-1}{}_{r}\,T_{b_r\ldots b_1}^{\nu}\;{}^{*}\Xi_{a'_x\ldots a'_r\ldots a'_1}^{\;\;\;\;\;\;\;\;\;\;\;\;\;b_r\ldots b_1}\\
&+T_{a'_x\ldots a'_1}^{\nu}-\sum_{2}^{x-1}{}_{r}\left(\left\{\Omega_{a'_x\ldots a'_n}^{\;\;\;\;\;\;\;\;\;b'_r}\,\delta_{a'_{p-1}\ldots a'_1}^{b'_{r-1}\ldots b'_1}\right\}+\omega_{a'_x\ldots a'_r\ldots a'_1}^{\;\;\;\;\;\;\;\;\;\;\;\;\;b'_r\ldots a'_1}\right)P_{b'_r\ldots b'_1}^{b_r\ldots b_1}T_{b_r\ldots b_1}^{\nu}-\\
&\qquad\qquad -P_{b'}^{b}\,\Omega_{a'_x\ldots a'_1}^{\;\;\;\;\;\;\;\;\;b'}\,T_b^{\nu}
\end{aligned}\right\}\ (5,2)$$

where ${}^{*}\Xi_{a'_x\ldots a'_r\ldots a'_1}^{\;\;\;\;\;\;\;\;\;\;\;\;\;b_r\ldots b_1}$ is a (linear) function of the $\Xi_{a'_x\ldots a'_r}^{\;\;\;\;\;\;\;\;\;b'}$ and the $\xi_{a'_x\ldots a'_r\ldots a_1}^{\;\;\;\;\;\;\;\;\;\;\;\;\;b_r\ldots b_1}$ and contains some $P_b^{a'}$, $P_{b'}^{a}$. In the right hand side we have to express $T_{b_q\ldots b_1}^{\nu}$ by $T_{a'_s\ldots a'_1}^{\nu}$ ($q=1,\ldots,r$, $s=1,2,\ldots,q$) using a similar formula to (2, 3) (with interchanged rôle of the parameters) [9]). In doing so we have finally the equation

[8]) The same device (the generalized Christoffel elimination) may be applied to any ($\xi\eta$)-tensor.

[9]) And the device

$$P_{a_2a_1}^{\;\;\;\;\;b'}=-P_{a_2a_1b}^{a'_2a'_1b'}P_{a'_2a'_1}^{\;\;\;\;\;b}=\Gamma_{a_2a_1}^{\;\;\;\;\;b}P_b^{b'}-\Gamma_{a'_2a'_1}^{\;\;\;\;\;b'}P_{a_2a_1}^{a'_2a'_1}$$

$$P_{a_3a_2a_1}^{\;\;\;\;\;\;\;\;b'}=\ldots$$

and so on.

$$\triangle_{a'_x} \dots \triangle_{a'_2} T^{\nu}_{a'_1} = P^{a'_x \dots a_1}_{a'_x \dots a'_1} \triangle_{a_x} \dots \triangle_{a_2} T^{\nu}_{a_1} + X^{\nu}_{a'_x \dots a'_1} \quad . \quad (5, 3)$$

where $X^{\nu}_{a'_x \dots a'_1}$ represents a function of the arguments $\Phi^{b_s \dots b_1}_{a_x \dots a_s \dots a_1}$ $\Phi^{b'_s \dots b'_1}_{a'_x \dots a'_s \dots a'_1}$, $T^{\nu}_{a_r \dots a_1}$ and $T^{\nu}_{a'_r \dots a'_1}$ $(r = 1, \dots, x,\ s = N+2-x, \dots N)$ as well as of the $P^{a}_{a'}$, $P^{a'}_{a}$ and does not contains the derivatives of the $P^{a}_{a'}$, $P^{a'}_{a}$. Let us now consider a transformation $\eta^{a} \longleftrightarrow \eta^{a'}$ with *constant* $P^{a}_{a'}$ $\left(\text{and } P^{a'}_{a}\right)$. Then any of the arguments already mentioned (with the exception of the $P^{a}_{a'}$ and $P^{a'}_{a}$) is a tensor with respect to this special transformation and consequently $\triangle_{a_x} \dots \triangle_{a_2} T^{\nu}_{a_1}$ is a $(\xi\eta)$-tensor, which means that

$$X^{\nu}_{a'_x \dots a'_1} = 0 \text{ for } constant\ P^{a}_{a'}, P^{a'}_{a}. \quad . \quad . \quad . \quad . \quad (5, 4)$$

Because the lefthand member does not contain any derivatives of the $P^{a}_{a'}$, $P^{a'}_{a'}$ the statement (5, 4) is equivalent to

$$X^{\nu}_{a'_x \dots a'_1} = 0 \text{ for any transformation at a generator point } P. \quad (5, 5)$$

Hence (5, 3) simplifies to an ordinary tensor law transformation at any generator point, which proves our statement.

Theorem (5, 2). The $(\xi\eta)$-tensor

$$H^{\nu}_{a_x \dots a_1} \equiv \triangle_{a_x} \dots \triangle_{a_2} T^{\nu}_{a_1}; \quad (x = 2, \dots, N) \quad . \quad . \quad . \quad (5, 6)$$

has the following properties:

a) *It is symmetric in the indices* $a_1\, a_2$

$$H^{\nu}_{a_x \dots a_2 a_1} = H^{\nu}_{a_x \dots a_1 a_2}. \quad . \quad . \quad . \quad . \quad . \quad . \quad . \quad (5, 7)$$

b) *It is of the* $\left.\begin{matrix}\xi-\\ \eta-\end{matrix}\right\}$ *order* $\left\{\begin{matrix}N+1 & (0)\\ x & (x)\end{matrix}\right.$.

c) *In the maximal case the ξ-vectors T^{ν}_{a}, $H^{\nu}_{a_x \dots a_1}$, $(x = 2, \dots, N)$ are linearly independent.*

d) *The linear space $\overset{x-1}{N}_{n_{x-1}}$ spanned by $H^{\nu}_{a_x \dots a_1}$ is in $\overset{x}{E}_{m_x}$ but not in $\overset{y}{E}_{m_y}$, $y < x$ and its dimension is*

$$n_{x+1} = m_x - m_{x-1}; \qquad (m_1 = m) \quad . \quad . \quad . \quad . \quad . \quad (5, 8)$$

Moreover $\overset{x-1}{N}_{n_{x-1}}$ is of the $\left.\begin{matrix}\xi-\\ \eta-\end{matrix}\right\}$ *order* $\left\{\begin{matrix}N+1 & (0)\\ x & (x)\end{matrix}\right.$.

Proof. We have in a privileged parameter system because of (4, 8c) and (5, 1)

$$\overset{\nu}{H}_{a_x \ldots a_1} = \overset{\nu}{T}_{a_x \ldots a_1} \text{ at } P; \quad (x = 2, \ldots, N) \quad . \quad . \quad . \quad (5, 9)$$

The statement *b*) of the theorem follows from (5, 1), the remaining statements follow at once from (5, 9).

Definition (5, 1). *The space* $\overset{x-1}{N}_{n_{x-1}}$ *as defined in the theorem* (5, 2) *will be termed the* $(x-1)$*st affine normal space of* A_m, $(x = 2, \ldots, N)$.

In the next paper we shall establish the FRENET formulas for the affine normal spaces.

Indiana University
Department of Mathematics

Bloomington (Ind.) USA

Astronomy. — *The Partition function for the elements in the Solar Atmosphere.* By W. J. CLAAS. (Communicated by Prof. M. G. J. MINNAERT.)

(Communicated at the meeting of March 26, 1949.)

1. *The influence of perturbations.*

The distribution of the atoms of an element over all the stages of excitation is of considerable importance for the interpretation of the solar spectrum. For conditions of local thermodynamic equilibrium, this repartition is described by BOLTZMANN's law $g_n e^{-E_n/kT}$, except for very high values of the quantum number n. Especially important is the partition function $u = \sum_n g_n \cdot e^{-E_n/kT}$ for a neutral atom and for the corresponding ion, which comes in when the amount of ionization is computed.

We shall consider particularly the influence of perturbing particles in the atmosphere, by which the formation of high electron orbits is made impossible. The nature of these perturbations is an interesting problem. Already long ago, physicists have pointed out two possibilities: UREY [1]) and FERMI [2]) compared the perturbations to these which occur in a VAN DER WAALS gas, while PLANCK [3]) considered the electrical perturbations due to the Coulomb-field of perturbing ions. This last effect has been recently treated by UNSÖLD [4]); he calculates the maximum potential energy which a bound electron can have in the neighbourhood of a perturbing ion, and puts this equal to the energy of the highest excited level which actually occurs. The probability that no perturbing ion is found within a distance r of the atom will be $e^{-\frac{4\pi}{3}N_1 r^3}$, where N_1 is the number of perturbing ions per cm³. For the case when this probability is e^{-1}, UNSÖLD finds that the highest quantum number which occurs is:

$$\log n^* = 1{,}62 + \tfrac{2}{3}\log Z - \tfrac{1}{6}\log P_e - \tfrac{1}{6}\log \vartheta, \quad \ldots \quad (1)$$

Z being the effective nuclear charge of the perturbed particle, P_e the electron pressure in dynes/cm²; $\vartheta = \dfrac{5040}{T}$.

2. *Perturbations by neutral atoms.*

Since the ionisation in the exterior layers of a star is relatively small, we may ask whether the perturbations by ions will be more considerable than these by neutral atoms; practically among these last ones we shall have to consider only the hydrogen atoms, because of their overwhelming abundance. These perturbations have been studied by FÜCHTBAUER [5]) and his collaborators in beautiful experiments; they are ascribed by FERMI [6]) to two different effects:

1. the perturbing atoms penetrate between the excited electron and the atomic nucleus; they are polarized in the field of the perturbed atom, which produces a change in the energy of the excited electron;

2. the excited electron in its orbit encounters several sharp potential holes, due to the presence of perturbing atoms; by this the total energy of the atom is modified.

In FÜCHTBAUER's experiments, the influence of the potential holes proved more important than that of the polarization. However, these experiments were made at pressures of at least 1 atmosphere and at temperatures between 350° K and 750° K. Such temperatures and pressures are very different from these, prevailing in a stellar atmosphere. A rough estimate shows, that in the solar atmosphere the polarization effect is the more important one; for this is proportional to the number of disturbing particules N, while the first effect is only proportional to $N^{1/3}$. Thus the low pressure and the high temperature both tend to diminish the perturbations, but this influence is more important for the potential holes. In the solar atmosphere, at an optical depth $\tau_0 = 0{,}75$, where $\log T = 3{,}79$, $\log P_g = 4{,}9$, the perturbation by polarization is about 5 times stronger than the perturbation by potential holes.

3. *A comparison between the perturbing effect of atoms and that of ions.*

The polarization effect is due to an interaction between the disturbed atoms or ions and the perturbing H-atoms. This problem has been treated by WEISSKOPF [7]). The interaction energy amounts to $E = \frac{e^2\,\alpha\,\overline{R^2}}{r^6}$, where $\alpha =$ polarisability of the hydrogen atom, $\overline{R^2} =$ the quadratic mean value of the radius of the excited orbit. The mean value of R^2 over all atoms with the same principal quantum number n and different auxiliary quantum numbers l, is found to be $\overline{R^2} = \frac{n^2}{2}\, a^2 \cdot 4n^2$ ($a =$ radius of the first BOHR orbit).

Ionization will take place if the interaction energy is equal to the energy which is needed for the ionization of the excited atom:

$$e^2 \cdot \frac{\alpha}{r^6} \cdot 2\,a^2\,n^4 = \frac{Rhc\,Z^2}{n^2} \quad \text{. . . . . (2}$$

By substituting the physical constants, we find

$$r = 8{,}56 \times 10^{-9} \times n \quad \text{. . . . . (3)}$$

The probability that there will be no perturbing H-atom within a distance r is: $e^{-\frac{4\pi}{3} N_H \cdot r^3}$.

So the correction factor which has to be applied to BOLTZMANN's distribution law, due to the perturbing influence of the hydrogen atoms, is found to be:

$$W_1 = e^{-\frac{4\pi}{3}\cdot\frac{P_g}{kT}\cdot r^3} = e^{-\frac{4\pi}{3}\cdot\frac{P_g}{kT}\cdot(8{,}56\times10^{-9})^3\cdot n^3} \quad \text{. . . . . . (4)}$$

The correction factor due to the influence of the ions is similarly:

$$W_2 = e^{-\frac{4\pi}{3}\cdot\frac{27\,e^6\cdot P_e}{(Rhc)^3\,Z^4\cdot kT}\cdot n^6} = e^{-\frac{4\pi}{3}\cdot 3{,}18\cdot 10^{-23}\cdot\frac{P_e}{Z^4\,kT}\cdot n^6} \quad . \; . \; . \quad (5)$$

The perturbations by ions are more important than these by H-atoms, if $W_2 < W_1$ vid. lic. if

$$\frac{4\pi}{3}\cdot 3{,}18\cdot 10^{-23}\cdot\frac{P_e}{Z^4\,kT}\cdot n^6 > \frac{4\pi}{3}\cdot\frac{P_g}{kT}\cdot(8{,}56\times 10^{-9})^3\cdot n^3.$$

Or, putting $Z = 1$, if the perturbed particles are neutral:

$$\log n > \tfrac{1}{3}(\log P_g - \log P_e) + 0{,}431 - 1. \quad . \; . \; . \; . \; . \quad (6)$$

Taking again $\tau_0 = 0{,}75$, $\log P_g = 4{,}9$ and $\log P_e = 1{,}5$, substitution in (6) yields: $\log n > 0{,}46$, $n > 3$. For disturbed ions $W_2 < W_1$, if $n > 9$.

Consequently *the influence of the ions is more important than that of the neutral H-atoms*; for the correction factor becomes appreciable only for levels of high excitation ($n > 10$).

4. *Calculation of the partition function.*

When applying the laws of BOLTZMANN and SAHA, the partition function u is needed. We separate u into two parts:

$$u = \sum^{n_0} g_n\, e^{-\frac{E_n}{kT}} + u_1 = u_0 + u_1. \quad . \; . \; . \; . \; . \; . \; . \quad (7)$$

The number n_0 is selected according to the following conditions:

1. Levels for which $n < n_0$ are populated according to the exponential distribution law;
2. levels for which $n = n_0$ may be considered as hydrogen-like.

In view of the computation of u_1 we choose the same $n_0 = 7$ for all elements. It is true that for several elements lower levels could already be treated as hydrogen-like. However, a uniform choice of n_0 has the advantage of an easier computation of the u_1 term in (7). Let r be the multiplicity of the levels for which $n \geq 7$; then

$$u_1 \doteq \int_7^\infty r n^2 \cdot e^{-\frac{E_n}{kT} - \frac{4\pi}{3}\cdot\frac{27\,e^6}{(Rhc)^3\,Z^4}\cdot\frac{P_e}{kT}\cdot n^6} \cdot dn. \quad . \; . \; . \; . \; . \quad (8)$$

We substitute $E_n = E_i - \dfrac{13{,}53\,Z^2}{n^2}$ with E_i = ionization potential of the atom ($Z = 1$) or of the ion ($Z \doteq 2$). We introduce $\vartheta = \dfrac{5040}{T}$, and take exponentials of 10:

$$u_1 = r\cdot 10^{-E_i\vartheta}\int_7^\infty n^2\cdot 10^{\frac{13{,}53\,Z^2\,\vartheta}{n^2} - \gamma\cdot\frac{P_e\vartheta}{Z^4}\cdot n^6}\, dn \quad . \; . \; . \; . \quad (9)$$

where

$$\gamma = \frac{4\pi}{3} \cdot \frac{e^6}{(Rhc)^3} \cdot \frac{27}{k} \cdot \frac{0{,}4343}{5040}\,; \log \gamma = 0{,}922 - 11.$$

Now put

$$v(\vartheta) = \int_7^\infty n^2 \cdot 10^{\frac{C_1}{n^2} - C_2 \cdot n^6} \cdot dn \quad . \quad . \quad . \quad . \quad . \quad . \quad (10)$$

where the parameters $C_1 = 13{,}53\, Z^2 \vartheta$ and $C_2 = \gamma \cdot \dfrac{P_e \cdot \vartheta}{Z^4}$ are easily computed. Then finally:

$$u_1 = r \cdot 10^{-E_i \vartheta}\, v(\vartheta). \quad . \quad . \quad . \quad . \quad . \quad . \quad . \quad . \quad (11)$$

The function $v(\vartheta)$ is computed by subdividing the integration interval and by developing the integrand within each segment in a Taylor series of the first or second degree. If, for $n > n_1$, $\dfrac{C_1}{n^2} \ll C_2\, n^6$,

$$\int_{n_1}^\infty n^2 \cdot 10^{\frac{C_1}{n^2} - C_2 n^6} \cdot dn = \int_{n_1}^\infty n^2 \cdot 10^{-C_2 \cdot n^6} \cdot dn =$$

$$= \frac{1}{6} \sqrt{\frac{\pi}{2{,}3026 \times C_2}} \cdot \{1 - \Phi\,(n_1^3 \cdot \sqrt{2{,}3026 \cdot C_2})\}.$$

The integral $v(\vartheta)$ converges and so does the partition function u. We computed this function $v(\vartheta)$ for neutral and for singly ionized atoms, for five values of ϑ. The relation between $\log v(\vartheta)$ and ϑ or $\log P_e$ is represented in fig. 1 and 2, for neutral atoms by the curves (1) and for ions by the curves (2). Practically $\log v$ is a linear function of $\log P_e$; in both cases $v \sim P_e^{-0{,}44}$.

The contribution $u_1 = r \cdot 10^{-E_i \vartheta}\, v(\vartheta)$ to the partition function u proves negligible for the ions of all elements, because of their high ionization potentials. For neutral atoms u_1 must be taken into account only for elements with low ionization potentials. If $E_i > 8$ Volt, u_1 can be entirely neglected.

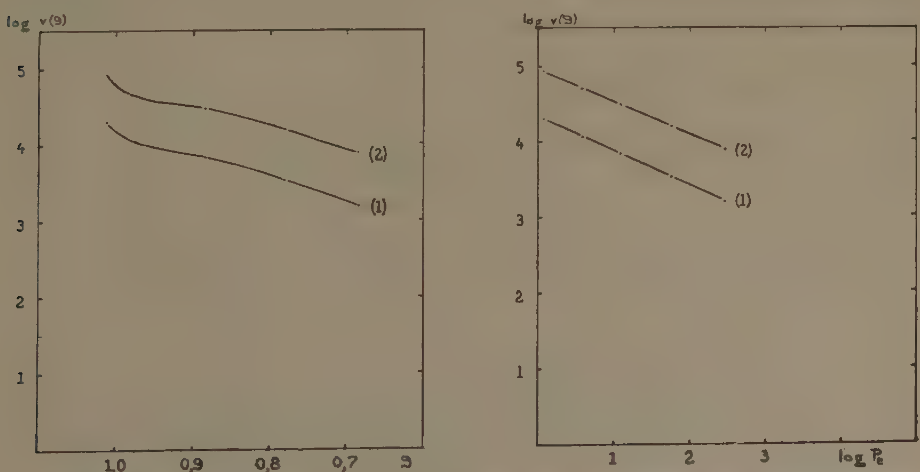

The auxiliary functions $v(\vartheta)$ and $v(P_e)$ in the solar atmosphere: (1) if the perturbed particles are atoms; (2) if they are ions.

For the easily ionized alcali metals, the contribution of u_1 is important; for these atoms, an appreciable influence of the electron pressure is found, next to the temperature influence. As we pass from the outer layers into the deeper parts of the solar atmosphere, the increasing temperature produces a stronger excitation of the high levels, while the increasing electron pressure produces an opposite effect. For most elements the influence of the temperature is preponderant; however, for the alcali metals and for *Ba* the pressure has the greater influence and u_1 decreases at first and increases only from a certain depth on (table 1).

TABLE 1. *Value of u_1 for easily ionized metals.*
Contribution of the higher levels ($n \geq 7$) to the partition function, at different levels of the solar atmosphere.

Element \ ϑ	1.022	0.980	0.939	0.817	0.781	0.684
Li	0.13	0.13	0.16	0.36	0.44	0.68
Na	0.23	0.22	0.28	0.58	0.68	1.00
K	1.54	1.36	1.57	2.62	2.85	3.48
Rb	2.22	1.92	2.22	3.55	3.80	4.53
Cs	4.42	3.68	4.11	6.15	6.46	7.11
Ba	0.40	0.38	0.49	1.03	1.21	1.82

We computed the contribution $u_0 = \sum^{n=6} g_n \cdot 10^{-E_n \cdot \vartheta}$ by adding the contributions of the individual levels. For elements with complicated electron systems so as *Ti, Fe, V, Co, Ni,* ...... terms with excitation potentials above $2V$ were combined into groups, and for each group a mean excitation potential was taken. Since u_0 depends only on ϑ, *our computations for u_0 may be used for all stellar atmospheres; however, u_1 applies only to the solar atmosphere,* since the concomitant influence of P_e which comes in is different from star to star. Table 2 gives u_0 and u for 4 values of ϑ.

5. Instead of introducing a correction factor to the BOLTZMANN distribution function, UNSÖLD [4]) proposes to limit the integration at the quantum number n^*, following from equation (1). The integral $v = \int_7^{n^*} n^2 \cdot 10^{\frac{C_1}{n^2}} dn$ is then to be computed by developing the exponential in a series and by integrating term by term. The result is practically the same as by our method, which gives bothways a very satisfactory confirmation. In UNSÖLD's method the influence of P_e is embodied in the choice of n^*. From a theoretical point of view our computation is slightly more satisfactory, since it does not cut off the integration in a rather artificial way at n^*.

It is a pleasure to thank Professor MINNAERT for stimulating discussions and criticism in the course of this investigation. I am grateful to Mr. B. B. VAN DEN HOORN for his kind help in translating FERMI's paper from "Il Nuovo Cimento".

TABLE 2. *The Partition Function.*

The contribution u_0 of the lower levels applies to any stellar atmosphere; the contribution of the higher levels and consequently the total partition function u applies only to the sun.

ϑ / Element	u_0				u			
	0.980	0.939	0.781	0.684	0.980	0.939	0.781	0.684
H	2.00	2.00	2.00	2.00	2.00	2.00	2.00	2.00
He	1.00	1.00	1.00	1.00	1.00	1.00	1.00	1.00
He+	2.00	2.00	2.00	2.00	2.00	2.00	2.00	2.00
Li	2.11	2.12	2.27	2.46	2.24	2.28	2.71	3.14
Li+	1.00	1.00	1.00	1.00	1.00	1.00	1.00	1.00
Be	1.02	1.03	1.07	1.13	1.02	1.03	1.07	1.13
Be+	2.00	2.00	2.01	2.01	2.00	2.00	2.01	2.01
B	6.00	6.00	6.00	6.00	6.00	6.00	6.00	6.01
B+	1.00	1.00	1.00	1.00	1.00	1.00	1.00	1.00
C	9.29	9.33	9.53	9.70	9.29	9.33	9.53	9.70
C+	6.00	6.00	6.00	6.00	6.00	6.00	6.00	6.00
N	4.05	4.06	4.15	4.26	4.05	4.06	4.15	4.26
N+	8.87	8.90	9.01	9.12	8.87	8.90	9.01	9.12
O	8.71	8.74	8.89	8.99	8.71	8.74	8.89	8.99
O+	4.01	4.01	4.03	4.05	4.01	4.01	4.03	4.05
F	5.66	5.68	5.73	5.77	5.66	5.68	5.73	5.77
F+	8.37	8.39	8.52	8.61	8.37	8.39	8.52	8.61
Ne	1.00	1 00	1.00	1.00	1.00	1.00	1.00	1.00
Ne+	5.36	5.39	5.49	5.55	5.36	5.39	5.49	5.55
Na	2.07	2.08	2.21	2.40	2.29	2.36	2.89	3.40
Na+	1.00	1.00	1.00	1.00	1.00	1.00	1.00	1.00
Mg	1.02	1.03	1.07	1.14	1.02	1.03	1.09	1.18
Mg+	2.00	2.00	2.00	2.01	2.00	2.00	2.00	2.01
Al	5.91	5.91	5.97	6.07	6.01	6.04	6.42	6.88
Al+	1.00	1.00	1.00	1.01	1.00	1.00	1.00	1.01
Si	9.61	9.71	10.06	10.35	9.61	9.71	10.07	10.37
Si+	5.77	5.79	5.81	5.84	5.77	5.79	5.81	5.84
P	4.46	4.53	4.90	5.26	4.46	4.53	4.90	5.26
P+	8.48	8.50	8.58	8.64	8.48	8.50	8.58	8.64
S	8.23	8.25	8.38	8.46	8.23	8.25	8.38	8.46
S+	4.17	4.20	4.40	4.61	4.17	4.20	4.40	4.61
Cl	5.30	5.32	5.44	5.50	5.30	5.32	5.44	5.50
Cl+	7.68	7.74	7.93	8.06	7.68	7.74	7.93	8.06
A	1.00	1.00	1.00	1.00	1.00	1.00	1.00	1.00
A+	4.90	4.93	5.11	5.20	4.90	4.93	5.11	5.20
K	2.22	2.25	2.62	3.07	3.58	3.82	5.47	6.55
K+	1.00	1.00	1.00	1.00	1.00	1.00	1.00	1.00
Ca	1.20	1.24	1.58	2.00	1.25	1.31	1.82	2.44
Ca+	2.23	2.27	2.50	2.74	2.23	2.27	2.50	2.74
Sc	12.21	12.67	15.50	18.94	12.23	12.70	15.62	19.19
Sc+	23.27	23.82	26.26	28.28	23.27	23.82	26.26	28.28
Ti	30.55	31.97	39.93	48.09	30.57	32.00	40.08	48.41
Ti+	56.49	58.18	64.30	69.41	56.49	58.18	64.30	69.41
V	49.45	51.23	61.15	71.31	49.48	51.28	61.37	71.78
V+	43.73	44.93	50.43	55.15	43.73	44.93	50.43	55.15
Cr	10.69	11.17	13.63	16.43	10.73	11.23	13.91	17 02
Cr+	7.34	7.59	9.11	10.79	7.34	7.59	9.11	10.79

TABLE 2. *(Continued.)*

Element \ ϑ	u_0 0.980	u_0 0.939	u_0 0.781	u_0 0.684	u 0.980	u 0.939	u 0.781	u 0.684
Mn	6.48	6.59	7.44	8.55	6.49	6.61	7.54	8.80
Mn+	7.77	7.89	8.57	9.23	7.77	7.89	8.57	9.23
Fe	26.93	27.86	32.59	36.60	26.93	27.87	32.63	36.76
Fe+	41.54	42.45	46.70	49.37	41.54	42.45	46.70	49.37
Co	31.94	32.97	38.14	42.80	31.94	32.98	38.17	42.89
Co+	28.13	29.06	32.95	35.90	28.13	29.06	32.95	35.90
Ni	28.95	29.42	31.67	33.52	28.95	29.43	31.70	33.61
Ni+	10.30	10.68	12.46	14.08	10.30	10.68	12.46	14.08
Cu	2.33	2.38	2.67	2.96	2.33	2.38	2.69	3.01
Cu+	1.03	1.05	1.10	1.21	1.03	1.05	1.10	1.21
Zn	1.00	1.00	1.01	1.02	1.00	1.00	1.01	1.02
Zn+	2.00	2.00	2.00	2.00	2.00	2.00	2.00	2.00
Ga	5.35	5.37	5.49	5.59	5.38	5.41	5.64	5.85
Ga+	1.00	1.00	1.00	1.00	1.00	1.00	1.00	1.00
Ge	8.21	8.34	8.87	9.27	8.21	8.34	8.88	9.29
Ge+	4.68	4.74	4.92	5.05	4.68	4.74	4.92	5.05
As	4.54	4.60	5.02	5.40	4.54	4.60	5.02	5.40
Se	5.91	6.00	6.43	6.70	5.91	6.00	6.43	6.70
Br	4.07	4.12	4.32	4.47	4.07	4.12	4.32	4.47
Br+	28.62	28.66	28.96	29.26	28.62	28.66	28.96	29.26
Kr	1.00	1.00	1.00	1.00	1.00	1.00	1.00	1.00
Kr+	3.68	3.72	3.91	4.06	3.68	3.72	3.91	4.06
Rb	2.28	2.33	2.75	3.28	4.20	4.55	6.55	7.81
Rb+	1.00	1.00	1.00	1.00	1.00	1.00	1.00	1.00
Sr	1.28	1.34	1.74	2.25	1.41	1.51	2.25	3.09
Sr+	2.18	2.21	2.42	2.65	2.18	2.21	2.42	2.65
Y	12.24	12.79	16.12	19.77	12.27	12.83	16.29	20.11
Y+	14.49	14.89	17.02	18.85	14.49	14.89	17.02	18.85
Zr	36.08	38.15	48.95	59.68	36.10	38.18	49.07	59.94
Zr+	47.72	49.54	57.75	64.52	47.72	49.54	57.75	64.52
Cb	25.68	25.85	26.82	27.63				
Cb+	36.12	36.86	39.64	41.68	36.12	36.86	39.64	41.68
Mo	8.82	9.12	10.93	12.85	8.83	9.13	11.00	13.03
Mo+	7.56	7.77	8.91	9.98	7.56	7.77	8.91	9.98
Ru	28.05	29.32	35.02	39.71	28.05	29.33	35.05	39.79
Ru+	19.74	20.50	23.75	26.40	19.74	20.50	23.75	26.40
Rh	24.39	25.32	29.70	33.44	24.39	25.32	29.72	33.49
Rh+	19.27	20.03	23.47	25.54	19.27	20.03	23.47	25.54
Pd	2.87	3.07	4.01	4.85	2.87	3.07	4.01	4.86
Pd+	6.86	6.95	7.33	7.62	6.86	6.95	7.33	7.62
Ag	2.00	2.00	2.01	2.02	2.00	2.00	2.02	2.04
Ag+	1.00	1.00	1.00	1.01	1.00	1.00	1.00	1.01
Cd	1.00	1.00	1.01	1.02	1.00	1.00	1.01	1.02
Cd+	2.00	2.00	2.00	2.00	2.00	2.00	2.00	2.00
In	4.62	4.66	4.85	4.97	4.67	4.73	5.07	5.33
In+	1.00	1.00	1.00	1.00	1.00	1.00	1.00	1.00
Sn	6.49	6.63	7.22	7.69	6.49	6.64	7.25	7.75
Sn+	3.92	3.97	4.17	4.31	3.92	3.97	4.17	4.31
Sb	4.83	4.93	5.44	5.89	4.83	4.93	5.45	5.91

TABLE 2. (*Continued.*)

Element \ ϑ	u_0 0.980	u_0 0.939	u_0 0.781	u_0 0.684	u 0.980	u 0.939	u 0.781	u 0.684
Te	4.87	5.00	5.59	6.05	4.87	5.00	5.59	6.05
X	1.00	1.00	1.00	1.00	1.00	1.00	1.00	1.00
Cs	2.50	2.57	3.17	3.87	6.18	6.68	9.63	10.98
Cs+	1.00	1.00	1.00	1.00	1.00	1.00	1.00	1.00
Ba	2.49	2.66	3.87	5.06	2.87	3.15	5.08	6.88
Ba+	4.38	4.48	5.16	5.69	4.38	4.48	5.16	5.69
La	20.74	21.47	25.15	28.56	20.99	21.80	26.08	30.08
La+	30.93	31.90	36.71	40.82	30.93	31.90	36.71	40.82
Eu+	13.44	13.55	13.99	14.42	13.44	13.55	13.99	14.42
Yb	1.05	1.07	1.17	1.28	1.09	1.12	1.36	1.63
Yb+	2.00	2.00	2.01	2.02	2.00	2.00	2.01	2.02
Lu	8.01	8.11	8.61	9.06				
Lu+	1.46	1.54	2.00	2.45	1.46	1.54	2.00	2.45
Hf+	13.71	14.40	17.75	20.73	13.71	14.40	17.75	20.73
Re	6.08	6.10	6.26	6.48	6.08	6.11	6.30	6.58
Pt	16.27	16.55	17.95	19.14	16.27	16.55	17.95	19.15
Au	2.40	2.46	2.70	2.92	2.40	2.46	2.70	2.92
Hg	1.00	1.00	1.00	1.00	1.00	1.00	1.00	1.00
Hg+	2.00	2.00	2.00	2.00	2.00	2.00	2.00	2.00
Tl	3.34	3.37	3.53	3.66	3.37	3.41	3.65	3.88
Tl+	1.00	1.00	1.00	1.00	1.00	1.00	1.00	1.00
Pb	3.50	3.57	3.85	4.09	3.50	3.57	3.87	4.15
Pb+	3.06	3.07	3.13	3.19	3.06	3.07	3.13	3.19
Bi	4.28	4.32	4.57	4.82	4.29	4.33	4.61	4.93
Bi+	3.10	3.11	3.22	3.34	3.10	3.11	3.22	3.34
Ra+	2.01	2.01	2.03	2.06	2.01	2.01	2.03	2.06

LITERATURE.

1. UREY, Ap. J. **49**, 1 (1924).
2. FERMI, Zs. f. Physik **26**, 54 (1924).
3. PLANCK, Annalen der Physik **75**, 673 (1924).
4. UNSÖLD, Zs. f. Ap. **24**, 355 (1948).
5. FÜCHTBAUER and collaborators, Zs. f. Physik **87**, 89 (1934); **89**, 63 (1934); **90**, 403 (1934).
6. FERMI, Il Nuovo Cimento, Nuova Serie, **11**, 157 (1934).
7. WEISSKOPF, Phys. Zs. **34**, 1 (1933); see also UNSÖLD, Physik der Sternatmosphären, p. 282 (1938).

Zoology. — *An electron-microscopical study of sperm IV.* (The sperm-tail of bull, horse and dog.) By L. H. BRETSCHNEIDER. (From the Zoological Laboratory, Utrecht, and the Department of Electron Microscopy, Delft.) (Communicated by Prof. CHR. P. RAVEN.)

(Communicated at the meeting of March 26, 1949.)

I. *Introductory.*

It was to be expected that a better insight into the structure of the tail of the spermatozoon could be obtained with the aid of electron-microscopic investigation than was previously possible by light-microscopy. To obtain a more or less satisfactory explanation of the complicated motorial automatism of the tail, it was necessary first to determine its morphological foundation. Our hitherto published communications (I, II, III) on this side of the question were confined to a description of the general structure of the tail; meanwhile, however, we have gained further knowledge of additional details, thanks to our being able to examine also the sperms of other animals besides the bull. Although the structural principle of the tail, so far as mammals are concerned, shows considerable mutual correspondence, our investigation nevertheless showed that a given structure can be analyzed far more easily in one species than in another, so that the facts obtained from the various species may be taken as mutually supplementary. One may pose the problem in the following way: "what is the structure of the mammalian sperm, as shown bij electron-microscopic examination?"

II. *Technique.*

As in our previous work, the investigation was carried out with the aid of the electron microscope of the Institute for Electron-Microscopy at Delft, at an emission voltage of between 80, 90, and 100 kv. For the technique we refer to our Communication No. III (L. H. BRETSCHNEIDER, 1949).

In addition to the techniques described therein, we also used in the present case a 5 % phenol solution, 10—20 drops of which, to 10 cm^3 aq. dest., was added to the suspension of spermatozoa in aq. dest. or in buffer solution.

This substance has a markedly corrosive action on proteins.

III. *The Neck region.*

The neck region, the articulation between the middle piece and the base of the head consists essentially of a sort of wreath formed by a number of points of attachment of sub-fibrils. The fasciculation of these

sub-fibrils into at least 2 articular bundles must be regarded as a secondary phenomenon. The neck region is covered on the outside by a thick membrane originating in the tail-collar which, only in the neck region, is strengthened by spiral bands and runs along covering the middle piece as a smooth membrane.

The variations in size and arrangement of the different parts of the neck, to be observed repeatedly in our electron-microscopic pictures, are caused by artificial changes occuring during the necessary drying process in the vacuum. The neck, as articulation point, is a most vulnerable part even in the living sperm; it is possible, under certain conditions, for the head to break off at this place. Thus, for example, the tail and the head may during the drying process, attach themselves to the substrate over a relatively large area, so that, during dehydration and its attendant shrinking effect, there is a force pulling at the neck region on both ends. The result of this is that the dimensions of the neck region, which is thus stretched, become greater than they naturally are. Added to this is the fact that, during dehydration, the originally cylindric neck region gets flattened, and becomes much broader. Only after fixation — when, may-be, the proteins have become more resistant against stretching —, say, with OsO_4, mercurochrome, Carnoy's mixture do the shape and size of the neck most conform to the natural state. But in this condition, by the compactness of the neck region, it becomes most difficult to get anything like an accurate picture of the various structural details. Thus, after previous fixation, the neck of the bull sperm had a length of 400 mμ and a width of 600 mμ, whereas after maximum stretching and without previous fixation the length was 800 mμ and the width 1 μ. In fact, the appearance of the neck region changes all according to the extent of these artificial modifications. This fact has led to differences of opinion, both in former light-microscopic research, but again in electron-microscopic investigations. The greater this flattening and deformation of the neck, the more details become visible, because it causes the enveloping membrane to tear open, whereby the fibrillar contents of the neck are spread out on a flat surface, whereas in the natural position, these structures cover one another and are closed in by the membrane. In the case of only slight flattening, we see two lateral bundles; when the flattening is more marked the number of fibrillar structures increases through spreading. Moreover, by proteolysis with bacterial enzymes, trypsin, chloramine-T or phenol (see technique in Part III), which act as solvents on all structures surrounding the fibrillar axis, we laid it bare as far as possible and so were better able to analyze it.

We also obtained further insight by comparing the spermatozoon of the bull with those of other species (horse and dog). It appears from the various data obtained that 8 out of the nine subfibrils of which the axis consists are each individually attached to the base of the head by a thickened insertion, as a shown in fig. 1 of the horse's sperm. These 8

insertion points are arranged in the form of a wreath around the central fibril No. 9, which, in its turn, is attached to the centrosome (*vide* the diagram, L. H. BRETSCHNEIDER, 1949). For the sake of better comparison, we have numbered these insertion points from left to right. In the projection — i.e. as we view the spermatozoon, as a rule, from one of its flat sides — we observe three fasciae, covering one another, whereas, in the case of maximum broadening of the neck region, the fibrils arrange themselves side by side, so that a greater number are laid bare. Owing to lack of room near the narrow base of the head, the sub-fibrils join up already at their insertion points in sets of two, three or four, thus forming a common insertion basis with a form of its own. This fusion may be clearly seen in fig. 3 and 5. The common basis of such an articular fascia, seen from above, shows a horse-shoe-like shape; viewed laterally, it is claviform, and fits with its slightly dome-shaped top into a correspondingly pan-shaped hollow of the base of the head. Between the respective surfaces of the two, there is a probably proteinic binding substance, which, when strongly stretched, pulls out into threads. The united sub-fibrillae too appear to be connected by a binding substance, because, after proteolytic treatment, their common insertion base falls apart into clean, separate sub-fibrils.

The centre of the base of the head has a crater-shaped, sunken part and contains the centrosome, whence the sub-fibril No. 9 begins. The entire neck region is covered by a membrane, which, anteriad, closes over the distal half of the head, and posteriad over the middle piece; this membrane orginates in the tail-collar. In this membrane, only in the part covering the neck region proper, there are, at regular distances, band-shaped thickenings, by way of strengthening structures. Around the wreath of fibrillea-insertions and against the base of the head, the 100—140 mμ wide "neck-ring" closes like a band. Just behind this neck-ring, a narrower band commences, of about 40—60 mμ, which runs in the form of a sinistrogyrate spiral as far as the beginning of the middle-piece, where it ends. We found, in the bull sperm, 10—12 windings (fig. 5); in the dog's sperm, 15—17 windings (fig. 6). The distance between the band-shaped windings is only $\pm$ 20 mμ, generally even less. Especially shadow-casts show up these bands to be elevations that should be regarded as local thickenings of the neck-membrane. The blacker colouring in the pictures is caused by the greater thickness of the structures that cover each other. From the last winding of this band, the membrane runs like a smooth enclosure along the rest of the middle piece as far as JENSEN's ring, at which point the cortical spirals of the tail membrane begin. Our original assumption that the neck region itself contains no spirals, and that the cortical spirals run uninterruptedly from the middle piece to the end of the tail, was shown on closer examination to be erroneous. We believed at first that the deeper black shown by the spiral bodies on the photographs covered and concealed

the course followed by the cortical spirals, so that they only became visible again at the tail. But both after shadow-casting and in one particular case, in which, owing to a secondary breach in the middle piece, the membrane at this spot was laid bare (fig. 2), it was shown that this membrane contains no spirals whatever. In the figure mentioned, we see the membrane, within the small curvature of the breach, torn away from the deeper layer, and slightly curled up on both sides, but otherwise perfectly smooth and homogeneous. It is evident, from the greater material now at our disposal, that, so long as the neck-membrane is not stretched and remains in its natural state, the spiral bands in the neck region close around it quite smoothly (*vide* 1947, fig. 4). Bij stretching, either longitudinally or laterally or both, the membrane bursts, and, with that, the spiral band also breaks to pieces. When this happens, it appears that the fibrillar structures underneath and the neck-membrane are so firmly joined together that the spiral fragments *ad locum* still adhere to the sub-fibrils (Fig. 1 and 7). This phenomenon at first led us to assume that the sub-fibrils showed regular cross-striations (L. H. BRETSCHNEIDER, 1947). Another point to be noted is that, in the case of extreme stretching of the sub-fibrils in the neck region, those parts of the fibrils to which a spiral fragment adheres are not stretched so much as the parts in between, a phenomenon which causes the sub-fibrils to show, at regular distances, thickenings and narrowings (Fig. 1). (*Vide* also L. H. BRETSCHNEIDER and W. VAN ITERSON, 1947).

IV. *The axial filament.*

The axial filament, which forms the fibrillar axis of the whole of the tail, consists — in the spermatozoa of the three species named — of 9 sub-fibrils, which, in the middle piece, are of unequal thickness. We can distinguish 2—3 classes of thickness; not until they get to the tail proper do the fibrils become of equal thickness. The widest of the sub-fibrils show an ellipsoid cross-section; the thinner ones are round, while their thickness decreases from the anterior towards the posterior end. In the middle piece the fibrils group themselves into two articular fasciae and a central fibril; in the tail proper they gradually form more and more a common compact, rod-shaped axis.

This composition of the axial filament, i.e. of 9 sub-fibrils, is not clearly seen until the different components surrounding the axis are removed. To this end we used trypsin (technique 6), chloramine-*T* (technique 4), and phenol. After careful corrosion nothing but the axial filament remains, which divides up into the single sub-fibrils. In pathologically modified sperms, in which the axial filament is characterized bij unequal length of the sub-fibrils, the latter, thanks to their being more loosely interconnected, can be analyzed more easily (fig. 8).

After treatment with trypsin or chloramine-*T*, the head usually breaks off owing to the binding substance being dissolved, so that the tail is laid

bare for inspection up to the point of its insertion. By this treatment JENSEN's spiral bodies, the tail plasma and the cortical membrane are also dissolved, so that nothing remains but the axial filament. It appears from a reconstruction of three successive photographs of such an axial filament (fig. 3) that 4 of the sub-fibrils are thicker, whereas 5 are thinner. From other pictures we may conclude that each articular fascia at the beginning of the filament is composed of two thick and two thinner fibrils. Each time two thicker fibrils lie together; they are adjoined by two thinner ones, so that we get the arrangement shown in fig. *A*. If we

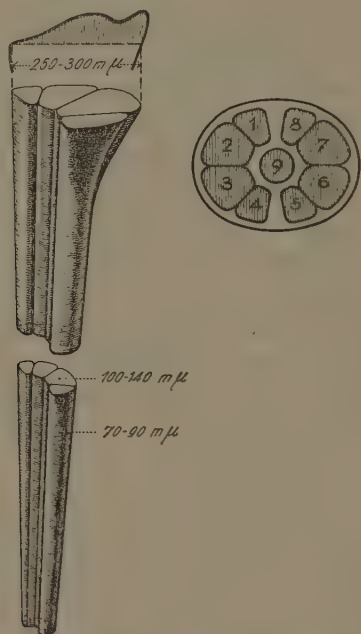

A. Articular strand and arrangement of the sub-fibrils in the middle piece.

project these on to the base of the head, and number the fibrils from left to right, they show a symmetrical picture in respect of the two transverse axes of the head. The size of the band-shaped sub-fibrils Nos. 2, 3, 6 and 7, immediately behind the neck, is $\pm$ 100—140 mμ; at the beginning of the tail, 80—100 mμ, and at the end of the tail, like the other sub-fibrils, 30—40 mμ. The fibrils Nos. 1, 4, 5, 8 and 9 measure, behind the neck, 70—90 mμ; at the beginning of the tail, 50—70 mμ, and at the end again 30—40 mμ. In some cases the central fibril (9) was already at the beginning of the tail, only 40—50 mμ, thick, and again, at the end, 30—50 mμ. From the arrangement of the fibrils in the dog's sperm (fig. 7) it follows that, in this case, the pairs of fibrils Nos. 1 and 8, and 4 and 5 each possess a common insertion, and are placed crosswise in respect of the two pairs 2 and 3, and 6 and 7. The independent position of fibril No. 9 is evident, among other things, from fig 8, taken

from a bull sperm, in which one of the articular fasciae (right) possesses longer sub-fibrils thans the other (left). The difference in thickness, too, is plainly visible here. Whereas, in some cases, the tail has a somewhat twisted course, it may be seen from the fact that it gets thinner at the points where it is twisted that it is not cylindrical in shape, but slightly flattened in the same direction as the flattening of the head. In the middle piece the four fibrils that are united into one articular fascia are shifted slightly towards one side, so that there is a small space between the two articular fasciae. Viewed, therefore, from the flattened sides, a light zone is visible between the fasciae (fig. 4). On looking from the narrow edge, one sees the entire width of an articular fascia. Only after the four thicker fibrils, referred to above, become thinner does the space between also disappear, after which the 8 sub-fibrils run like a regularly formed cylinder around the central fibril No. 9.

The axial filament is enveloped in a plasma covering. In the middle piece the two spiral bodies of JENSEN are embedded in this plasma covering, while, in the tail, the plasma fills the space between the filament and the cortical membrane in a homogeneous layer.

V. *Discussion.*

On comparing our electron-microscopic findings in regard to the mammalian spermatozoon with the light-microscopic observations of previous authors, we shall be able either to rectify or to formulate more concretely certain statements. Thus, it has been customary — for understandable reasons, such as the extreme smallness of the structures to be investigated, whose sizes are in the neighbourhood of 0,1 μ — to regard the thickened insertion base of the articular fasciae, light-microscopically, as granula. In the same way, the fragments of the spiral bands in the neck region, which fall asunder after dehydration, present the appearance, when seen light-microscopically, of more markedly stainable granula. Since the separate bands, as such, are invisible by light-microscopic means (40—60 mμ), they can only be observed by this means, if a fairly large group of them are joined together. As early as 1886, BALLOWITZ described, in the two diverging articular fasciae, the insertion with the aid of a granulum which he took to be a divided centrosome. Later, MEVES (1899), in his classic investigation on the Cavia sperm, described three proximal and three distal granula in the neck region, which he considered to be derivatives of the proximal and distal centrosome, respectively. RETZIUS (1910) gives a number of illustrations showing, on the articular fasciae, and even on the sub-fibrils, three granula (centrosome derivatives), one behind the other; this shows that this eminent investigator already succeeded in distinguishing certain separate, adjoining bands in the neck region. Thanks to the theory of the identity of centrosomes and basal granula of cilia and flagella — formulated independently by both LENHOSSEK and HENNEGUY (1898), this

problem was also transferred to the granula in the neck of the sperm, which were regarded as belonging to the same class. Many an explanation relative to the movement of the tail was also connected up with the same theory. In spite of the fact that this theory has been abandoned long since, and that no indication has ever been found of the existence of a division of the centrosome into basal granula during spermiogenesis, the term "centrosome derivatives" to denote a series of neck region granula has maintained itself up to the present. No doubt we may conceive the thickened insertion bases of the sub-fibrils — correspondingly to the structure of similar motorial organella as vibrissae, cilia and flagella — as "basal granula". On comparing these organella with the sperm tail we find, indeed, an essential correspondence and only a difference in degree. According to KOLTZOFF (1906), ERHARD (1909), KLEIN (1926–'32), the vibrissae of cells and the cilia of the Ciliata possess a central fibril by way of a fixed axis. BROWN (1945) found, for the flagella of Flagellates — electron-microscopically — two axial fibrils, while, already since BALLOWITZ (1886–1912), the structure of the axial filament in spermatozoa has been known to consist of several fibrils. Thus, we found, up to the present, 9 sub-fibrils in the bull, the horse, the dog *Myotis* and *Gallus*. HARVEY & ANDERSON (1943) found, in *Arbacia*, 9—10 sub-fibrils. BALLOWITZ found 9 sub-fibrils in *Fringilla*, *Copris*, *Chrysomela*, *Colothus*, and *Hydrophilus*. We ourselves found 18 sub-fibrils, i.e. a multiple of 9 — in *Cavia*. In cilia, flagella and the sperm tail this fibrillary axis is enveloped by a plasmatic enclosure forming a more or less firm membrane, which finishes before the end of the fibrillary axis, the latter finishing as a free terminal piece. Both in the case of the flagella of Flagellates and in that of the sperm tail, spiral fibrils run in the cortical membrane around the organellum (BROWN, 1945); while KLEIN (1929) also observed in the cilia of the Ciliates — with the aid of silver nitrate — rings placed at regular distances (although explaining these differently). In every case there is a basal granulum at the basis. All according to the size of the motorial organellum, we therefore find more or fewer fibrils in this axis, the plasmatic envelope being accordingly thicker or thinner, respectively, and the basal granulum either larger or smaller. We may say, therefore, that the differences between cilia, flagella and sperm tails are merely gradual ones.

Notwithstanding the fact that BALLOWITZ (1886–1912) and RETZIUS (1909–1912) already demonstrated the insertion of the articular fasciae immediately at the base of the head, we still continue to find — even in the most recent textbooks —, in the schemata of the mammalian sperm, the insertion of the tail being placed only behind the "neck": MAXIMOV (1945); ROMEIS (1938); METZ (in Cowdry, 1934); BRANCA and VERNE (1942); DE GROOT (1944), amongst others. The neck is described as an envelope which is supposed to contain merely a clear "filling" or "connecting substance". The composition of the axial filament of

individual sub-fibrils, too, which was discovered as early as 1879 by Jensen, and by Ballowitz in 1886, still continues to be known under the indifferent name of "involucrum". If there is anything at all that "envelops", then it is the plasma envelope surrounding the axial filament, not the sub-fibrils, which, on the contrary, constitute the central, fixed axis.

Following the above rectification of certain older results, we would briefly revert to our own observations, which too need some correction. As we intend to explain in more detail in subsequent communications, the beginning of the spiral body of Jensen is situated, in different spermatozoa — also in those of the same species — at varying levels. In cases where it is not placed immediately at the beginning of the middle piece, we see that the 10—17 spiral bands of the neck region continue their course some way into the middle piece. This fact led us to assume, at first (1947), that these spiral bands run along the entire tail, including the middle piece, without interruption. We have rectified this erroneous supposition in the diagram in fig. *B* (Part. III). Further, the cross striation of the sub-fibrils, which we believed to have observed, turned out to have been suggested simply by an artificial interruption of the spiral bands in the neck region. It was probably a similar erroneous interpretation that must have led Harvey & Anderson (1943) to affirm the presence of cross striations in the sperm tail of *Arbacia*. It was suggested electron-optically by the over-crossing of longitudinal fibrils and spiral fibrils.

VI. *Summary.*

With the aid of a renewed electron-microscopic investigation of three different mammalian sperms (bull, horse and dog), further structural details were described, supplementary to those previously published. By the application of proteolysis, or of phenol as a solvent, the axial filament was freed of all surrounding structures, thereby rendering it accessible to separate analysis. Comparative examination of the spermatozoa of different animal species facilitated the interpretation of structural details which could hardly be done justice to in the electron-optical investigation of a single species. A description is given of the insertion of the sub-fibrils with basal granula at the base of the head; their varying arrangement into articular fasciae; their thickness and their shape. A number of spiral bands giving firmness to the structure were convincingly, observed in the membrane of the "neck", which bands, in contrast to our previous assumption, come to an end at the beginning of the middle piece. The middle piece itself is surrounded by a smooth membrane; the cortical spiral fibrils begin only at Jensen's ring. The structures supposed by us to be "cross striations", at the beginning of the sub-fibrils, proved to be caused by artificial fragmentation of the band structures in the membrane of the neck region.

The writer desires to express his appreciation and gratitude to Miss W. VAN ITERSON and Dr A. L. HOUWINK for their assistance in the electron-microscopic documentation, and to the Landbouw-organisatie T.N.O. (Agricultural Organization for Applied Scientific Research), for the financial aid granted him for this research work.

LITERATURE.

BALLOWITZ, E., Handwörterbuch d. Naturwissenschaften, **9** (1913).
BRANCA, A. and J. VERNE, Precis d'Histologie. Masson, Paris (1942).
BRETSCHNEIDER, L. H. and W. v. ITERSON, Proc. Kon. Ned. Akad. v. Wetensch, Amsterdam, **50** (1947).
BRETSCHNEIDER, L. H., Proc. Kon. Ned. Akad. v. Wetensch., Amsterdam, **52** (1949).
BROWN, H. P., Ohio Journ. of Sci. **85** (1945).
EIMER TH., Verhandl. physic. med. Gesellsch. Wuerzburg, **6** (1874).
GROOT, A. DE, Leerboek bijzondere weefselleer, Oosthoek, Utrecht (1947).
HARVEY E. B. and TH. F. ANDERSON, Biol. Bull. **85** (1943).
HENNEGUY, Journ. d'Anat. et de la Phys. **27** (1891).
JENSEN, O. S., Struktur der Samenfaeden, Bergen (1879).
KLEIN, B. M., Arch. f. Protistenk., **65** (1929).
KOLTZOFF, N. K., Biol. Zentralbl. **26** (1906).
LENHOSSEK, M. v., Arch. f. mikr. Anat. **51** (1898).
———, Verhandl. Anat. Ges., Kiel (1898).
MAXIMOW A. A. and W. BLOM, Textbook of Histology, Saunders, N. York (1930).
METZ, CH. W. in E. V. COWDRY, Special Cytology, Hoeber, N. York (1934).
MEVES, F., Arch. f. mikr. Anat., **54** (1899).
RETZIUS, G., Biologische Untersuchungen, Stockholm (1881—1912).

EXPLANATION OF FIGURES.

Fig. 1. Horse sperm with sub-fibrils after chloramine. Shadow cast. Orig. magn. 20.000 ×.

Fig. 2. Bull sperm. Fragment of middle piece with subfibrils and membrane. Orig. magn. 65.000 ×.

Fig. 3. Bull sperm. Axial filament after digestion with trypsin and impregnation with OsO_4. Orig. magn. 20.000 ×.

Fig. 4 and 5. Bull sperm. Articular strands and neck with spiral bands. Orig. magn. 25.000 ×.

Fig. 6 and 7. Dog sperm. Spiral band of the neck and sub-fibrils after phenol. Orig. magn. fig. 6: 23.000 ×, fig. 7: 20.000 ×.

Fig. 8. Abnormal bull sperm with loose sub-fibrils. Orig. magn. 20.000 ×.

Fig. 1 and 2.

Fig. 3, 4 and 5.

⊢⊣ Indicates 1 μ in all pictures.

Fig. 6 and 7.

Fig. 8.

L. H. BRETSCHNEIDER: *An electron-microscopical study of sperm IV.*
(The sperm-tail of bull, horse and dog.)

Zoology. — *Spermiation in Rana and Salamandra*. Preliminary note [1]).

By G. J. VAN OORDT, F. CREUTZBERG and N. SPRONK. (Zoological Laboratory, Dept. of Endocrinology, University of Utrecht.) (Communicated by Prof. CHR. P. RAVEN.)

(Communicated at the meeting of April 23, 1949.)

In 1929 HOUSSAY and LASCANO GONZALEZ showed that after transplantation of the anterior part of the mammalian pituitary in male specimens of *Bufo arenarum* sperms are released from the testes in a remarkably short time. This observation has been confirmed later by RUGH (1935) in *Rana* and by many others; from it GALLI-MAININI (1947) derived his pregnancy-test, for which many species of *Bufo*, as well as of *Rana*, may be used.

In a recent communication (VAN OORDT and KLOMP, 1946) we have introduced the term s p e r m i a t i o n for the liberation of sperms from the testis, a term which is analogous to ovulation, the process of discharging the ova from the ovary.

The subject of the present investigation is a study of spermiation in representatives of Anurans and Urodeles. As experimental animals hibernating *Rana esculenta* and *temporaria* and *Salamandra salamandra* were used.

We have found on the one hand that spermiation can be provoked easily by gonadotrophins [2]) in these species; on the other hand important differences were observed in the way in which this process takes place in Anurans and Urodeles respectively.

Rana spec. In intact *Rana*-specimens spermiation is accomplished easily after administration of gestyl, a pregnant mare serum gonadotrophin, or pregnyl, a pregnancy urine preparation. In a specimen of *Rana esculenta*, which has been injected with a dosis of 2—3 I.U. of pregnyl pro gram body-weight, sperms are already found in the cloacal urine after about 1 hour.

As we were also interested in the resumption of spermatogenesis in the testis tubules after spermiation, we have tried, by repeated injections, to get testis tubules totally free from sperm. However, in *Rana* it is extremely difficult to accomplish this phenomenon. After 9 doses of pregnyl had been administered in 22 days to a specimen of *Rana esculenta*, most of the testis-tubules were not yet empty (fig. 1).

In this species it was difficult to ascertain, whether a resumption of spermatogenesis took place after administration of such a large quantity

[1]) 26th communication of the "Werkgemeenschap voor Endocrinologie", part of the "National Council for Agricultural Research T.N.O.".

[2]) These preparations were kindly supplied by the Direction of Organon N.V., Oss.

of pregnyl, as control specimens may also show many spermatogenetic cysts in the tubules of the winter-testis. In *Rana temporaria* however, in which the testis-tubules contain only very few spermatogonia and numerous compact sperm-bundles in winter, the formation of spermatogenetic cysts and therefore the resumption of spermatogenesis was very distinct in several cases after 3 or more gestyl-injections (fig. 2). Of course this spermatogenesis may be provoked by the pituitary, as the experimental frogs were not hypophysectomized, but it seems more likely that the resumption is (directly?) caused by the injected gonadotrophins.

From the above follows that in *Rana* spec. there is a distinct, direct (?) influence of pregnyl on the testis-tubules, which results in the liberation of sperms from these tubules.

Salamandra salamandra. It is a well-known fact that in Urodeles the testis structure is very different from that of the Anurans. In the newts (*Triturus* spec.) as well as in the Spotted Salamander (*Salamandra salamandra*) the winter-testis possesses numerous tubules, filled with bundles of sperm, loosely attached to Sertoli-cells, and with very few spermatogonia and tubules, totally filled with germ cells in the early spermatogenetic stage (especially spermatogonia) which show very few or no cell-divisions. These tubules form two areas, which may be called the sperm- and the spermatogenetic part, with a transition-zone between them (fig. 3). The testis of *Salamandra* belongs to the multiple type; in every lobe a sperm- and a spermatogenetic part are present, whereas in the narrow connecting tissue only male primary sex cells are to be found.

Spermiation is very easily caused in the sperm-part. Already after 2 doses of 4—5 I.U. of gestyl pro gram body-weight (the second dose given 48 h. after the first) practically all sperms are released from the testis-tubules and 5 h. after the second injection the testis is totally devoid of sperms (fig. 4).

Moreover, it is interesting that in experimental as well as in control salamanders, killed by means of chloroform, sperm and mucus were present in the cloaca, even before they died, but that in the cloaca of control salamanders which had been decapitated, no sperm or mucus secreted by the cloacal glands could be found. Between the experimental animals and the controls, however, there was a conspicuous quantitative difference, which became especially distinct on microscopical investigation of the testes: control specimens which had been killed by chloroform showed little spermiation, whereas in gonadotrophin-treated animals spermiation was mostly total and the efferent ducts of the testis were packed with sperm.

After spermiation the following processes take place in the "empty" testis-tubules (fig. 4):

1. a distinct increase in size of the Sertoli cells, which pass over into large inflated cells, filling almost the whole diameter of the tubules, and
2. the formation of large cells, very similar to male primary sex-cells.

G. J. VAN OORDT, F. CREUTZERG and N. SPRONK: *Spermiation in Rana and Salamandra.*

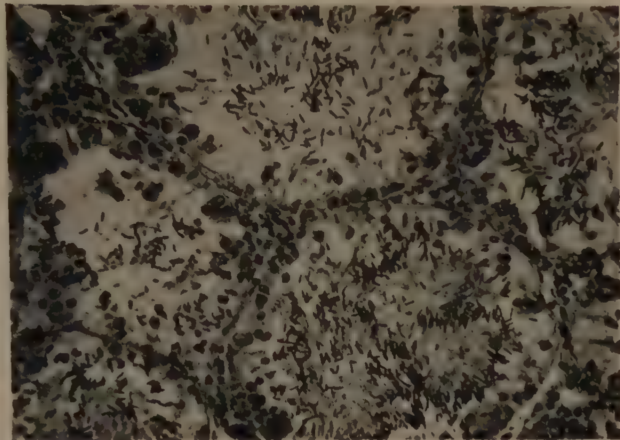

Fig. 1.

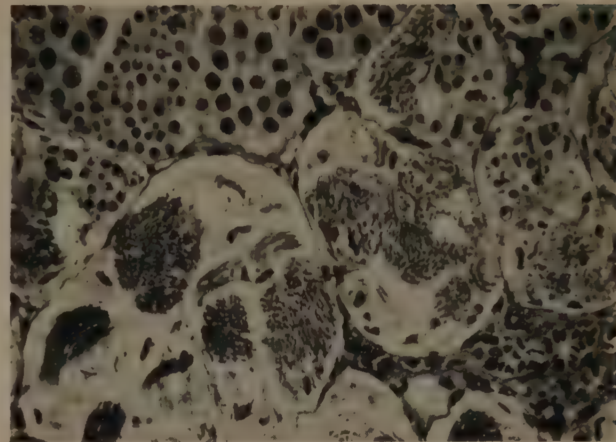

Fig. 3.

Fig. 2.

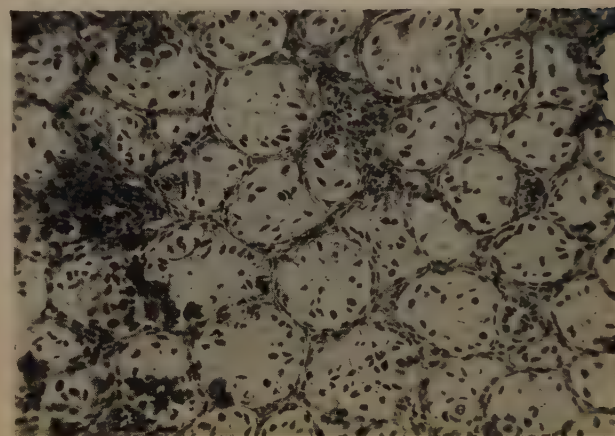

Fig. 4.

From the above it follows that spermiation can be caused by gonadotrophins in *Rana* as well as in *Salamandra*. The way in which spermiation takes place is very different, however: gradually in frogs, very rapidly in the salamander. Though we have given the salamanders a relatively larger quantity of gonadotrophic hormones than the frogs, we think that the differences in the way in which spermiation is accomplished may be explained with the help of the biology of the investigated animals:

Male frogs of most species generally possess large seminal vesicles in which sperm is stored before and during the breeding season. Therefore it is not necessary that sperms are liberated from the testis tubules at once, and we may assume that under a rather prolonged but weak influence of the anterior lobe of the pituitary, spermiation takes place gradually in spring. In the salamander, however, the formation of spermatophores, consisting of a large quantity of sperm and of mucus, secreted by the cloacal wall, is a process which must take place rapidly; hence, in the reproductive period the sperms are suddenly released from the testis in one large mass, presumably under the influence of a large amount of hypophyseal gonadotrophin. Therefore total spermiation can only be provoked experimentally by many repeated injections of gonadotrophins in *Rana* and by already 2 consecutive injections of these hormones in *Salamandra*.

Summary.

Spermiation, i.e. the process of liberation of sperms from the testis, can be provoked easily in *Rana* and *Salamandra* by means of gestyl as well as pregnyl. Consequently both gonadotrophins have a distinct (direct?) influence on the testis-tubules.

In *Rana* it is almost impossible to get total spermiation: after more than 9 dosages of pregnyl administered in 22 days, most of the testis-tubules of a specimen of *Rana esculenta* still possessed sperms. Resumption of spermatogenesis after gonadotrophin-injections was especially distinct in *Rana temporaria*.

On the other hand spermiation is easily accomplished in *Salamandra salamandra*; all sperms are released from the sperm-part of the Salamander-testis after 2 dosages, the second being given 48 h. after the first.

The differences in the way in which spermiation is accomplished in these Amphibians are explained with the help of the biology of the investigated animals.

REFERENCES.

GALLI-MAININI, C., J. Clin. Endocrin. **7** (1947).

HOUSSAY, B. A. & J. M. LASCANO-GONZALEZ, Rev. Soc. Argent. Biol. **5** (1929).

OORDT, G. J. VAN and H. KLOMP, Proc. Kon. Ned. Akad. v. Wetensch., Amsterdam, **49** (1946).

RUGH, R. R., Proc. Soc. exp. Biol. a. Med. **36** (1937).

DESCRIPTION OF PLATE.

Fig. 1. Spermiation of *Rana esculenta* after 9 doses of 2—3 I.U. of pregnyl pro gram body-weight, administered in 22 days. Large quantities of sperm are still present in the testis-tubules.

Fig. 2. *Rana temporaria*. Distinct resumption of spermatogenesis after 3 injections of 2—3 I.U. of gestyl pro gram body-weight.

Fig. 3. *Salamandra salamandra*. Section through testis of a control specimen. At the upper side of the figure the spermatogenetic, at the bottom-side the sperm-part.

Fig. 4. Spermiation of *Salamandra salamandra* after 2 injections of 4—5 I.U. of gestyl pro gram body-weight. In the tubules of the sperm-part only enlarged Sertoli-cells and a few male primary sex cells are present; no sperms.

Geology. — *Tectonics of the Mt. Aigoual pluton in the southeastern Cevennes, France.* Part II. By D. DE WAARD. (Communicated by Prof. H. A. BROUWER.)

(Communicated at the meeting of March 26, 1949.)

11. *Tectonics of the slaty country rock.*

In the slates cleavage planes have been measured in radial strips as far as 10 km from the pluton and round about the contact. The poles of the cleavage planes of the measurements not too close to the contact in the whole area are plotted in tectonogram fig. 5. The local density with close

Fig. 5. Pole diagram (55 poles) of the slaty cleavage exept near the granite contact. Contours 45—27—18—9 %. Crosses indicate the axes of ribs and minor folds.

contour intervals points to a very regular strike and dip of the slaty cleavage with an average of about N 138 E, 34 NE.

Generally, cleavage planes in slates have been developed without being the direct consequence of stratification. Locally however cleavage planes may be found parallel to the original bedding. The original bedding in the studied area is usually obliterated. In some localities hard beds of quartzite have been found parallel to the slaty cleavage, indicating a local parallelism of primary and secondary structures. Elsewhere microscopic examination of slates brings out that ordinary flat cleavage planes intersect small folds in the original stratification.

Slaty cleavage, being a better developed kind of fracture cleavage, is usually ascribed to shearing action of tectonic movements. The rock material gives way to the stress by differential movement along shearing planes. The direction of motion of the tectonic unit of which the Mt. Aigoual region is a small part, must thus be found within the plane of cleavage. In the same way ribs or minor folds and most of the joint systems

in the slates have been formed during the orogeny. They give additional clues about the direction of orogenic motion.

Minor folds are usually well developed in the southern part of the area. In the northern area an analogous phenomenon is to be seen in small straight ribs of about 2 mm wave length in the cleavage planes. Connection between ribs and small folds have been found as transitions and combinations of both forms in the field and after plotting the axes of folds and ribs in the diagram, fig. 5, they clearly exhibit uniformity of directions.

The average trend of these folds (N 140 E) is about the strike of the slates, most of them pitching a few degrees north-west. In some cases a second system perpendicular to the first is developed. Their axes are plotted in the north-east section of the diagram.

As folds usually originate by compression of material, the compression or motion of the strata in the Mt. Aigoual area must have taken place in NW—SE direction. Small folds and ribs however may be interpreted as drag folds. In that case the pitch of the drag folds is about parallel to the pitch of the major structures, being here nearly horizontal. Together with the relationship of cleavage planes to tectonic motion the direction in which the motion occurred is found, viz. perpendicular to the minor folds and within the cleavage planes, resulting in a direction of about NE—SW, dipping NE. Whereas French geologists consider the southern part of the Central Massif to be originated by southward motion, the foregoing conclusions with respect to the Mt. Aigoual area point to a tectonic motion directed about 30° upward to the S.W. with a folding axis slightly dipping to the N.W.

Most joints in slates are to be considered too as caused by tectonic motion. Everywhere in the Mt. Aigoual region slates are fractured in at

Fig. 6. Pole diagram (72 poles) of joint systems in slates. Contours $5\frac{1}{2}$—3 %. Hatched area indicates the average of schistosity of fig. 5.

least two systems of joints. A combination of all measured joints in slates not too close to the contact is shown in fig. 6. The poles of the joint planes appear to form densities in a broad girdle whose axis is the average

cleavage of the slate. This indicates a preponderant jointing perpendicular to the cleavage plane.

In this girdle dominant densities of poles are broadly concentrated in a NW—SE direction, which indicates a preponderance of joints perpendicular to both cleavage and minor folds and they may thus be considered as tension joints. The smaller concentration of poles in the NE corner of the diagram — being joints in the direction of the minor folds — may be seen as the less developed set of the two shearing systems of which the slaty cleavage is by far the most important.

In fig. 7 the plane of the diagram is made the plane of the average slaty cleavage by rotation of this average to the centre of the diagram. The concentration of perpendicular joints is now clearly shown as a peripheral girdle. Addition of the rotated axes of ribs and minor folds of

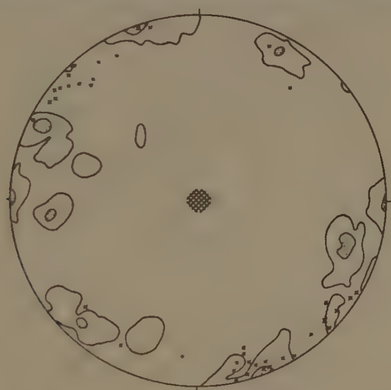

Fig. 7. Same diagram as fig. 6 after rotation of the average of schistosity to the centre of the diagram. Crosses are the rotated axes of ribs and minor folds of fig. 5.

fig. 5 in the same tectonogram gives the relation between the directions of the ribs and folds and the NW—SE densities of joints which are considered as to be caused by tension.

The above mentioned features of the slates are combined in block diagram fig. 8. It shows in outline the relation of joints and folds to each

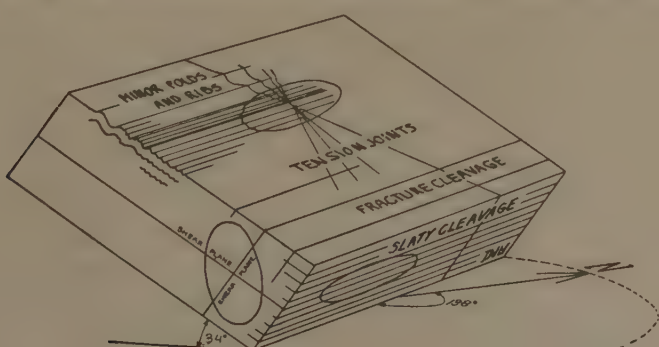

Fig. 8. Block diagram of the tectonic features in the slates in relation with the strain ellipsoid.

other and to the strain ellipsoid of which sections are drawn on the sides of the diagram.

12. *Tectonics of the country rock near the contact.*

Besides a normal small variability in strike and dip of the slaty cleavage, big divergences have been measured near the contacts of the granite. The structure map (in: DE WAARD, 1949) shows these variations especially in the country rock near the northern and eastern boundary of the pluton. The other contacts too, nearly always have divergences in the strikes of the slates. As a whole these divergences are found in a zone up to 500 meters round about the pluton. Strikes in this zone are systematically bent to the ENE. As much as 70° divergence has been observed. Bending of the strike in this zone is accompanied by alteration in dip. Usually dips near the contact are much stronger. The normal dip of the slates of about 30° tot 35° increases to 40° and 45° and sometimes over 60° towards the granite contact.

These divergences are plotted in tectonogram fig. 9. The poles of the

Fig. 9. Pole diagram of the slaty cleavage in the neighbourhood of the granite contact. Dots indicate data in the northern and northwestern, circles in the southern and southeastern contacts. The average of the normal schistosity is shown by the hatched area.

slaty cleavage of the country rock are shown together with the average of the normal schistosity (hatched spot). They occupy a much larger area in the diagram than those of the slates farther away from the contact. Variations of about 60° at both sides of the average occur and most dips are considerable steeper. In the diagram a separation has been made between the country rock NW and SE of a plane perpendicular to the average strike of the slates through the centre of the pluton. North and west of this plane strikes are mostly turned anti clockwise (dots) and in the southeastern part in clockwise direction (circles) in the same measure and both with increase of dip.

Clearly these phenomena have been caused by the intrusive movement during the *mise en place* of the granite. The upward movement of the

granite mass pushed upward the slates close to its contacts. Lifting up strata with a certain strike and dip can mean alteration in dip as well as in strike.

This is illustrated in the theoretical block diagram fig. 10. In the case

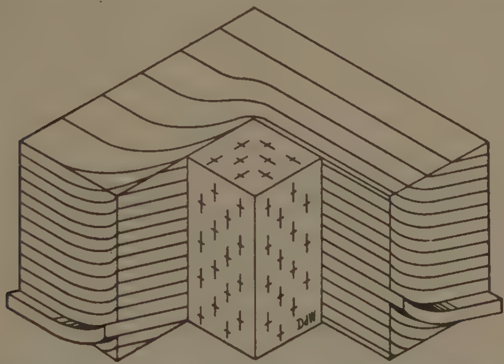

Fig. 10. Block diagram showing the theoretical alteration in strike and dip of the slates by upward bending at the contacts of the pluton, parallel and at right angles to the strike of the slaty cleavage.

in question the uplift of the slates in the country rock is shown in the increase in dip as well as in bending of its strike to the NE. These phenomena may thus be seen as large drag features. They are one more evidence of the intrusive character of the pluton.

13. *Faults and dikes in the country rock and the contact planes of the pluton.*

A glance at the structure map shows striking regularities in the directions of faults, dikes and contact planes of the pluton. This is indicative of a similar age and origin of these different features.

As mentioned in paragraph 3 faults have not been found cutting granite dikes. They are younger however than quartz veins and the development of schistosity and joint systems in the slates. In one locality drag features are observed in the adjoining country rock of a granite dike, but this drag is caused before the consolidation of the dike. Thus faults must have been active during the intrusive motion of the granite. This age determination of course does not imply any denial of the possibility of faults having been formed along existing fractures in the slate.

All observed faults, dikes and contact planes in the mapped area are compiled in tectonogram fig. 11. Besides some scattered pole axes two areas of increased density are shown. Most of the pole axes are concentrated in the SE corner of the diagram. A second and smaller concentration is visible in the middle of the SW quadrant. Compared with the diagram of the joint systems in the slates of fig. 6, the largest concentration coincides with the area of joints in the SE corner of this diagram which is interpreted as the area of tension joints in the slates. The smaller

concentration in the SW quadrant is the area of the slaty cleavage in fig. 5. The great majority of faults, dikes and contact planes thus may be considered as occurring along existing joint systems in the slates.

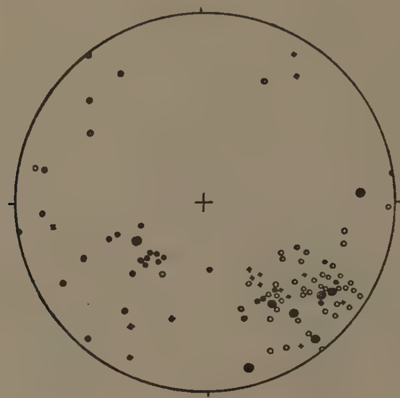

Fig. 11. Pole diagram of faults (crosses), granitic dikes (circles) and lamprophyre dikes (dots) in the country rock and the contact planes (double circles) of the pluton.

Most of the contact planes of the pluton occupy the area of tension joints in the diagram. Only in one case the cleavage plane of the slate has been used. More than 80 % of all granite dikes penetrated tension joints. Few of them intruded along the slaty cleavage. Most lamprophyre dikes preferred the cleavage planes of the slates. About 30 % penetrated tension joints. There may be a relation between the usually far away intrusions of lamprophyre dikes and their preference of penetration in the slaty cleavage. Faults occur in the joint system areas as well as the secondary fracture cleavage areas in the NE and SW margins of the diagram.

As appears from the structure map faults are arranged more or less parallel to the nearest granite contact. If drag features have been observed uplift proved to be at the side of the contact and downthrow at the other. The drag features indicate in this way an uplift of the country rock round about the pluton.

The faults nearest to the granite are shown in outline in fig. 12. The dip of all faults is rather steep; less than 50° has not been found. In the north faults are dipping N. All except one have downthrow to northern directions. The exception near the NE contact is presumably connected with the peninsula of slates in the pluton and has in this way only local significance. East and west of the pluton faults dip away from the contact except two in the south-east of the map which are very steep.

As mentioned above, movements along these faults must have taken place somewhat before or during the intrusion of the granite. It is obvious that these movements are in causal relation with the intrusive motion of the granite. The intrusive forces must have arched the country rock which caused tension in the slates and penetration of the granite mass along

Photo 1. Scenery in the northern part of the Mt. Aigoual region. The reticular pattern in the vegetation of this hill is caused by erosion differences on its surface as a result of dikes and faults in the slates.

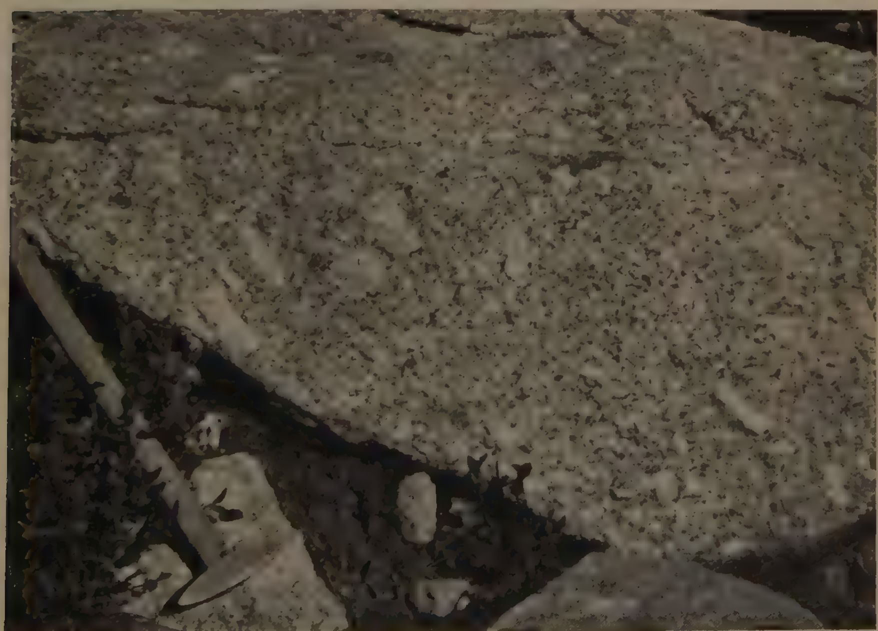

Photo 2. Ordinary type of the Mt. Aigoual granite with oriented phenocrysts of orthoclase.

Photo 3. Joint systems in the granite.

Photo 4. Example of joint systems in the slates.

open joints. This was accompanied by movements of blocks of rock along joints of the slates which effected uplift of the country rock in the neighbourhood of the intrusion.

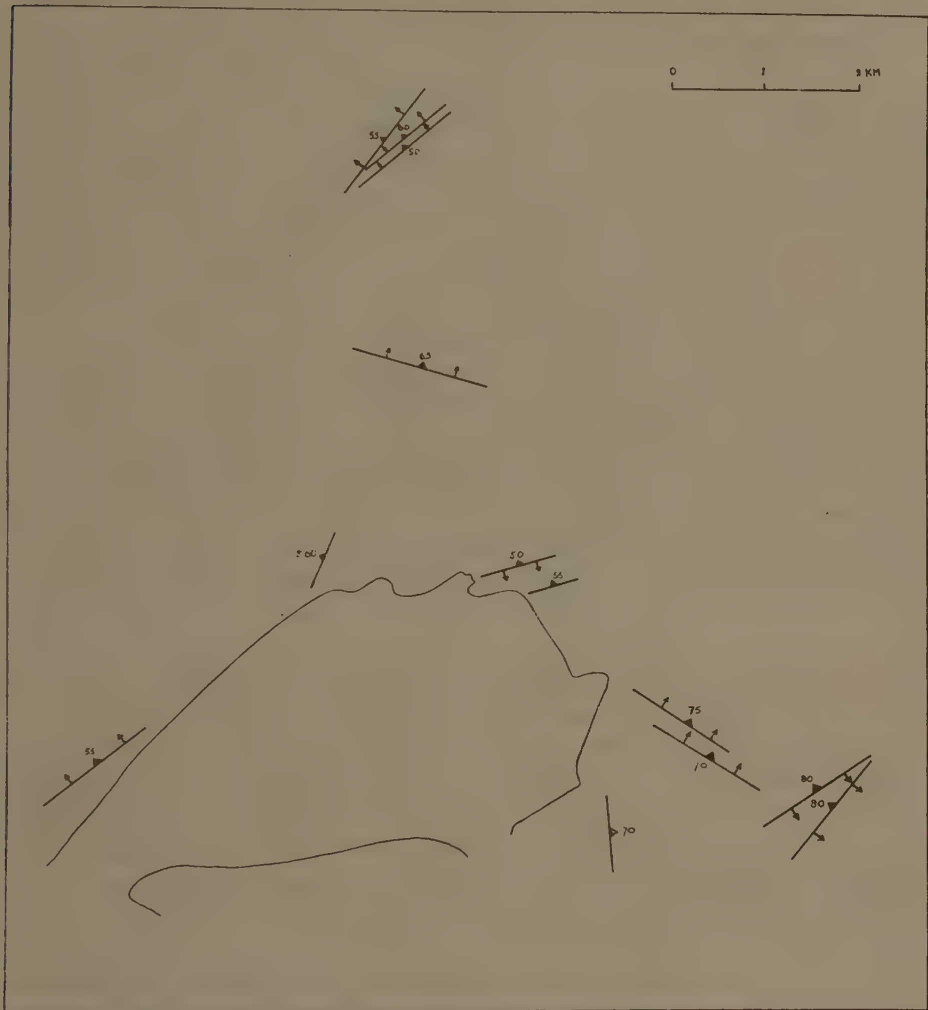

Fig. 12. Outline map of all faults near the pluton. Observed drag features are shown by arrows; the direction of the arrows indicates the downthrow side of the fault.

14. *The mise en place of the granite.*

In the preceding paragraphs all observed structural phenomena of the Mt. Aigoual pluton and its country rock have been discussed successively. They are subordinate parts in a complicated occurrence, each giving its own piece of evidence. Taken together they tell a rather complete story of an important geological event, the story of the emplacement of the granite.

The history of this area starts with Palaeozoic — probably Cambrian —

sedimentation of mainly argillaceous material, exudation of quartz veins and folding probably in the sudetic phase of the variscan orogeny. The latter created slates, locally phyllite and quarzite, and developed ribs, minor folds, slaty cleavage, tension joints and secondary fracture cleavage, indicating the stress effects on the rock in this part of the orogeny.

In this rock the granite mass occupied room. The substance cannot have been rich in easily volatilized constituents and the temperature has not been very high; the contact metamorphic zone is poorly developed, no assimilation features have been found at the contacts, acid dikes and veins are scarce. Nor can it have been very liquid during its *mise en place*; oriented crystals compose flow structures which indicate the presence already of a great part of the crystals. The occupied room must have been relatively high in the earth's crust, which is shown by the straight and sharp contacts of the pluton and the faulting features.

Thus the substance — magma *sensu lato* or better "mush" — has been a viscous flowing, partly crystallized mass of relatively low temperature and poor in easily volatilized constituents in a relatively shallow depth in the earth's crust. The mush consolidated slowly within the pluton into porphyritic granite and somewhat quicker in most dikes into granite porphyry having the same composition of quartz and feldspar phenocrysts in a matrix with different coarseness of grain. Somewhere inside the pluton body differentiation processes must have taken place and acid and basic dikes were formed. The source of the lamprophyre dikes has probably been deeper in the pluton which coincides perhaps with their relatively great distance from the plutonic outcrop.

The mush flowed upward as appears from the dome-shaped flow structures. It forced its way upward according to the upward bended slates near the contact and it arched even the intruded area which became evident by the uplifted blocks of country rock round the contact. The structural habitus of the pluton may be summarized according to the nomenclatures of HANS CLOOS (1928) and BALK (1937) as follows. A small, oval, mainly periclinal, autonomous pluton of porphyritic granite with flow facies in at least two domes of flow lines and layers, is discordantly and parallel to joint systems, mainly conformably, disharmoniously and posttectonic intruded as a nuclear pluton in the variscan orogen.

As mentioned in paragraph 8 the flow structures of the pluton seem to be incomplete. The structures in the SE of the outcrop are part of a dome of flow layers of which the other part must be hidden SE of the pluton border. Inconformable structures in the south and the east of the outcrop give the impression of continuation of internal structures under the adjoining country rock. The drawn-out flow structures and the enormous dike swarms north and east of the pluton outcrop also seem to point to a hidden extension of the pluton body.

All mentioned phenomena indicate a larger pluton than the exposed

outcrop not far below the present surface. Most of the adjoining country rock must thus be part of the roof of the pluton. Upthrown blocks of slates, faulted or separated along pre-existing fractures form part of this roof. The granite must have forced its way upward, arched the roof as a whole and made room by further lifting up parts of the roof and by penetrating its fractures.

This is illustrated by the series of sections in block diagram fig. 13. Faults and dikes border blocks of walls and roof. Their bottom is the cleavage plane of the slates. The NW contact is steep; continuation of the pluton is drawn to the north and east. North of the outcrop the granite body must be very near. The numerous dikes border floating blocks of slates.

15. *Comparative observations in adjacent massifs of the Cevennes.*

By a rapid survey in 1948 comparative studies have been done in surrounding massifs (fig. 1). South of the Mt. Aigoual pluton is the much larger St. Guiral pluton which is possibly connected with the Mt. Aigoual pluton by the bottle-neck in the SW of the latter. From the St. Guiral pluton a massif — about 30 km long — stretches away to the east, dilating in the Mt. du Liron massif. North of the Mt. Aigoual is the Mt. Lozère massif, the largest massif of the Cevennes region. The mentioned massifs form together an interrupted horseshoe including a large area of slates open to the NE.

Preponderant resemblances in structure and petrology have been observed in the visited areas. The massifs consist mainly of identical grey-coloured porphyritic granite with large phenocrysts of orthoclase. In the Mt. Lozère massif and to a less extent in the Mt. du Liron massif the phenocrysts may be missing locally, the type of rock in all other aspects remaining the same. In the Mt. du Liron massif masses of aplitic granite have been found. It is the same type of granite but without phenocrysts and with less biotite often passing into normal aplite. As near the Mt. Aigoual pluton, dikes of granite porphyry, quartz porphyry, tonalite porphyry, aplite, pegmatite and lamprophyre occur. Flow structures, sharp and straight contacts with narrow and feebly developed contact zones are also typical in these massifs. Their posttectonic and intrusive character are equally evident.

This wide-spread homogenity, petrological as well as structural, in the massifs of the Cevennes points to a same source of the material which intruded after the orogenic movements into different places in the mainly slaty country rock. Of less importance — but mentioned because of petrological resemblances — is at least one small outcrop of augen gneiss in the neighbourhood of one of the granite contacts. There is no relationship however between the postectonic granite and the much older augen gneiss. The latter has been mapped in detail and it turned out to be a small massif of orthogneiss, intruded as well but much earlier. There may be some relation in the source of both rocks.

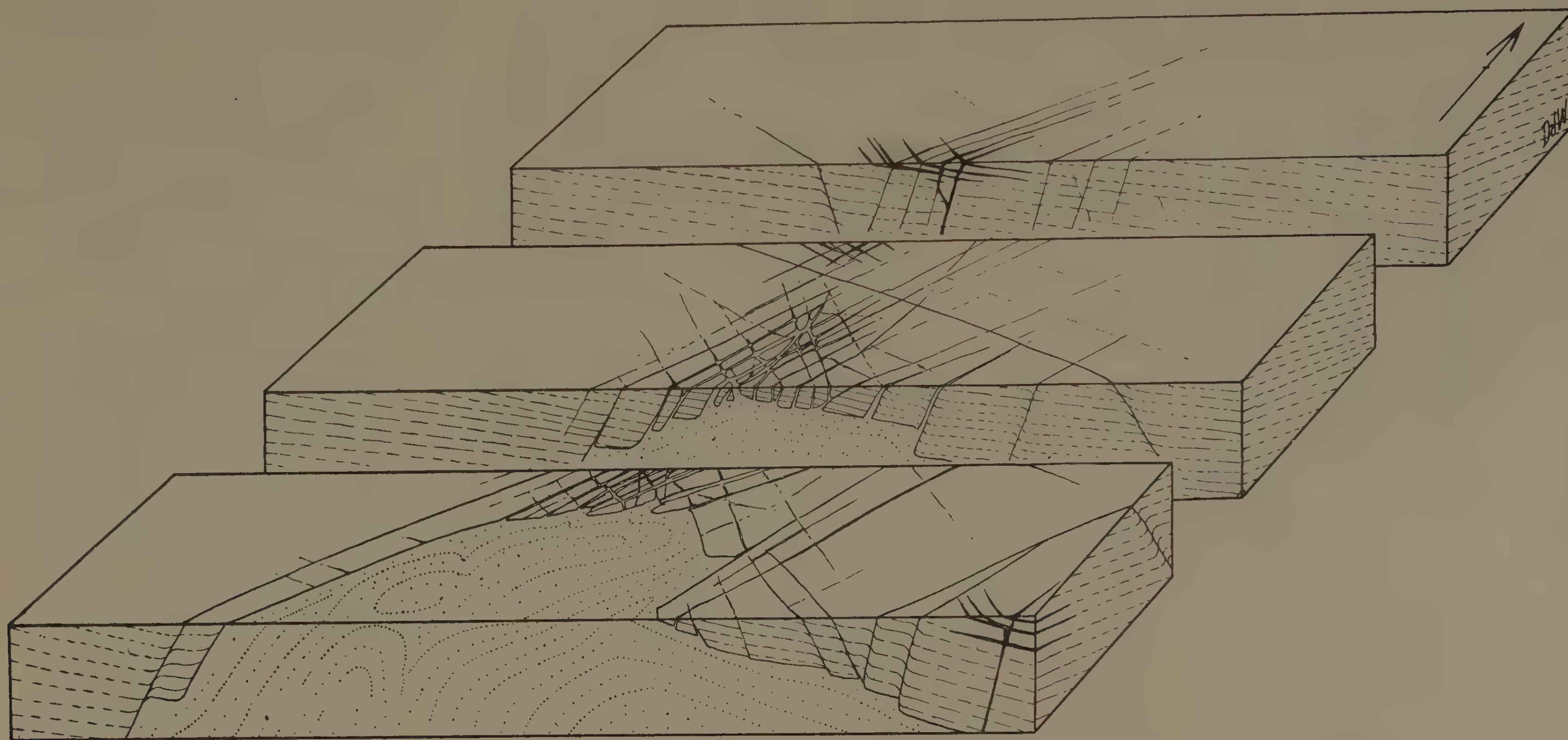

Fig. 13. Block diagram of the northern part of the mapped area showing the mean structural phenomena and their continuation into the depth.

16. *Concluding remarks in relation with granite problems.*

For a long time the mechanism of intrusion has been a matter of discussion. Stoping, enlargement of a magmatic chamber by the breaking off of blocks from the walls and roof is opposed by organized upward flow of the magma through the crust and doming of its roof. In the case in question there is nothing found supporting stoping. On the contrary all features point to a doming mechanism of intrusion. Domes of flow structures, slates dragged upward near the contacts, dragged faults indicating raised blocks of rock near the pluton and long-distance faults showing arching of the roof give evidence of a forcing upward of the magma and enlargement of the magmatic chamber by doming of the roof.

During recent years the discussions concerning the origin of granite have increased considerably. The purely magmatic origin of granite is opposed by migmatization, refusion and metamorphic diffusion. The structure of the Mt. Aigoual pluton and as far as observed in all granite massifs of the Cevennes proves evidently the existence of magma or mush and magma flow. The granite has been a mobile substance during its *mise en place* and there are no indications for metamorphic diffusion in the present magmatic deposit. No indications have been found, supposing a special conception about the origin of the mobile granite mass in the depth before its intrusion.

REFERENCES.

BALK, R. (1937) — Structural behavior of igneous rocks — Geol. Soc. America, Memoir 5, 1937.

BAULIG, H. (1928) — Le Plateau Central de la France et sa bordure méditerranéenne; étude morphologique — Paris, 1928.

BERGERON, J. (1889) — Étude géologique du massif ancien situé au sud du Plateau Central — Ann. Sc. Géol., XXII, 1889.

— —— (1904) — Note sur les nappes de recouvrement du versant méridional de la Montagne Noir et des Cévennes aux environs du Vigan — Bull. Soc. Géol. France, IV série, 4, 1904.

CLOOS, H. (1928) — Zur Terminologie der Plutone — Fennia, 50, 2, 1928.

DEMAY, A. (1931*a*) — Contribution à l'étude de la tectonique hercynienne antestephanienne dans les Cévennes méridionales et dans le Rouergue — Bull. Soc. Géol France, V série, 1, 1931.

———— (1931*b*) — Les nappes cévenoles — Mém. Carte Géol. France, 1931.

———— (1934) — Contribution à la synthèse de la chaine hercynienne d'Europe. Étude du plan axial de l'évolution et de l'orogénèse hercyniennes — Bull. Soc. Géol. France, V série, 4, 1934.

———— (1935) — Sur le jeu alternant ou simultané des phénomènes magmatiques et dynamiques dans les Cévennes septentrionales — Comptes Rendues Ac. Sc., Paris, 200, 1935, pp. 2197—2199.

———— (1942) — Microtectonique et tectonique profonde. Cristallisations et injections magmatiques syntectoniques —Mém. Carte Géol. France, 1942.

FABRE, G. et L. CAYEUX (1901) — Alais, avec notice explicative — Carte Géol. France au 1 : 80.000, 209, 1901.

GAERTNER, H. R. VON (1937) — Der Bau des Französischen Zentralplateaus — Geol. Rundschau, 28, 1937.

HEIM, R. C. (1949) — Petrology of the Mt. Aigoual area in the southeastern Cevennes, France — (in print).

RAGUIN, E. (1930) — Problèmes tectoniques dans les terrains cristallins du Centre de la France — Bull. Soc. Géol. France, IV série, 30, 1930.

——— (1946) — Géologie du granite — Paris, 1946.

ROQUES, M. (1941) — Les schistes cristallins de la partie Sud-Ouest du Massif Central Français — Mém. Carte Géol. France, 1941.

THIÉRY, P. (1923) — Alais, 2-ème éd. avec notice explicative — Carte Géol. France au 1 : 80.000, 209, 1923.

WAARD, D. DE (1949) — Tectonics of the Mt. Aigoual pluton in the southeastern Cevennes, France. Part I. — Proc. Kon. Ned. Akad. v. Wetensch., Amsterdam, **52**, 389, 1949.

Petrology. — *On metamorphic rocks from the island of Kabaëna in the East-Indian Archipelago.* By C. G. EGELER. (Communicated by Prof. H. A. BROUWER.)

(Communicated at the meeting of April 23, 1949.)

In this paper a description will be given of a number of metamorphic rocks from Kabaëna, a small island situated directly South of the south-eastern peninsula of Celebes and West of the islands of Moena and Boeton. These rocks form part of the collections of the Geological Institute of the University of Amsterdam. They were partly collected by Prof. H. A. BROUWER and co-workers when visiting Kabaëna during the Celebes expedition of 1929 and partly by geologists of the Mining Department at Bandoeng, which presented the Geological Institute with a type-collection [1]).

I herewith wish to thank Prof. BROUWER for his courtesy in placing this material at my disposal and especially for discussing with me the results of my microscopical investigations in connection with the metamorphism on Celebes.

I. Thermally metamorphosed rocks

Garnetiferous biotite-hornfelses

2691 *Schistose garnet-biotite-hornfels with bands of a garnet-epidote-amphibole-rock.* in the Oe. Lakambola.

The only rock of this type examined is a somewhat folded variety, showing violet-brown and greenish grey bands in irregular alternation.

Under the microscope the brown bands appear to consist of a *schistose garnet-biotite-hornfels*, the structure of which is truly hornfelsic, notwithstanding the parallel arrangement of the mica flakes. The biotite is developed in small reddish brown crystals of a uniform size. For the rest the matrix is mainly formed by granular quartz and plagioclase (andesine). Garnet is represented by reddish, six-sided or more or less rounded crystals, generally of less than 0.5 millimetre in diameter, intensely cracked and often containing abundant inclusions. Both the garnet and the biotite are somewhat chloritized. Some parts of the rock are rich in colourless mica, which is considered an alteration-product of the felspar. Minerals of the epidote-group occur in a considerable amount, sometimes in separate zonary crystals partly recognized as clinozoisite, and also in turbid sausuritic aggregates. Titanite and rutile are accessory constituents, together with some pyrite.

The greenish bands contain much garnet, while further a pale coloured

[1]) The rocks collected by Prof. BROUWER c.s. may be distinguished from those from the Mining Department by the series-number 18.

amphibole is found in a considerable quantity, partly formed as a transition-product of a monoclinic pyroxene which still appears to be fairly abundant locally. The epidote-group is again represented by various members, especially zoisite. The interstitial mass consists mainly of quartz. Some muscovite occurs, presumably formed out of felspar.

This rock is of some interest as it closely resembles some of the schistose biotite-hornfelses which are so abundantly represented in western Celebes, where they are considered to have originated out of low-grade crystalline schists by the thermal influence of granodioritic intrusions (Lit. 4). On Kabaëna, however, no acid intrusive rocks are known to occur and the micaceous hornfelses of the type mentioned above are attributed to the thermal metamorphism caused by basic magmas [2]).

Lime-silicate-hornfelses

18—34 *Grossularite-hornfels rich in pumpellyite.* In contact with an albite-diabase in the upper course of the Oe. Lakambola, closely above the point where the road from Tangkeno crosses the river.

18—36 *Banded lime-silicate-rock with bands of partly pumpellyitized grossularite-hornfels and of crystalline limestone.* Same locality.

18—37a *Grossularite-hornfels.* In the Oe. Lakambola, somewhat more upstream.

18—37b *Banded lime-silicate-rock with bands of partly pumpellyitized grossularite-hornfels and of grossularite-bearing crystalline limestone.* Same locality.

The sample of the *grossularite-hornfels 37a* is a massive grey rock of a characteristic hornfels type. Under the microscope a colourless lime-garnet appears to be by far the most important constituent, occurring in a finely granular "groundmass" consisting of albite together with minute (some hundredths of a millimetre in length) pale green prisms determined as monoclinic pyroxene. Garnet is developed in six-sided or more or less rounded crystals, strikingly equigranular and averaging 0.2 millimetre in diameter. Optical anomalies are common, the birefringent areas showing a characteristic sector arrangement. The garnet contains abundant inclusions, especially of ore, pyroxene and minute needles considered as rutile. Sometimes a number of grossularite grains are cemented by a single calcite crystal. One or two grains of titanite are found. Ore is very abundant; it is chiefly represented by pyrrhotite, scattered through the rock in irregular grains.

Megascopically the rock *37b* also has the appearance of a normal *lime-silicate-hornfels,* in which light grey bands alternate with darker grey ones.

Under the microscope this rock shows several features of interest.

The lighter coloured bands appear to consist of crystalline limestone, the calcite developed in fairly large, closely interlocking crystals. Small, rounded crystals of grossularite are noticed in some parts of these bands. Swarms of small, colourless prisms, presumably consisting of zoisite, occur locally. The limestone band examined is intersected by veins of pumpel-

---

[2]) A rock from the North of Kabaëna was described as a diorite by WUNDERLIN, but an approximate analysis yielded a SiO_2-content of only 48 % (Lit. 12).

lyite; irregular patches of pumpellyite are also noticed within the carbonate mass. In the veins the pumpellyite occurs in fibrously developed crystals, averaging several tenths of a millimetre in length. The mineral is very pale coloured and shows a faint pleochroism from pale green (n_β) to almost colourless (n_α and n_γ). The optic axial plane has a transverse position, so that n_β is parallel to the longitudinal direction of the crystals and the elongation varying. The refringence is fairly strong; with the aid of the immersion method in sodium light a value of $\pm$ 1.68 was found for n_β. The birefringence is moderate; with the aid of the universal rotation stage and the Berek-compensator a birefringence of 0.018 was found. A measurement in a single crystal of the optic axial angle gave a value of 32° for $2V_\gamma$; it should be noted, however, that the mineral shows a distinct zonary structure. The dispersion $\varrho < \nu$ appears to rather weak for pumpellyite.

The pumpellyite vein continues from the limestone band into one of the darker grey bands, and here the mineral is associated with varying quantities of albite, some calcite, deep green chlorite-like matter and pyrrhotite.

The dark grey band shows a rather complicated structure. It partly consists of a very finely granular aggregate of albite, minute crystals of monoclinic pyroxene, some grossularite especially concentrated near to the contact with the limestone band, and much pyrrhotite. In this fine-grained lime-silicate-rock rounded or lenticular patches occur, consisting of a felty aggregate of very fine-crystalline pumpellyite. Evidently the process of pumpellyitization began at certain points causing the formation of these concentrations which apparently have grown at the expense of the other minerals. In other places this process appears to have become so intensive that entire areas now consist of closely packed lenticular pumpellyite patches, often of more than a millimetre in length and showing a distinct tendency towards a parallel arrangement (see figure). The matrix between

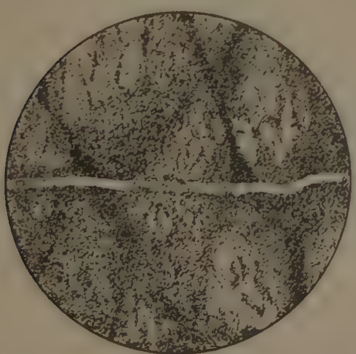

Lenticular pumpellyite aggregates in a partly pumpellyitized lime-silicate-hornfels (18—37b) found near a diabase dike in the upper course of the Oe. Lakambola. An albite-vein is seen intersecting the rock; where this vein cuts the very fine-crystalline pumpellyite patches it is filled up with pumpellyite crystals of a considerably larger size, which appear to be more or less parallel-ranged comforming with the general orientation of the patches. Approx. $\times$ 30.

these pumpellyite concentrations is formed by a greyish turbid aggregate, presumably mainly consisting of very fine-crystalline pyroxene together with much ore (pyrrhotite), some interstitial albite and occasionally some titanite. A few grossularite crystals are also present. It should be noted that the actual determination of the very fine-crystalline pumpellyite concentrations was made possible by the fact that the band in question is

intersected by narrow veins of albite and pumpellyite. These sometimes cut the pumpellyite "eyes", in which case the two parts generally appear connected in the vein by larger pumpellyite crystals.

Another of the dark grey bands examined contains much well-developed grossularite, again embedded in a finely granular matrix of albite, pyroxene, pyrrhotite and some calcite. It is a grossularite-hornfels resembling the rock 18—37*a*.

The *lime-silicate-rocks* 18—34 and 18—36 are closely related to the type described above, so no separate description need be given.

The lime-silicate-hornfelses described above are formed by the contact-metamorphism induced by albite-diabases on a series of dark coloured limestones and calcareous slates. It is an interesting feature of these grossularite-rich rocks that the felspar is albite. It seems likely that this phenomenon should be attributed to albitization caused by the soda-rich diabases responsible for the metamorphism.

Another noteworthy fact is the abundant occurrence of pumpellyite as a hydrothermal mineral both in the diabases and in the contact-rocks. This again points to the fact that this mineral — which was described for the first time in 1925 by PALACHE and Miss VASSAR — has a considerable distribution in the East-Indian archipelago in rocks of various type. In the last few years occurrences have been recorded from several localities: in eastern Celebes, for instance, pumpellyite appears to be an important constituent of various igneous as well as metamorphic rocks (Lit. 8), in the western part of Celebes it has been found in albite-diabases (Lit. 3, p. 26), whereas lately the mineral has also been found in eastern Borneo, in spilites and albite-diabases of the Danau-formation (Lit. 9).

The peculiar structure arising from the pumpellyitization of some of these lime-silicate-hornfelses (see the description of the rock 18—37*b* and the figure) is of special interest.

II. Regionally metamorphosed rocks

Micaceous schists

18—6 *Muscovite-schist.* In the Oe. Emeloro, downstream of Menoero.

18—39 *Piedmontite-bearing garnet-muscovite-quartz-schist with porphyroblastic plagioclase.* In the upper course of the Oe. Lakambola, upstream of the point where the road from Tangkeno crosses the river.

The *muscovite-schist* 18—6 is a phyllitic rock showing no special features of interest.

The *piedmontite-bearing garnet-muscovite-quartz-schist* 18—39 is a considerably higher grade type, especially characterized by the occurrence of plagioclase porphyroblasts. The chief constituents are quartz and muscovite. In some highly micaceous bands a distinct folding is observed. The garnets vary much in size (up to 1.5 millimetres in diameter); irregular shapes predominate; some of the crystals are shattered and occasionally the mineral seems to be partly recrystallized. Trains of ore particles which

emphasize the foliation pass mostly undisturbed through the larger garnet specimens; sometimes also a certain degree of rotation is observed. The piedmontite is developed in small, elongated prisms, parallel-ranged and showing the characteristic intensive pleochroism from deep yellow (n_α) to violet (n_β) and carmine red (n_γ); the mineral is locally associated with epidote [3]). The lenticular felspar porphyroblasts, attaining sizes up to 2.5 millimetres, consist of sodic andesine. Inclusions are abundant, especially of parallel-ranged piedmontite prisms and of ore, but also of quartz, muscovite, tourmaline and apatite. Some chlorite is associated with the muscovite; some brown mica-like matter is locally concentrated.

Gneissic rocks

18—41 *Amphibole-garnet-zoisite-gneiss.* In the upper course of the Oe. Lakambola, upstream of the point where the road from Tangkeno crosses the river.
2691 *Biotite- and amphibole-bearing garnet-plagioclase-gneiss.* In the Oe. Lakambola.
2629 *Gneissic garnet-epidote-augite-quartz-rock.* Along the beach at Dongkala.

The rather fine-grained *amphibole-garnet-zoisite-gneiss* 18—41 shows some relationship to some of the amphibolitic rocks described below. Garnet is very abundant, occurring in porphyroblastic crystals. Often the garnets are shattered and dragged out and locally recrystallization appears to have taken place. Changes to biotite and chlorite are common. Amphibole is present in bluish green porphyroblasts, which are often much chloritized. Clinozoisite and zoisite are abundant, often accompanied by sericitic mica which is considered as an alteration-product of felspar. Sometimes the sodic plagioclase is still preserved as turbid crystals partly changed to albite. In general, however, the interstitial mass consists of quartz. Some much chloritized biotite is also present. A few, apparently relict crystals of monoclinic pyroxene are observed, partly changed to chlorite and amphibole. Carbonate occurs in a considerable quantity in between the other minerals; titanite is the main accessory constituent.

The *biotite- and amphibole-bearing garnet-plagioclase-gneiss* 2691 is a somewhat divergent type, with plagioclase, quartz and garnet as characteristic minerals, together with smaller quantities of amphibole, biotite and chlorite. Retrograde metamorphism has again caused shattering and chloritization of the garnet, chloritization of the biotite and sericitization and sausuritization of the felspar (oligoclase).

The *gneissic garnet-epidote-augite-quartz-rock* 2629 is a completely divergent type. The sample shows an irregular alternation of deep green, lighter green and greyish bands, all three specked with red garnets. Under the microscope the deep green bands appear to consist mainly of pyroxene and quartz, with varying amounts of epidote, plagioclase, garnet and amphibole. The pale green augite is developed on irregular poiciloblastic crystals of varying size (up to 2.5 mm), which appear partly changed to

[3]) An occurrence of piedmontite on the neighbouring island of Boeton was stated by the author in a metamorphic radiolarite (18—27), found as a cobble in the Oe. Moekito.

fibrous bluish green amphibole. The amphibole also occurs separately, sometimes formed at the expense of the epidote. The larger amphibole crystals sometimes show deeper coloured cores. Quartz forms an irregular mozaic. The plagioclase (oligoclase-andesine to andesine), which occurs in varying amounts in the quartzitic matrix, is generally much altered. Clusters of garnet locally occur; the crystals, which attain sizes up to several millimetres in diameter, are generally irregularly shaped, though more or less idioblastically developed specimens are also observed. Magnetite is very abundant.

In the lighter green bands epidote is the main rock-forming mineral; certain discontinuous streaks consist almost exclusively of yellow, equigranular epidote. Generally, however, pyroxene is fairly abundant too. Some layers are very rich in quartz, sometimes in association with much altered plagioclase. Garnet is again abundant locally. A considerable amount of titanite occurs, while ore is much less abundant than in the deep green bands.

The greyish bands are very rich in quartz, with varying amounts of felspar, augite, epidote and ore.

Amphibolites and amphibole-schists

18—39× *Epidote-amphibole-schist.* In the upper course of the Oe. Lakambola, upstream of the point where the road from Tangkeno crosses the river.
18—46× *Epidote-amphibole-schist.* Cobble in the Oe. Lakambola.
2680 *Epidote-amphibole-schist.* In the Oe. Rantinoli.
300 *Epidote-amphibolite.* On Poelou Damalawa Besar, NE of Dongkala.
18—40× *Quartz-rich plagioclase-amphibole-schist.* In the upper course of the Oe. Lakambola, upstream of the point where the road from Tangkeno crosses the river.
246 *Quartz-rich plagioclase-amphibole-schist.* Along the road from Dongkala to Sikele.
626 *Quartz-rich plagioclase-amphibole-schist.* In the Oe. Kala-Ero.
1523 *Quartz-rich plagioclase-amphibolite.* In the Oe. Lakambola.
298 *Amphibole-schist.* On Poelou Damalawa Besar, NE of Dongkala.
299 *Amphibole-schist.* Same locality.
2636 *Amphibole-schist.* Along the path N of the Oe. Lambale.
18—46 *Garnetiferous plagioclase-amphibolite.* Cobble in the Oe. Lakambola.
18—41× *Garnet-epidote-amphibolite.* In the upper course of the Oe. Lakambola, upstream of the point where the road from Tangkeno crosses the river.
18—42 *Garnet-epidote-amphibolite.* Same locality.
2647 *Garnet-amphibolite.* In the Oe. Lambo.
2654 *Quartz-rich garnet-amphibole-schist.* In the Oe. Lapondoowe.

The collection investigated contains a considerable number of amphibolitic rocks. They are distinguished as amphibolites or amphibole-schists merely in accordance with respectively a massive or a more schistose structure.

The *epidote-amphibole-schists* 18—39×, 18—46× and 2680 are fairly low-grade rocks containing bluish green amphibole, epidote and plagioclase as characteristic constituents. The felspar, which has a composition near oligoclase, is much sausuritized. Some quartz is always present.

The *epidote-amphibolite* 300 is a divergent variety, consisting of epidote

and amphibole, almost to the exclusion of other minerals. Originally some felspar has been present but now this mineral is entirely changed to sericite and zoisite. A few relict crystals of monoclinic pyroxene are present.

The *quartz-rich plagioclase-amphibole-schists* 18—40×, 246 and 626 differ from the rocks above mentioned in so far that here epidote does not occur as an important rock-forming constituent. Amphibole and lime-bearing plagioclase are the chief minerals, together with varying amounts of quartz. The plagioclase, which ranges in the various rocks from oligoclase-andesine to calcic andesine, is often much altered. Some epidote may occur; a small quantity of colourless mica and chlorite is also sometimes present. Titanite is generally the main accessory mineral.

A more highly amphiboliferous type is represented by the *amphibole-schists* 298, 299 and 2636. These mainly consist of stout crystals of bluish green amphibole, mostly attaining a length of several millimetres. Some felspar occurs, though always much broken down and changed to zoisite, sericite or prehnite; often turbid patches are the only indication of the original presence of plagioclase. Rutile is always a characteristic accessory constituent.

The *garnetiferous plagioclase-amphibolite* 18—46 is a coarsely granular rock. The pale greenish amphibole is developed in large, broad crystals, often with abundant inclusions. Garnet is represented by irregularly shaped poiciloblastic individuals, with inclusions i.a. of plagioclase, amphibole, rutile, titanite and ore. The plagioclase is an intermediate andesine, well-twinned and somewhat sausuritized. Some quartz occurs. Rutile, often associated with ore, is very abundant. The non-garnetiferous *quartz-rich plagioclase-amphibolite* 1523 is a closely related variety.

The *garnet-epidote-amphibolites* 18—41× and 18—42 form a well-distinguished type. They mainly consist of a deep greyish brown amphibole and epidote, while garnet is present in varying quantities. The rock 18—42 appears to be especially rich in garnet, developed in irregularly rounded crystals, averaging several millimetres in diameter. Sometimes amphibole is enclosed. The garnet appears to be much altered to green chlorite. The amphibole, which shows a strong pleochroism from greyish brown (n_γ) to brown (n_β) and yellow-brown (n_α), occurs in large crystals; with the aid of the universal rotation stage the optic axial angle was measured as $2V_\alpha = 72°$; the extinction angle $n_\gamma/c = 18°$. This amphibole is considered to be a relict of igneous origin. Towards the exterior changes to a more fibrous, bluish green variety are observed; sometimes also the brown amphibole is changed to chlorite, in which case strings of minute titanite grains are observed along the cleavage lines. The younger, bluish green amphibole also occurs independent of the brown variety. Almost the entire interstitial mass consists of an aggregate of epidote, often associated with muscovite. In the rock 18—42 one or two relict crystals of monoclinic pyroxene are observed, almost changed to chlorite. Titanite and leucoxene are very abundant; titaniferous iron ore occurs, sometimes in pseudomorphs

after titanite; sometimes these minerals form peculiar vermicular patches. Some rutile and apatite are also present. The *garnet-amphibole* 2647 is a closely related type in which a small amount of felspar has been spared.

Lastly the *quartz-rich garnet-amphibole-schist* 2654 should be mentioned as a considerably divergent variety. Amphibole is again the principal constituent, but here the mineral is developed in smaller, more fibrous crystals, of an olive green colour. Quartz is very abundant. Originally the rock must have contained a considerable amount of plagioclase, but now this mineral is mostly changed to colourless mica. Some pyroxene occurs, in course of alteration to chloritic matter.

There is little doubt that many of the amphibolites and amphibole-schists described above are of igneous origin. Besides from characteristic structural features, this may in some cases be concluded from the occurrence and general character of relict amphiboles (see e.g. the garnetiferous amphibolites 18—41×, 18—42 and 2647). Other types again show some resemblance to the sausurite-gabbros from Kabaëna (see e.g. the plagioclase-rich amphibolites 18—46 and 1523). The amphibole-schists 298, 299 and 2636 may represent rather melanocratic equivalents of these sausurite-gabbros which have been subjected to considerable stress. In some cases, (e.g. the quartz-rich plagioclase-amphibole-schists 18—40×, 246 and 626), the origin is uncertain. The highly quartziferous garnet-amphibole-schist 2654 is considered to be of sedimentary origin.

Crystalline limestones

18—3 *Crystalline limestone.* In the Oe. Emeloro, W of Dongkala.
18—4 *Crystalline limestone.* Same locality.
18—40 *Muscovite-rich crystalline limestone.* Occurring as a band in amphibole-schists, in the upper course of the Oe. Lakambola, upstream of the point where the road from Tangkeno crosses the river.
18—51 *Crystalline limestone.* Along the path mounting from the Oe. Lakambola to Poö.
263 *Crystalline limestone.* Along the road from Dongkala to Sikele.
1463 *Crystalline limestone.* In the Oe. Emeloro.
1497 *Crystalline limestone.* Along the horse-path from Langkema to Timoekolek.
1516 *Crystalline limestone.* Along the path from Tangkeno to Sambara Kambola.
2632 *Epidote-rich crystalline limestone.* Along the beach at Dongkala.

In the *muscovite-rich crystalline limestone* 18—40 there is a well-marked parallel elongation of the calcite crystals, which show an intensive polysynthetic twinning. The rock contains a considerable quantity of colourless mica and further quartz and a subordinate amount of clino-zoisite. A gradual transition of the limestone into a calc-epidote-chlorite-muscovite-schist is observed.

The *epidote-rich crystalline limestone* 2632 is a more massive type. It is a patchy greenish and brownish rock, which under the microscope besides the main constituent calcite, appears to contain a considerable amount of epidote and quartz and more subordinate amounts of muscovite, an almost

colourless chlorite-like mineral, titanite, leucoxene, apatite and haematite. The carbonate-mass is specked with small quartz grains; sometimes also lenticular quartz concentrations are found. The epidote occurs in prismatic crystals, often showing an ideal development. An interesting feature is the partial alteration of some of the epidote crystals to sericite, a change which generally preceeds from cracks in the epidote; replacement of epidote by calcite is also observed. It is a well-known fact that the epidote minerals are but seldom subject to alteration, though some instances have been described, e.a. from Celebes (Lit. 8, p. 149).

The other *crystalline limestones* investigated show but few features of interest, so no separate descriptions need be given. They are for the greater part considered to be of a lower grade than the varieties described above. The grain-size varies considerably. Carbonate is always the chief constituent, while quartz is generally present in a subordinate amount. Some types, however, appear to be fairly rich in quartz and often this mineral is concentrated in irregular dark patches together with i.a. sericite, chlorite, ore and a considerable quantity of carbonaceous matter.

Comparison with Celebes.

Up till now very little was actually known about the petrology of Kabaëna. A small number of eruptive and metamorphic rocks was described by WUNDERLIN, the metamorphic group comprising only amphibolitic varieties (Lit. 12). It is clear, however, that the island, with its schist-formation and its peridotitic intrusions, forms the continuation of the southeastern peninsula of Celebes. Here more petrological data are available, thanks to descriptions given by WUNDERLIN (Lit. 12) and GISOLF (Lit. 5) and thanks to the results of the Celebes expedition of 1929 (BROUWER, Lit. 2, 3, and DE ROEVER, Lit. 8).

The regional distribution on the southeastern peninsula, of rocks metamorphosed in the glaucophane-schist facies, shows that here there is a close relationship to the metamorphism in the eastern part of Central Celebes. DE ROEVER (Lit. 8), in his study on the igneous and metamorphic rocks in eastern Central Celebes, distinguishes between a metamorphism in the epidote-amphibolite facies, which is older than the radiolarites and the ophiolitic and spilitic igneous rocks, and a younger, presumably alpine, glaucophanitic metamorphism. He proves that many varieties, such as e.g. those intermediate between amphibolitic and glaucophanitic rocks, have been subjected to polymetamorphism. In an appendix the same author gives the names of a number of rocks from southeastern Celebes, together with some brief remarks. It appears that here too both amphibolitic and glaucophanitic rocks are represented and special attention is drawn to the occurrence of a plagioclase-amphibolite in the W. Sesoh, SE of Lake Towoeti. Another interesting fact is the occurrence in the W. Aloehoeno

---

[4]) See also SCHMIDT (Lit. 10).

(NW of Teetedopi) of a rock intermediate between a glaucophanite and an amphibolite, and therefore polymetamorphic. Indeed it seems likely that the polymetamorphism which has played such an important part in the geological history of Central Celebes, can also be traced in the southeastern part of the island, and that here the glaucophanitic metamorphism was also preceded by an amphibolitic metamorphism. The occurrence, on the peninsula, of amphibolites containing lime-bearing plagioclase, may point to the fact that the older metamorphic phase has sometimes been of a somewhat higher grade (amphibolite facies) than in eastern Central Celebes, where the epidote-amphibolite facies was not exceeded.

For a comparison between Celebes and Kabaëna it is especially important to know the nature of the metamorphism in the more southern part of the southeastern peninsula. It appears that in Roembia both amphibolites and glaucophanitic rocks occur, the latter i.a. at Liano, not far from the coast directly opposite to Kabaëna (Lit. 12) [5]. No polymetamorphic phenomena are described from this area, but a further study of the crystalline schists, with the probability of polymetamorphism in mind, might lead to interesting results.

The detailed study, published in this paper, of metamorphic rocks from Kabaëna, shows that here the regional metamorphism was mainly in the amphibolite facies, as proved by the frequent occurrence of amphibole in association with lime-bearing plagioclase (varying from albite-oligoclase to andesine [6]). To these medium to higher grade schists are reckoned the amphibolites and amphibole-schists, the gneissic rocks, the piedmontite-bearing garnet-mica-schists and the higher grade crystalline limestones. In contrast with eastern Celebes no indications of a glaucophanitic metamorphism are found.

Further a few thermally metamorphic rocks (lime-silicate-rocks) are described, which have been formed out of dark coloured limestones and other calcareous sediments where these are intruded by albite-diabases in the upper course of the Oe. Lakambola. This flysch-like series is but feebly metamorphosed and therefore considered younger than the crystalline schist-formation occurring close by (somewhat more upstream). Though the age of the sediments is not known the occurrence of the diabasic intrusions is of some help in solving the problem of the age-

---

5) On the neighbouring island of Boeton the schist-formation — found only in the upper course of the Oe. Moekito in the South — mainly consists of plagioclase-amphibolites and epidote-chlorite-schists (Lit. 6 p. 4). No glaucophanitic rocks are found. The schists, according to HETZEL, are older than the upper-triassic formation occurring on the island.

6) The paragenesis observed in many of these rocks of amphibole and lime-bearing plagioclase with minerals of the epidote-group, is attributed to the general physical conditions and in the first place to the stress which prevailed during the metamorphism and which made a still higher lime-content in the felspar impossible (see e.g. TURNER, Lit. 11, p. 81).

relations [7]). BROUWER considers the albite-diabases in eastern Central Celebes and on the southeastern peninsula to belong to the same differentiation-series as the gabbro-peridotitic rocks and consequently to be of about the same age (Lit. 3). It seems highly probable that the same is the case on Kabaëna, where basic and ultrabasic rocks are widely distributed. The difficulty remains that the actual age of the gabbro-peridotitic rocks in the east arc of Celebes and on Kabaëna is insufficiently known; an upper-mesozoic to lower-tertiary age of many of these rocks seems most probable [8]).

Taking these various facts into consideration it seems reasonable to assume that the regional amphibolitic metamorphism on Kabaëna, which is older than the ophiolitic rocks, may be correlated with the older (pre-radiolarite and pre-ophiolite and -spilite) metamorphism distinguished on Celebes. Further it seems likely that the intrusion of the diabases, causing the contact phenomena in the flysch-like series, may be roughly correlated with that of the gabbro-peridotitic rocks which on Celebes appear to have preceded the younger phase of metamorphism responsible for the glaucophanitic rocks. The question why no traces of this glaucophanitic metamorphism have been found in the rocks investigated from Kabaëna, remains unanswered.

Summary.

The collection investigated comprises both thermally and regionally metamorphosed types.

Most of the thermally metamorphic rocks, viz. the lime-silicate-hornfelses rich in grossularite, are formed by contact-metamorphism of calcareous sediments, caused by albite-diabases. Post-metamorphic pumpellyitization has given rise to peculiar structures in some of these hornfelses.

The regionally metamorphic rocks can be divided into a number of medium to higher grade crystalline schists — e.g. epidote-amphibole-schists, plagioclase-amphibolites and amphibole-schists, garnetiferous amphibolites, garnetiferous gneisses, piedmontite-bearing garnet-mica-schists with porphyroblastic plagioclase and crystalline limestones — and a number of lower grade types, e.g. phyllitic mica-schists and crystalline limestones.

A comparison is made with eastern Celebes where two different phases of metamorphism have been distinguished. It is suggested that the higher grade crystalline schist-series on Kabaëna may represent the older phase of metamorphism on Celebes, which is considered to be older than the

[7]) On Boeton contact phenomena caused by gabbroid and diabasic intrusions in the upper-triassic Winto-series have been recorded by BOTHÉ (Lit. 1), while HETZEL states that in this flysch-like series dikes and sills of diabase are a common phenomenon (Lit. 6, p. 21).

[8]) See i.a. BROUWER (Lit. 3, p. 24), BOTHÉ (Lit. 1, p. 100) and HETZEL (Lit. 6, p. 21).

ophiolitic rocks. No traces are found, in the rocks investigated from Kabaëna, of the younger, glaucophanitic metamorphism occurring on Celebes. It appears that the thermal metamorphism is younger than the regional metamorphism causing the higher grade crystalline schists. It is pointed out that the diabasic rocks responsible for the thermal metamorphism may be related to the gabbro-peridotitic intrusions occurring in the east arc of Celebes and consequently approximately of the same age.

REFERENCES.

1. BOTHÉ, A. CH. D., Voorloopige mededeeling betreffende de Geologie van Zuid-Oost-Celebes. De Mijningenieur, 8, 97—103 (1927).
2. BROUWER, H. A., Geologische onderzoekingen op het eiland Celebes. Verh. Geol. Mijnb. Gen. voor Ned. en Kol., Geol. Ser. **10**, 39—217 (1934).
3. ————, Geological explorations in Celebes. Summary of the results. In: Geological explorations in the island of Celebes under the leadership of H. A. BROUWER. Amsterdam, 1—64 (1947).
4. EGELER, C. G., Contribution to the petrology of the metamorphic rocks of western Celebes. In: Geological explorations in the island of Celebes under the leadership of H. A. BROUWER, Amsterdam, 175—346 (1947). Also published as thesis, Amsterdam (1946).
5. GISOLF, W. F., Mikroskopisch onderzoek van gesteenten uit Z.O. Selébès. Jaarb. Mijnw. Ned. Indië. Verh., 66—113 (1924).
6. HETZEL, W. H., Verslag van het onderzoek naar het voorkomen van asfaltgesteenten op het eiland Boeton. Versl. en Med. Betr. Ind. Delfstoffen, **21**, Batavia, (1936).
7. PALACHE, C. and H. E. VASSAR, Some minerals of the Keweenawan copper deposits: pumpellyite, a new mineral; sericite; saponite. Amer. Min. **10**, 412—418 (1925).
8. ROEVER, W. P. DE, Igneous and metamorphic rocks in eastern Central Celebes. In: Geological explorations in the island of Celebes under the leadership of H. A. BROUWER, Amsterdam, 65—174 (1947).
9. ————, Occurrences of the mineral pumpellyite in Eastern Borneo. Bull. of the Bur. of Mines and the Geol. Surv. in Indonesia, **I**, **1**, 16—17 (1947).
10. SARASIN, P. and F., Entwurf einer geographisch-geologischen Beschreibung der Insel Celebes. (1901), with petrographical descriptions by C. SCHMIDT.
11. TURNER, F. J., Mineralogical and structural evolution of the metamorphic rocks. Geol. Soc. Amer., Mem. 30, (1948).
12. WUNDERLIN, W., Beitrage zur Kenntnis der Gesteine van Südost-Celebes. Samml. Geol. Reichsmus. Leiden, 9, 244—280 (1913).

Amsterdam, Geological Institute of the University.

Crystallography. — *Transformation of gnomograms and its application to the microchemical identification of crystals.* II. By D. W. DIJKSTRA. (Memorandum of the Crystallographic Institute of the Rijks-Universiteit at Groningen.) (Communicated by Prof. J. M. BIJVOET.)

(Communicated at the meeting of February 26, 1949.)

§ 11. Two applications of the method dealt with in the previous part will be discussed here.

a. TERPSTRA describes in his book [6]) how to make a pasteboard model of a crystal of cane sugar. The gnomogram is shown in fig. 228 (p. 275), and represented in our fig. 14 by full lines, the poles being indicated by dots. In order to make it possible to reproduce the face (001) in its true form another gnomogram has to be constructed with the pole (001) in its centre; then an orthogonal parallel projection onto the plane of drawing will produce the face with the angles between the edges having the correct values. This modified gnomogram is shown in TERPSTRA's fig. 230 (p. 280). In our fig. 14 the required transformation has been performed as described in the first part of this article (§ 8*a*; cf. figg. 6 and 12) without any numerical values of the angles having been used. The —·—·—·—·— lines represent the modified gnomogram, the circlets its poles.

(The small distance between (001) and the centre, $13\frac{1}{2}°$, causes the old zone line $h' = 0$ to coincide in the drawing practically with the new one $h = 0$, and (001) likewise with P_n. In the original drawing the radius of the gnomon circle being 6 cm the distance between O' and (001) is equal to 6 tan $13\frac{1}{2}° = 1{,}44$ cm and that between O' and P_n to 2×6 tan $6\frac{3}{4}° = 1{,}42$ cm).

b. The method can be useful in microchemistry, when microscopical crystals have to be identified [7]); the measuring of the angles by means of a goniometer then being impossible or at least very difficult, an ordinary microscope provided with a revolving stage with graduation is used. The investigator will see the crystal, resting with one of its faces upon the object glass, projected orthogonally onto that plane and thus will be able to measure the angles by which the edges intersect in this image. When he has some notion or other of the chemical identity of the crystal, he can look up the data on the crystallographic properties of this substance, surmise on which of its faces the crystal may rest and then construct its orthogonal projection onto this plane (if desirable onto several). If the constructed angles and the measured ones agree, the crystal will be thus identified. Moreover the orientation of the crystal on the object glass

6) P. TERPSTRA, "Kristallometrie" (Groningen, 1946) p. 279 seqq.
7) J. D. H. DONNAY and W. A. O'BRIEN, Anal. Ed. Ind. & Eng. Chem. **17**, 593 (1945).

will be known and the question will be answered as to which of its edges are seen as lines in the image formed by the microscope.

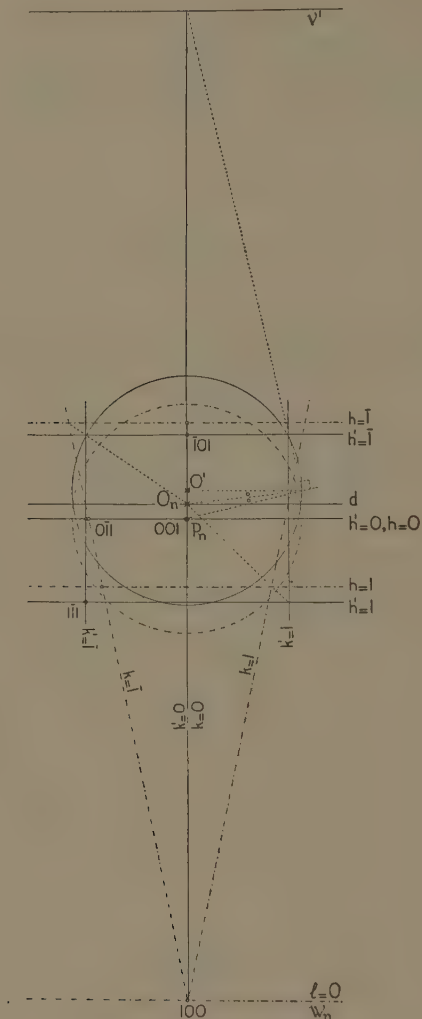

Fig. 14

In order to elucidate this we will take silverdichromate as an example, the formation of this substance being used in microchemistry to identify both silver ion and chromate ion [8]). A correct performance of the reaction will result in tolerably large, well shaped crystals, coloured yellow to reddish-brown, in most cases plate-shaped and sometimes so thin that no colour is to be seen. If the crystal shown by the microscope is expected to be silverdichromate, this conjecture can be verified as follows:

---

[8]) BEHRENS–KLEY, "Mikrochemische Analyse" (1915), vol. 1, pp. 87 and 121. F. EMICH, "Mikrochemisches Praktikum" (1924) p. 88.

The image of the crystal is copied as seen in the microscope (fig. 15 *B, C, D*). The angles between the lines in this image can be measured, if the crystal is a suitable one, with an exactitude of about ½°, or measurements can be taken on a microphotograph of the crystal.

GROTH [9]) describes the crystal of silverdicromate, measured by SCHABUS. The crystals are apt to be plate-shaped, the face (100) predominating, and elongated in the direction of the *c*-axis. The table of angular values is from TERPSTRA [6]) p. 190.

Face	φ	ϱ
b	0°	90° 0′
a	70° 35′	90° 0′
μ	136° 11′	90° 0′
ω	113° 2′	56° 41′
o	40° 29′	65° 8′
c	68° 9′	32° 51′
ϱ	258° 7′	11° 39′

From these angular values the gnomogram shown in fig. 15 is constructed as usual, the angles φ being located on the gnomon circle and the distances $R \tan \varrho$ (R being the gnomon distance) being laid off from the centre on the radii through the corresponding points.

From the description of its habit the crystal may be expected to rest upon the object glass with face *a* {100}; obviously the gnomogram has to be changed into another one, having the pole (100) in its centre. The polar distance of *a* being 90° the bisector of $\angle O'OA$ (fig. 5) forms with the line OO' an angle of 45°, so *d* (fig. 15*A*) can be drawn tangent to the circle in its point of intersection with $O'a$. Now O_n will be represented by this point of intersection and v' by the line through $O' \parallel d$ (see § 5 and § 8 (*a*)).

It will, however, not be necessary to perform the transformation completely, only the directions of the new zone lines — and not the zone lines themselves — being wanted, since in the construction of an orthogonal projection only this simple proposition is used: the orthogonal projection e' of the edge *e* between the faces *A* and *B* onto the plane of drawing will be perpendicular to the zone line through the poles *a* and *b* of these faces [10]).

Now after transformation (§ 6, fig. 6*b*) the zone lines will be parallel

[9]) P. GROTH, "Chemische Kristallographie", vol. 2, p. 591.

[10]) The demonstration of this proposition runs as follows: $Oa \perp A$, so $Oa \perp$ any line in face *A*, including the edge *e*; $Ob \perp B$ and so $\perp e$ too. This means $e \perp$ the plane through Oa and Ob and — the zone line through the poles *a* and *b* lying in this plane — $e \perp$ this zone line. The perpendicular OO' is dropped onto the plane of drawing, and this line OO' will be $\perp$ the zone line too. The zone line, being $\perp e$ and $\perp OO'$, thus will be $\perp$ the plane through *e* and OO', which is the plane projecting *e*. The line of intersection e' of the plane of drawing and this plane now will be $\perp$ the zone line.

to the lines connecting O_n with the points of intersection of the original zone lines with v'. So the directions of the new zone lines (represented

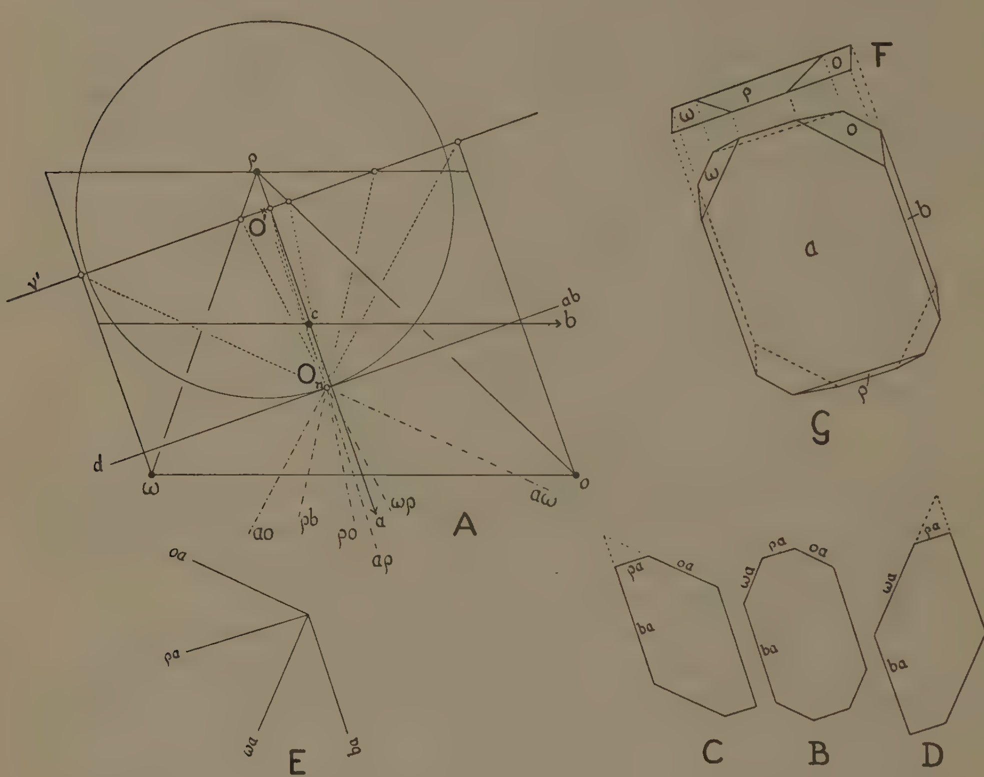

Fig.15

by —·—·—·—·— lines) can be constructed as a pencil through O_n that will result, when the points of intersection of v' with the original zone lines are connected with the point O_n.

The projections of the edges, being perpendicular to these zone lines, will form a pencil similar to the one through O_n but rotated through 90°. The crystal being likely to rest on *a* {100}, in the first place the directions of the new zone lines through *a* will be constructed.

On a piece of transparent paper the directions obtained from the crystal itself are laid off from one point (fig. 15 *E*); this is laid on top of the pencil constructed through O_n and now the pencils are tested as to their similarity by rotation, which then should make them coincide. If this should not happen, then turn the paper upside down and try again, as the crystal may as well lie on the face (100) as on ($\bar{1}00$). In the case dealt with here the pencils turn out to coincide exactly, which justifies the conclusion that the crystal will be almost certainly one of silver-dichromate lying with face (100) uppermost.

As of each zone line it is known through which pole it passes including *a*, the lines in the image formed by the microscope which can be made to coincide with the zone lines, can be determined as the edges between these faces and face *a*.

Some elaboration in this case being worth while, the top view of the crystal is designed (fig. 15*F*), its lines being drawn perpendicular to the zone lines of the original gnomogram.

Then the projection of the crystal onto plane *a* is designed (fig. 15*G*), which will result when from the points of intersection in the top view perpendiculars are dropped onto the line *d* and the edges between the faces are added, each of them being perpendicular to the corresponding zone line in the transformed gnomogram. The outline of this fig. 15*G* agrees with the image of the crystal as seen by microscope (In fig. 15*G* the faces μ and *c* have not been reproduced because none of the crystals measured showed their edges.)

If the crystal is a very thin plate, the observed outline will be that of its upper face (fig. 15*B*), the absence of face ω resulting in fig. 15*C* and that of face *o* in fig. 15*D*. All of these shapes have been observed.

These figg. *C* and *D* are almost similar to each other, especially if one of them should lie upside down; both figures can be defined as rhombs with the acute corners cut off. Moreover the angular values turn out to differ only slightly. The methods of analytic geometry have been followed in the calculation of the under mentioned angular values from the gnomogram. This calculation is, as the construction described above, very simple. The construction being restricted to intersections of lines and connections of points the calculation runs as follows: the coordinates of the given poles are determined and the equations of the zone lines, then the coordinates of their points of intersection with v' and last of all the equations of the lines connecting these points of intersection with O_n, their direction coefficients being the tangents of the angles they form with the *X*-axis. Only the results of this calculation will be mentioned here.

The obtuse angle of the rhomb, formed by *ab* and $a\omega$ in fig. *D*, is equal to 135° 45′, that between *ab* and *ao* in fig. *C* to 137° 16′.

The line *ao*, which cuts off the acute corner of the rhomb, forms in fig. *D* angles of 132° 4′ and 92° 11′ and in fig. *C* of 134° 55′ and 87° 49′.

The fact that the angles, in connection with the attainable accuracy of the measurements are practically equal, is very confusing, if the above interpretation should be wanting. In BEHRENS–KLEY the acute angle of the rhomb is recorded to be equal to 43°. In fig. *C* this angle is equal to 42° 44′, in fig. *D* to 44° 15′, the value 43° probably being the average of the values found for edges that were held to be the same, actually being different ones.

In this case *C* and *D* cannot be distinguished by the orientation of the extinction directions, the plates frequently being so thin, that in spite of the strong reddish-brown colour of silverdichromate they will show in white

light only a faint greyish colour, which makes the interference colour between crossed NICOLS of so low an order that the extinction direction cannot be determined with a reasonable degree of exactitude.

In general an exact calculation of the angular values will not be necessary, since the results of the construction will have about the same degree of exactitude as those obtained from the image formed by the microscope. If however, as in the case of silverdichromate, a slight difference between some of them might bring about some confusion, the required certainty can be easily obtained by means of calculation.

Finally I wish to express my gratitude to Prof. Dr P. TERPSTRA, Groningen, and to Dr W. F. DE JONG, Delft, for the interest shown to me, when this article was being written.

Rotterdam, October 1948.

Astronomy. — *Magnitude effects in G-type stars.* By P. J. GATHIER.
(Communicated by Prof. M. G. J. MINNAERT.)

(Communicated at the meeting of March 26, 1949.)

Summary.

Equivalent widths have been measured for Ca I λ 4227 and Sr II λ 4077 in the spectra of 14 stars — supergiants, giants, dwarfs — with all about the same spectral type as the sun. The observed values are satisfactorily explained by the theory of stellar atmospheres. The damping constant is found to be five to ten times larger for dwarfs than for giants and supergiants.

Introduction.

The material consists of 14 stellar spectra, taken by Professor MINNAERT at the McDONALD Observatory with the Cassegrain spectrograph, equipped with two quartz prisms. The focal length of the camera was 50 cm, the dispersion was 40 A/mm near H_γ; the plates cover the region $\lambda\lambda$ 3500—4700. The stars investigated are dwarfs, giants and supergiants of the spectral types *F*5—*G*5. Nine of the plates carried a calibration, obtained with a tube photometer. Since the exposure times did not differ by more than a factor two and since all plates were developed in the same way, it was possible to construct one mean density curve for the whole material. The spectra have been recorded by means of the Utrecht microphotometer on a 60-fold scale.

We proposed to study for these stars the relation between the observable quantities: the absolute magnitude M and the spectral type, and the theoretical parameters: temperature and effective gravitational acceleration. Just because the atmosphere of the sun has been studied so well, these stars of a similar type are well fitted for a comparative theoretical investigation.

A search for luminosity characteristics.

The stars which have been selected are but little different in spectral type; since their absolute magnitudes vary over a considerable range, vid. lic. from $M = +6$ to $M = -6$, it seemed interesting to look in the first place for spectral lines which are very sensitive to variations of the absolute magnitude. With the purpose to find such characteristic lines, the galvanometer deflections on the registrograms were compared for giants and for dwarfs, without converting them into intensities. In figure 1 these values are compared for the dwarf star ζ Her GO IV and for the supergiant β Aqu GO I^b. A hundred points were obtained, scattered about

a main line; this is not a straight line under an angle of 45°, because the plates have not the same density. Some points are lying well away from

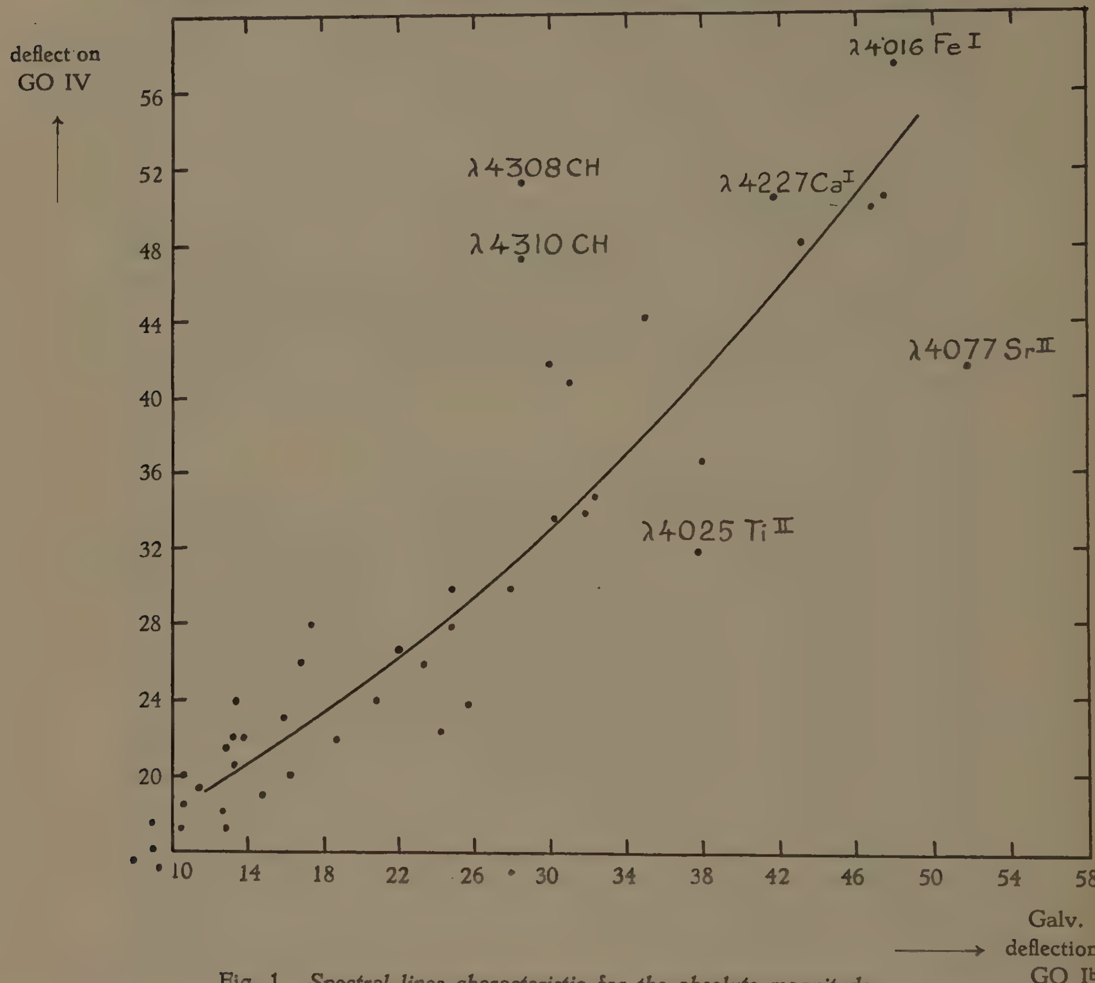

Fig. 1. *Spectral lines characteristic for the absolute magnitude.*
Comparison between the galvanometer deflections for several spectral lines in a dwarf and in a supergiant.

it: these represent lines which are much stronger or much weaker in giants than in dwarfs. Strikingly stronger in giants are for example Sr II λ 4077 and Ti II λ 4025, while the CN-bands and Ca I λ 4227 are conspicuously weaker. These are just the lines, generally used as criteria of the luminosity for *G*-type stars. For some of these lines the variations of the galvanometer deflection with the spectral type have been determined and the ratio between the deflections for two spectral lines has been investigated as a function of the absolute magnitude (figure 2). Here for the determination of the spectral type, MORGAN's classification [1]) has been

[1]) MORGAN, KEENAN, EDITH KELLMAN, An atlas of stellar spectra.

used (table I). Two interesting lines, namely Ca I λ 4227 and Sr II λ 4077 have been studied into more details, with the purpose to connect the theory of the stellar atmospheres with the observations.

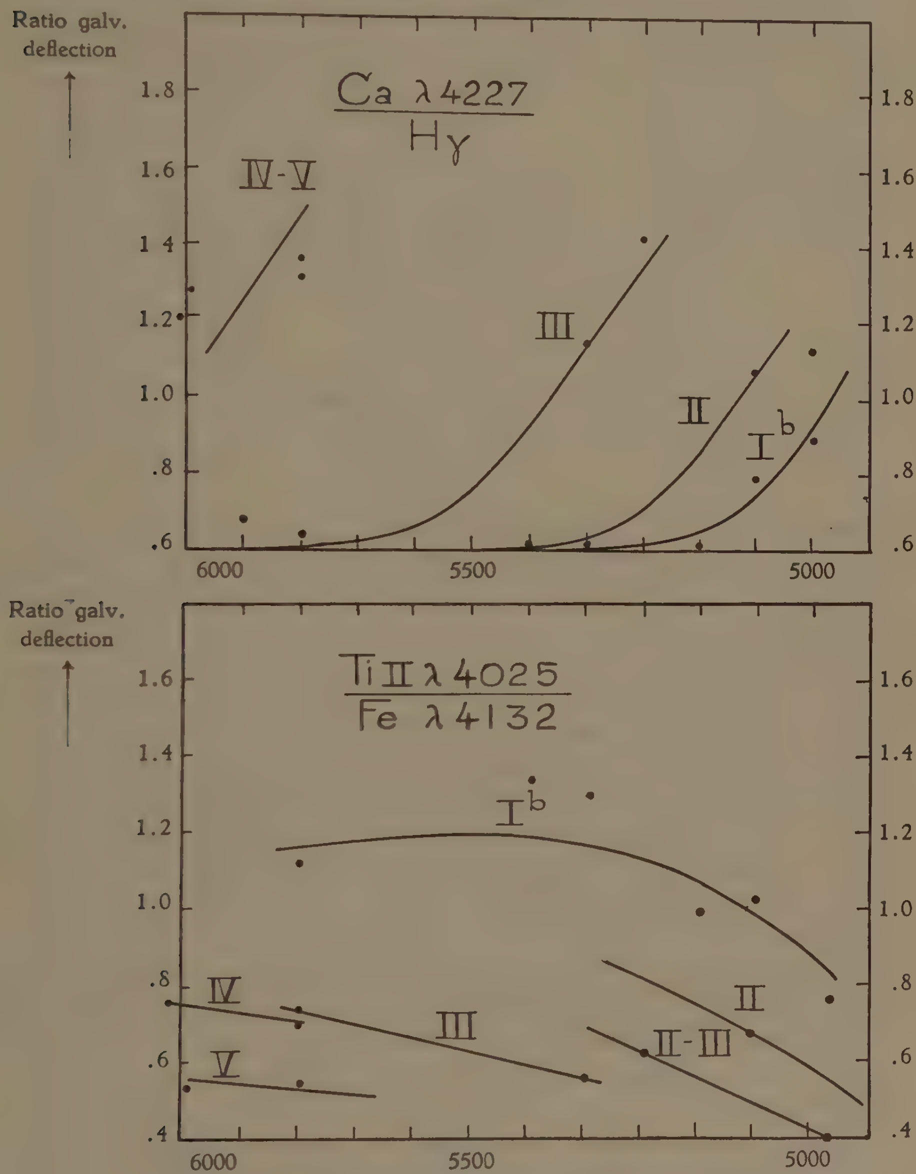

Fig. 2. The ratio of the galvanometer deflections:
1) for Ca I λ 4227 and H_γ;
2) for Ti II λ 4025 and Fe I λ 4132.
Variation of these ratio's in stars of different absolute magnitudes and effective temperatures.

Ca I λ 4227.

The equivalent width W_λ was measured on the available 14 stellar spectra.

TABLE I. Stars observed for spectral line intensities.

Star	Spectrum	M	W_{4077}	W_{4227}	T_{eff}° K
β Aqu	G0 I^b	−3	2.0	1.4	4950
ζ Her	G0 IV	+3.2	1.0	1.4	5800
α Per	F5 I^b	−3	1.55	0.95	5800
$\varkappa$ Cet	G2 V	+5.0	0.77	1.5	5900
δ C Ma	F8 I^a	−6	2.3	1.5	5000
9 Peg	G2 I^b	−2.3	1.65	2.0	4700
$\varkappa$ Cet	G2 V	+5.0	0.8	1.5	5900
β Lep	G2 II	−2.0	1.0	1.4	5000
η Cas A	G0 V	+4.9	0.6	0.9	6050
v Peg	F8 III	+0.7	0.9	0.9	5700
ϱ Pup	F6 II	−0.3	1.3	1.1	5800
γ Cyg	F8 I^b	−4.3	1.8	1.1	5300
α Sag	G1 II	−1.9	1.35	1.35	5100
η Peg	G2 II—III	−1.0	1.25	1.5	5100
9 Peg	G2 I^b	−2.3	1.7	1.9	4700
v And	F8 IV	+4.9	0.75	1.2	6000

Because λ 4227 is a resonance line and all Ca-atoms are in the fundamental level, the number of absorbing atoms is determined by the ionisation temperature T_{ion}. According to investigations on spectra taken with a considerable dispersion T_{ion} will be very much the same as the effective temperature T_{eff}.

With the help of the data of BECKER [2]) and KUIPER [3]) the relation between the effective temperature and the spectral type has been determined for each of MORGAN's luminosity classes (table I).

In figure 3 the measured W_λ-values are plotted as a function of T_{eff}, values of W_λ determined by other writers being also included. Two different sequences are clearly shown, one for the dwarfs and another one for the giants and supergiants.

The following simple theory was used for the calculation of the equivalent widths of Ca I λ 4227 in stellar atmospheres, characterized by different values of T and the effective gravitational acceleration g. The total number of calcium-atoms in a stellar atmosphere is determined by:

1. The total number of all atoms or ions in that part of the atmosphere which can be considered to be transparent;
2. the Ca-abundance, A_{Ca}, defined as the fraction of the atoms or ions in the atmosphere which are either Ca I or Ca II;
3. the equilibrium between the number of Ca-atoms and Ca-ions, as given by SAHA's law for every value of T and p_e, the electron pressure.

For the calculation in these three steps, the numerical values of the different quantities will be chosen as well as possible in accordance with

---

[2]) BECKER, Zs. f. Ap. 25, 145 (1948).
[3]) KUIPER, Ap. J. 88, 429 (1938).

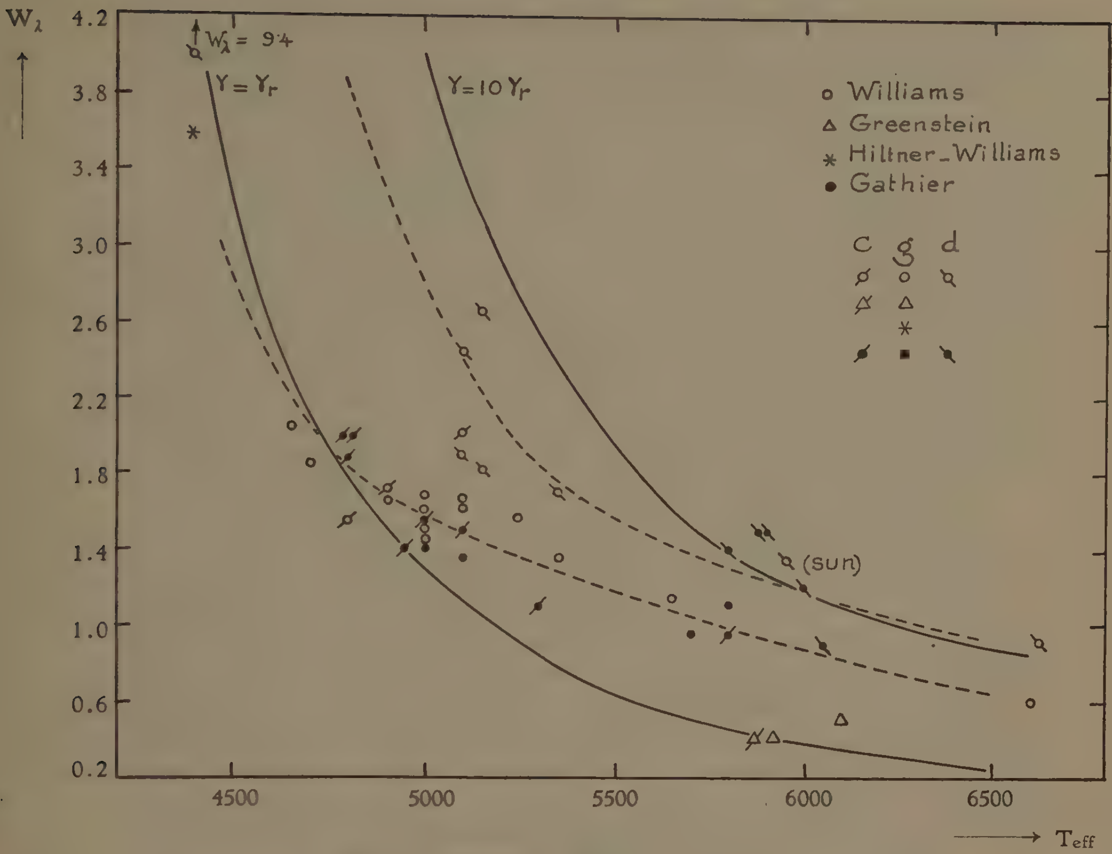

Fig. 3. *Equivalent widths of Ca I λ 4227.*
Fulldrawn lines: theoretical equivalent widths for $\gamma = \gamma_r$ and for $\gamma = 10\,\gamma_r$.
Dotted lines: observed values of W_{4227} as a function of temperature, for giants-supergiants (left line) and for dwarfs (right line).
The dispersions used are (near H_γ):
WILLIAMS [4]) 17 A/mm; GREENSTEIN [5]) 3 A/mm;
HILTNER–WILLIAMS [6]) 3 A/mm; GATHIER 40 A/mm.

earlier results of other authors. If N is the average number of atoms or ions per cm^3 and H is the effective height of the atmosphere, we have:

$$NH = \frac{\tau_0}{\mu\, m_H\, \varkappa}$$

where τ_0 is the effective optical depth, μ the mean atomic weight, m_H the mass of the H-atom and $\varkappa$ the continuous absorption coefficient [7]).

We assume [8]) $\mu = 1.5$ and provisionally $\tau_0 = 0.7$, which is a convenient value for the sun [9]).

---

[4]) WILLIAMS, P. A. S. P. **48**, 113 (1936).
[5]) GREENSTEIN, Ap. J. **107**, 151 (1948).
[6]) HILTNER–WILLIAMS, A Photometric Atlas of Stellar spectra.
[7]) UNSÖLD, Physik der Sternatmosphären 1938, Chapter XII.
[8]) Miss ROSA, Zs. f. Ap. **25**, 9 (1948).
[9]) TEN BRUGGENCATE, Veröff. Univ. Sternw. Göttingen **76** (1947).

At present it seems well established that the continuous absorption for stars of the spectral type investigated is due to the H^--ions; the absorption coefficient $\varkappa$ is known from theory [10].

For A_{Ca} a value 1.45×10^{-6} has been taken. The electron pressure p_e can be expressed as a function of T and the gas pressure p. With the aid of the relation $p = \frac{\tau}{\varkappa} g$ we introduce g as parameter instead of p_e [11]. So, if N_a is the number of active Ca-atoms, it is possible to calculate $N_a H$ for every value of T and g (fig. 4). From this figure one can see that in

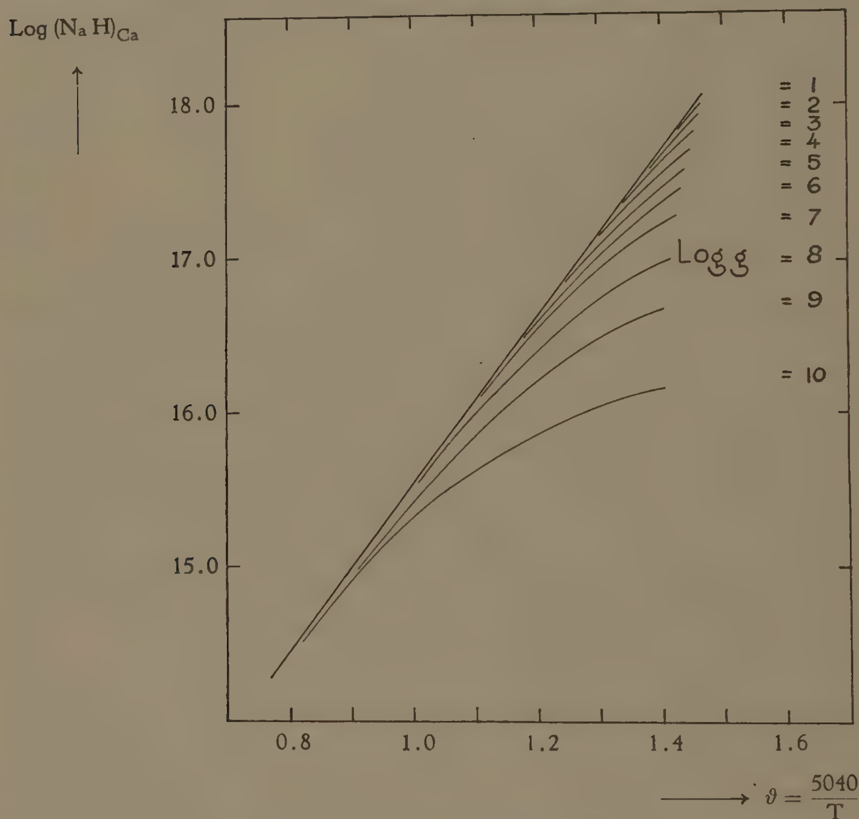

Fig. 4. *The theoretical number of active Ca-atoms,* for different temperatures and effective gravitational accelerations.

the temperature range here investigated, since log g is always < 5, the values of $N_a H$ cannot be expected to be different for dwarfs and for giants.

The Ca-line at λ 4227 is a strong line and so its equivalent width can be calculated by the relation:

$$W_\lambda = \frac{\lambda^2}{c} \sqrt{\frac{e^2}{mc} N_a H \gamma f}.$$

[10]) CHANDRASEKHAR and MÜNCH, Ap. J. **104**, 446 (1946).

[11]) Compare also Miss ROSA, Zs. f. Ap. **25**, 4 (1948).

The best value for f is 1.2. About the damping there is always the uncertainty how much of it is due to the radiation and how much to collisional damping. Therefore W_λ has been calculated for two different cases:

1. for pure radiation damping, $\gamma = \gamma_r = 1.6 \times 10^8$; and
2. for the damping as derived from the solar spectrum, which is ten times the damping caused by radiation. In figure 3 both theoretical cases have been considered.

In comparing the theoretical curves with the observations, it is found that the E.W., measured on small dispersion plates, are in general too great; GREENSTEIN, working with the Coudé-spectrograph, finds lower values which are much closer to the theoretical ones. This effect has been found many times before; it may be due to blends, which are not well discerned if the dispersion is small; or perhaps to photographic effects. We conclude that probably some correction of the order of —0,4 A will have to be applied to our measurements, but that the main differences between the luminosity classes will subsist and that the values of the damping constants will not materially be altered.

The giants and supergiants are pretty well in agreement with the theoretical curve for $\gamma = \gamma_r$. Evidently γ is greater for dwarfs, because the pressures in their atmospheres and the collisional damping are much higher than in giants or even supergiants. To the change from giants to supergiants corresponds no further decrease of γ; this seems to show that we have already reached a minimum value for γ in the giants, which must evidently be γ_r. Thus for stars with $M < 3$ or $\log g < 2$, we have $\gamma = \gamma_r$, while for larger values of M the damping increases rapidly. For the sun ($M = 5$, $\log g = 4.4$) usually $\gamma = 10\ \gamma_r$ is adopted; WRIGHT supposes that this applies to all dwarfs [12]).

From figure 3 a somewhat smaller value for γ is deduced but this may be due to our assumption, that the effective optical depth is the same in dwarfs and in giants. Moreover, the material is still too small to derive more definitive values.

Sr II λ 4077.

Also for this spectral line the equivalent widths have been measured on the available plates (figure 5). The theoretical values of λ 4077 have been calculated in the same way as for λ 4227. For the Sr-abundance we assumed 2.35×10^{-9} [13]), while for all other quantities the same numerical values as for λ 4227 have been used. In figure 5 on the left side the theoretical values of W_λ have been plotted for $\gamma = \gamma_r$, and at the right for $\gamma = 10\,\gamma_r$. The assertion that $\gamma = \gamma_r$ for giants and supergiants and $\gamma = 10\,\gamma_r$ for dwarfs seems well-confirmed; the g-values from figure 5

[12]) WRIGHT, Dom. Ap. Obs. 8, 1 (1948).
[13]) UNSÖLD, Zs. f. Ap. 24, 306 (1948).

agree in a satisfactory way with those, mentioned in the literature for supergiants, giants and dwars [14], [15], [16].

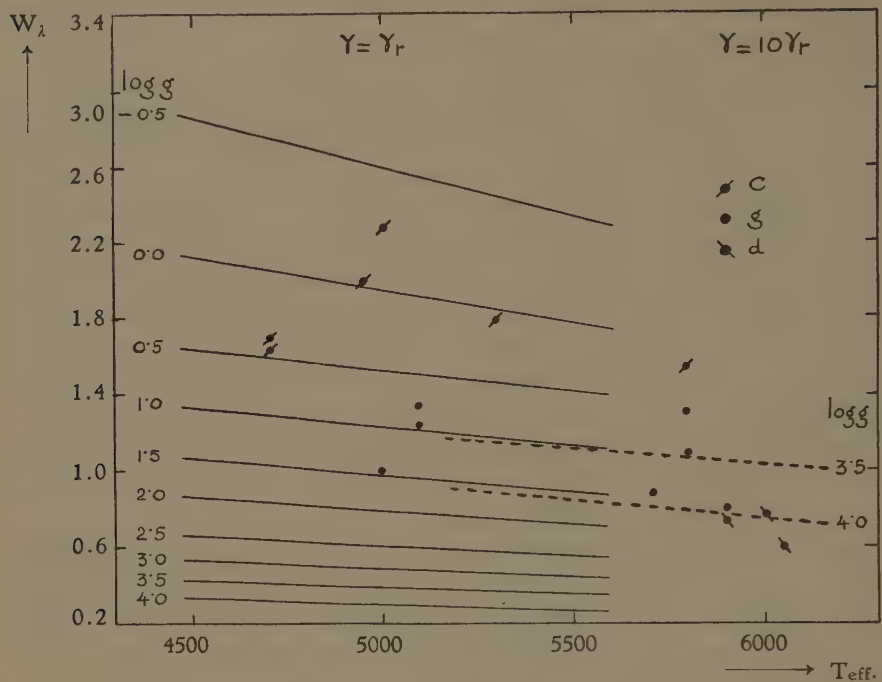

Fig. 5. *Equivalent widths of Sr II λ 4077.*
Fulldrawn lines: the theoretical values of W_{4077} for different values of log g, computed for $\gamma = \gamma_r$.
Dotted lines: the same for $\gamma = 10\,\gamma_r$. The points represent the measured W_{4077}.

I am much indebted to Professor M. MINNAERT, who suggested this investigation and gave me his continuous help.

---

14) GREENSTEIN, Ap. J. **107**, 151 (1948).
15) WRIGHT, Dom. Ap. Obs. 8, 1 (1948).
16) PANNEKOEK and VAN ALBADA, Publ. Astr. Inst. Univ. Amsterdam, **6** (1946).

Botany. — *De hypothese voor de erfelijkheidsformules van de twee zuivere lijnen I en II van Phaseolus vulgaris op grond van kruisingsproeven.* II. By G. P. FRETS. (Communicated by Prof. J. BOEKE.)

(Communicated at the meeting of January 29, 1949.)

We gaan nu over tot het onderzoek van de erfelijkheid van de bonen met de grootste breedten en resp. met een zeer grote en een niet zeer grote lengte van de F_3-zaadgeneratie van 1935. Daarvoor gaan we de erfelijke samenstelling van enige bonenopbrengsten van tab. 5 na.

TABLE 5. The beanyields with the greatest mean breadths of F_3-1935 and comparison beanyields of the I- and the II-line of 1935.

N	Pl.	n	B	Gr. var.	Sm. var.	L	Gr. var.	Sm. var.
F_3-1935. 1—6. The mean length is great; 7—12 the mean length is small.								
1	73	35	95.4	112	73	159	183	120
2	71	29	96.3	104	85	155.6	182	138
3	95	52	98	105	89	155	177	139
4	63	50	97.6	111	78	153.5	174	127
5	84	52	91.5	98	83	149.7	167	133
6	60	64	92.7	104	81	149.5	166	119
7	93	56	91.7	102	80	136.3	155	115
8	47	75	91.8	113	80	140.6	160	119
9	58	47	96.7	113	83	142.3	157	117
10	80	100	92.5	105	78	143.9	171	120
11	68	51	96.9	115	78	144.2	170	126
12	87	58	95.7	106	75	146.7	164	107
	I-line 1935							
	1	36	96.4	117	73	158.2	193	128
	16	45	94.7	130	73	160.2	216	125
	10	49	90.6	106	66	149.3	178	112
	II-line 1935							
	22	48	90.4	97	76	120.8	130	98

Dimensions in 0.1 mm. The standarddeviations and variation coefficients are omitted. The mean error (m) of the mean dimensions is for the lengths, $m_l = 1.5$—2.5, for the breadths $m_b = 1$—2.

Pl. 73. De bonenopbrengst van pl. 73 heeft de grootste gemiddelde lengte van de bonenopbrengsten van de F_3-generatie van 1935. De uitgangsboon voor pl. 73 is van pl. 81, F_2-1934 en heeft eveneens een zeer grote lengte (de grenswaarde) en grote breedte (tab. 6 en fig. 1, blz. 427). De formule van de gemiddelden van de bonenopbrengst van pl. 81 is $L_1\, l_2\, B\, Th$, cl. 1b. De bonenopbrengst van pl. 81 bevat, naast bonen met een grote breedte en een zeer grote lengte, zoals de uitgangsboon voor pl. 73, ook

TABLE 6. The heredity of beans of some beanyields of F_3-1935 with great mean breadths. Four succeeding generations.

N.	Pl.	Bean	L	B	Th	W	LB	LTh	BTh	N.	Pl.	n	L	B	Th	W	LB	LTh	BTh
Initial beans are crosses (F_1) I×II and II×I										F_2 — 1934. Averages									
1	II×I		124	79	67	43	64	54	85	1	81	90	142	87	70	62	61	49	80
2	II×I		128	84	68	50	66	53	81	2	82	91	141	85	69	59	61	49	81
3	I×II		152	86	68	58	57	45	79	3	70	51	139	92	74	69	67	53	80
4	I×II		154	90	67	61	58	44	75	4	76	64	134	88	69	59	66	52	79
Initial beans of F_2 — 1934 for beanyields of F_3 — 1935										F_3 — 1935. Averages									
1	81	4p 1b	155	96	67	73	61	43	69	1	73	35	159	95	63	66	60	40	66
2	82	13p 3b	158	90	71	71	57	45	79	2	93	56	136	92	67	59	67	49	74
3	70	6p 3b	132	94	77	70	71	58	82	3	58	47	142	97	64	63	69	45	66
4	76	12p 2b	149	93	64	62	62	43	69	4	68	51	144	97	66	67	67	46	69
Initial beans of F_3 — 1935 for beanyields of F_4 — 1936										F_4 — 1936. Averages									
1	73	2p 1b	183	112	73	101	61	40	65	1	309	38	154	100	65	66	66	42	64
2a	93	1p 2b	134	94	71	61	70	53	76	2a	352	23	140	88	63	56	63	45	72
2b	93	6p 2b	155	102	75	74	66	48	74	2b	353	24	131	85	60	48	65	46	70
2c	93	10p 1b	116	83	56	39	72	48	68	2c	354	25	143	91	65	61	64	45	71
3a	58	1p 2b	152	113	60	75	74	39	53	3a	259	21	119	85	53	41	71	44	62
3b	58	7p 1b	167	110	64	83	66	38	58	3b	260	23	126	86	58	45	68	46	67
4a	68	1p 1b	170	109	65	98	64	38	60	4a	291	15	140	96	55	55	69	39	57
4b	68	4p 4b	143	96	72	68	67	50	75	4b	292	25	132	90	55	46	68	42	61
4c	68	9p 3b	156	103	75	87	66	48	73	4c	293	23	129	88	59	47	68	46	67
4d	68	13p 2b	137	100	68	68	73	50	68	4d	294	14	134	93	63	55	69	47	68
Initial beans of F_4 — 1936 for beanyields of F_5 — 1937										F_5 — 1937. Averages									
1a	309	7p 1b	178	113	57	84	63	32	50	1a	239	25	162	101	66	81	62	41	65
1b	309	3p 1b	168	107	71	77	64	42	66	1b	151	13	149	89	61	59	60	41	68
1c	309	3p 3b	142	103	69	66	73	49	67	1c	152	21	149	90	68	68	61	46	76
1d	309	3p 5b	150	99	68	69	64	45	69	1d	153	29	137	85	61	54	62	45	72
2		—								2	—								
3aa	259	6p 1b	135	95	56	50	70	42	59	3aa	206	29	131	87	61	54	66	47	70
3ab	259	6p 2b	128	95	55	49	74	43	58	3ab	207	28	125	89	55	45	71	44	62
3b	260	3p 1b	139	89	59	52	64	42	66	3b	208	30	131	86	62	53	66	47	72
4a	291	—								4a	—								
4ba	292	3p 1b	147	101	63	64	69	43	62	4ba	221	32	144	92	66	67	64	46	72
4bb	292	6p 1b	161	103	62	74	64	39	60	4bb	222	30	157	95	64	74	61	41	67
4bc	292	6p 2b	158	104	68	76	66	43	65	4bc	223	29	152	94	70	71	62	46	74
4bd	292	6p 3b	153	100	67	71	65	44	67	4bd	224	26	141	91	64	62	65	45	70
4ca	293	5p 1b	144	96	71	68	67	49	74	4ca	225	29	135	88	63	57	65	47	72
4cb	293	5p 2b	138	94	74	65	68	54	79	4cb	226	29	134	90	66	60	67	49	73
4d	294	2p 1b	140	102	68	67	73	49	67	4d	227	30	127	86	57	47	68	45	66

bonen met een grote breedte en een niet zeer grote lengte e.a. Bij de bonenopbrengst van 35 bonen van pl. 73, F_3-1935 (tab. 7) zijn 9 bonen met de grote breedte, $b = 10.1$—11.2 mm. Al deze 9 bonen hebben een zeer grote lengte $l = 16.6$—18.3 mm. Er zijn 11 bonen met de grote breedte 9.6—10.0 mm. Ook deze 11 bonen hebben alle een zeer grote lengte $l = 15.7$—17.5 mm. Van 7 bonen met de breedte, $6 = 9.1$—9.5 mm, is de lengte $l = 14.5$—15.3 mm. Van de overige 8 bonen is de breedte, $b = 7.3$ (dan volgt

TABLE 7. The breadths and lengths of the beans of 4 beanyields of F_3-1935 with great mean breadths of which the first (pl. 73) has a very great mean length whereas the mean length of the 3 other beanyields is not very great and comparison beanyields of the I- and the II-line of 1935.

Pl.	I	I	I	II	F_3	F_3	F_3	F_3	Pl.	I	I	I	II	F_3	F_3	F_3	F_3
	1	16	10	22	73	93	58	68		1	16	10	22	73	93	58	68
Br.	Length of beans								Br.	Length of beans							
66			112						90				120		137	135	
72			115						90				127			137	
73	128	132	124		120				90				124				
76				98					90				123				
77	132	132	134						90				118				
77		135	127						90				117				
78		131						126	90				127				
78		135							91	162		144	122	152	136	139	135
78		134							91	148			126		126		136
78		125							91				121		134		
79			127						91				127		148		
80	146	128				121			91				128				
80	138					118			92		167		127	149	136	138	143
81		137			128	115			92		166		130	145	141	140	
81						120			92		163		127		146	131	
82		140				131			92				120		136		
82						134			92				123		145		
83			142	116	141	129	118		92						144		
83						116			93		152	155	128	153	141	117	144
83						118			93			156	120	153	138	138	142
84			134	111		133			93			150	123		138	129	141
84			142						93			150			130	138	146
84			139						93			152			133	145	
85		140	145			140		129	93						142		
85		131	147						93						137		
86	142	149	157	120	136	138	135	133	94				127	149	134		141
86	148		151	114		141			94					150	135		135
86	145		143			130			94						132		
87	145		140	115		125			94						139		
87	148		142	116		134			94						139		
87	152					136			94						128		
87	141								94						143		
87	149								95	159		160	118		146	140	
88	155	151	149	116	146		136	134	95			166	127			140	
88	148	147		110	152				95			154	119				
88				105					95			157	127				
88				123					95			155	123				
89	152	171	153	120		134	137		95			145					
89				120			138		96		159	150	124	161	145	140	140
89				121			137		96		157	158	122	157	146	142	153
89				128					96					158	142	140	143
89				114					96						141	133	145
89				116					96								141
90		154	157	123	156	142	130	137	97	158	152	160	130	158	142	152	149
90		157	153	118	154	142	139	144	97	165	169	164		169	139	142	145

TABLE 7 (*Continued*).

Pl.	I	I	I	II	F_3	F_3	F_3	F_3	Pl.	I	I	I	II	F_3	F_3	F_3	F_3
	1	16	10	22	73	93	58	68		1	16	10	22	73	93	58	68
Br.	Length of beans								Br.	Length of beans							
97	157	177				136	153	148	103	161		159				157	152
97		165					146	142	103	168		153		174		144	148
97							144		103					171		150	145
98	164	168	149			174	141	156	103					176		148	156
98		192	163		175			145	104		181					145	
98		182			159			140	105	177				183			146
99			163		168			145	105								156
99								146	106			175					
99								133	107	178	158			176		155	
99								146	107							151	
99								154	108		173					160	
99								149	108		181						
99								139	109		180						170
99								136	110	162	160					167	
100		167	148		166		150	143	110	168	183						
100					161		141	140	110	188	182						
100							152	145	111	148							
100								137	111	167							
100								150	112		195			183			
101					166			150	112		196						
101					166			146	113							152	
101					178			153	115	183							
102	175	162	178			155	152	153	115	186							
102		171	160			152	147		117	193							
102			157				139		121		179						
102							147		130		216						

8.0)—9.0 mm, en de lengte, $l = 12.0$ (dan volgt 12.5)—15.6 mm. De bonenopbrengst van pl. 73 bevat dus veel bonen met een grote breedte (9.6—11.2 mm) en een zeer grote lengte (formule $L_1 L_2 B_1 b_2$), daarbij is er geen met een grote breedte en niet zeer grote lengte (formule $L_1 l_2 B_1 b_2$). Er is overeenstemming met bonenopbrengsten van de I-lijn van 1935 (tab. 7 en blz. 425).

Van pl. 73 is in 1936 een boon voortgekweekt. Ze leverde pl. 309, F_4-generatie 1936, fig. 2, blz. 430. Van de 38 bonen van deze bonenopbrengst, hebben 22 bonen de grote breedte $b = 10.1$—11.3 mm. Twee bonen ($b = 10.2$ en $= 10.3$ mm) hebben de lengte $l = 14.2$ mm, één boon ($b = 10.3$ mm) heeft de lengte $l = 14.5$ mm. Vijf bonen ($b = 10.1$, 10.4—10.8 mm) hebben de lengte $l = 15.0$—15.5 mm. De overige 14 bonen hebben alle een lengte groter dan 15.5 mm ($l = 15.6$—17.8 mm). De bonenopbrengst van pl. 309 bevat brede en minder brede peulen. De brede peulen bevatten zeer brede bonen. Deze bonen hebben een hoge L B-index (L B = 68—73). Daardoor is ook de gemiddelde L B-index hoog, ($LB_{gem} = 66$, tab. 6) en ligt in het characterogram L B hoog (fig. 2b). De bonenopbrengst is ten opzichte van bonen met de form. $L_1 L_2 B_1 b_2$ niet geheel eenvormig. Ze bevat veel bonen met een grote breedte en een zeer grote lengte, zodat de samenstelling van de bonenopbrengst wel wijst op de erfelijkheid van bonen met de form. $L_1 L_2 B_1 b_2$ voor de lengte en de breedte.

Van pl. 309 zijn in 1937 4 bonen voortgekweekt. Ze leverden pl. 239 en 251—253, F_5-1937. De uitgangsboon van pl. 309 voor pl. 239 is de boon met de grootste breedte en de grootste lengte van deze bonenopbrengst. De breedte is zeer groot, daardoor is de L B-index vrij hoog (tab. 6) en ligt ook in het characterogram (fig. 3a) L B vrij hoog.

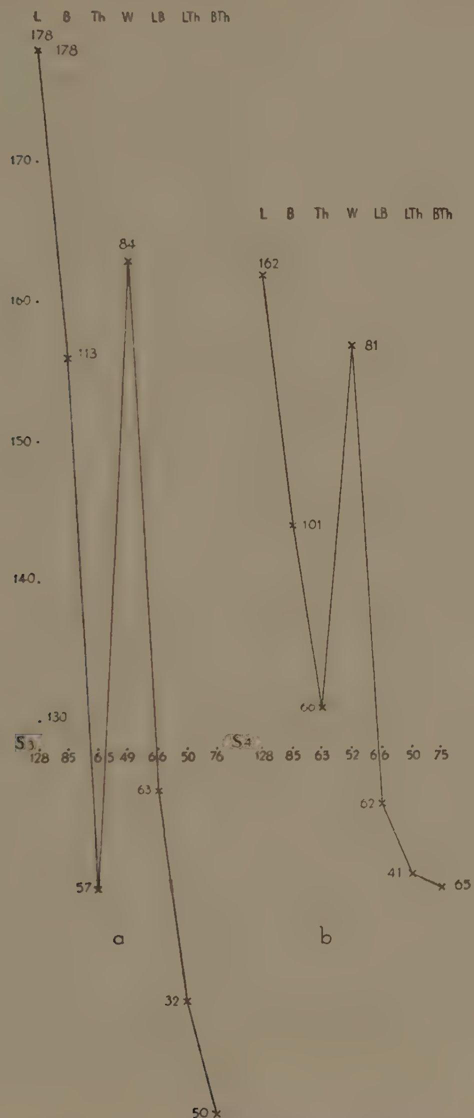

Fig. 3. *a.* Characterogram of 7 p l b, initial bean of pl. 309, F_4-1936 for pl. 239, F_5-1937. *b.* Idem of the average of the beanyield of pl. 239, F_5-1937. S_3 = Standardcharacterogram of 1936; S_4 = id. of 1937.

De bonenopbrengst van 25 bonen van pl. 239, F_5-1937, fig. 3*b*, bevat veel bonen met een grote breedte en een zeer grote lengte. Van 13 bonen met de grote breedte, b = 10.1—10.9 mm, is de lengte 15.8—17.5 (van één boon, b = 10.3 is l = 15.2 mm). Van 7 bonen met de grote breedte b = 9.6—10.0 mm, is de lengte, l = 15.7—17.0 mm. Van de overige 5 bonen is b = 8.9—9.5 mm en de lengte, l = 14.8—15.4 mm. De samenstelling van de bonen-

opbrengst van pl. 239 beantwoordt voor de lengte en de breedte aan de form. $L_1 L_2 B_1 b_2$. De uitgangsboon 7 p i b van pl. 309, F_4-1936 voor pl. 239 heeft voor de lengte en de breedte de form. $L_1 L_2$ $B_1 b_2$ in homozygote of bijna homozygote vorm. De uitgangsbonen van pl. 309 voor de pl. 151—153 F_5-1937 zijn de 1ste, 3de en 5de (laatste) boon van dezelfde peul. De lengten van deze 3 bonen verschillen zeer (tab. 6).

Pl. 151. De 13 bonen van de kleine bonenopbrengst van pl. 151 bevat 9 bonen met de grote breedte 9.8—8.6 mm. Van deze 9 bonen hebben er 4 de zeer grote lengte 16.6—15.6 mm. De L B-index is, L B = 57—60. Van de 5 overige van deze 9 bonen is de lengte, l = 13.8—15.1 mm; tweemaal is de L B-index, L B = 59; van 3 bonen is zij 64—67. Een boon heeft dus een hoge L B-index, bovendien een grote breedte (b = 9.2 mm) en een niet zeer grote lengte (l = 13.8 mm). Ze beantwoordt aan de form. $L_1 l_2$ $B_1 b_2$. Er zijn twee grensgevallen. Vier bonen hebben de breedte 8.0 (dan 8.4)—8.5 mm en de lengten 13.6—15.6 mm. De L B-index is, L B = 54—62 (dan 58). De bonenopbrengst van pl. 151 bevat vooral bonen met de form. $L_1 L_2$ $B_1 b_2$ en enkele met de form. $L_1 l_2$ $B_1 b_2$. De uitgangsboon van pl. 309 voor pl. 151 is niet homozygoot voor de form. $L_1 L_2$ $B_1 b_2$.

Pl. 152. De uitgangsboon van pl. 309 voor pl. 152 is een zeer goed voorbeeld van een boon met de form. $L_1 l_2$ $B_1 b_2$ (tab. 6). Van de 21 bonen van de bonenopbrengst van pl. 152 hebben er 19 de grote breedte, b = 8.6—9.8 mm. Acht er van hebben de zeer grote lengte 15.6—17.2 (dan 16.2) mm. De index van deze 8 bonen is laag, L B = 57—59. Van 4 bonen is de lengte l = 15.2—15.4 mm; van deze bonen is L B = 56—64 (dan 63). De 7 bonen met de niet zeer grote lengte 12.9—14.9 (dan 14.4) mm, hebben alle een hoge index, L B = 63—69. De bonenopbrengst van pl. 152 heeft een gemengde samenstelling. Ze bestaat bijna uitsluitend uit bonen met een grote breedte (van één boon is b = 8.2 mm en er is een onvolgroeide boon). Daarvan zijn er met een zeer grote, doch ook met een niet zeer grote lengte. Er zijn veel bonen met een lage en met een hoge L B-index. Er zijn 10 bonen met de L B-index 55—60 (7 met L B = 55—57) en 9 met de L B-index 63—69. De uitgangsboon, ofschoon phaenotypisch duidelijk $L_1 l_2$ $B_1 b_2$ is genotypisch heterozygoot.

Pl. 153. De uitgangsboon van pl. 309 voor pl. 153 heeft een grotere lengte dan die voor pl. 152 en een kleinere lengte en breedte dan die voor pl. 151 (tab. 6). Van de bonenopbrengst van 29 bonen zijn er 12 met de grote breedte 8.7—9.4 mm. Er zijn er enige met een zeer grote lengte en vele met een niet zeer grote lengte. Er zijn 8 bonen met een hoge L B-index, L B = 63 (dan 65)—69. Er zijn zeer veel bonen met een kleine breedte, b = 7.5—8.5 mm. Daarbij zijn er 7 met een kleine lengte. Er zijn hoge en lage L B-indices. Van 7 bonen is L B = 63 (dan 65) —67, van 10 bonen is L B = 54—61. Ook de bonenopbrengst van pl. 153 is samengesteld. Naast bonen met de formules $L_1 L_2$ $L_1 l_2$ zijn er met de form. $L_1 l_2$ $B_1 b_2$. Er zijn ook veel bonen met de form. $L_1 l_2$ $b_1 b_2$ en $l_1 l_2$ $b_1 b_2$.

Uit de samenstelling van de bonenopbrengsten van de pl. 151—153 blijkt, dat de uitgangsbonen van pl. 309 voor deze planten de form. $L_1 L_2$ $B_1 b_2$ niet in de homozygote vorm hebben. Ze blijven hierin achter bij de uitgangsboon van pl. 309 voor pl. 239. Wel zijn de gemiddelde L B-indices van de pl. 151—153 laag. Deze bonenopbrengsten, besluiten we, steunen wel de opvatting, dat de uitgangsboon van pl. 73 voor pl. 309 in belangrijke mate homozygoot is voor de form. $L_1 L_2$ $B_1 b_2$.

De gegevens van de descendentie en de ascendentie van de bonenopbrengst van pl. 73, F_3-1935, die betrekking hebben op een onderzoek over 4 generaties, bevestigen, dat van deze bonenopbrengst de formule voor de lengte en de breedte $L_1 L_2$ $B_1 b_2$ is. Er blijkt de erfelijkheid uit van bonen met een grote breedte en een zeer grote lengte. Het gaat er steeds om, om de erfelijkheid te herkennen te midden van een grote niet-erfelijke variabiliteit.

Pl. 93. De bonenopbrengst van pl. 93 heeft de kleinste gemiddelde lengte van de bonenopbrengsten met een grote gemiddelde breedte van de F_3-generatie van 1935 (tab. 6). De bonenopbrengst van 56 bonen van pl. 93 (tab. 7) bevat slechts 2 bonen met de grote breedte, b = 10.2 mm. Deze bonen hebben niet een zeer grote lengte (l = 15.5 en = 15.2 mm). Er zijn 8 bonen met een breedte van b = 9.6—10.0 mm (de grootste breedte is b = 9.8 mm). De lengte van deze bonen, is l = 13.6—14.6 mm. Er zijn dus geen bonen met een grote breedte en een zeer grote lengte. Maar de grootste breedten treffen we ook niet aan in de bonenopbrengst van pl. 93. Er zijn 25 bonen met de breedte, b = 9.1—9.5 mm; de lengte is l = 12.8 (dan volgen l = 13.0 en 13.2)—14.8, (dan volgt l = 14.6) mm. Het is een zeer gelijkmatig samengestelde groep bonen met een grote breedte, waarbij er geen enkele is met een zeer grote lengte. De uitgangsboon voor pl. 93 is van pl. 82, F_2-1934. Deze boon heeft een matig grote breedte en een zeer grote lengte. De overige 5 bonen van de peul van de uitgangsboon hebben alle een kleinere lengte (l = 13.2—15.2 mm).

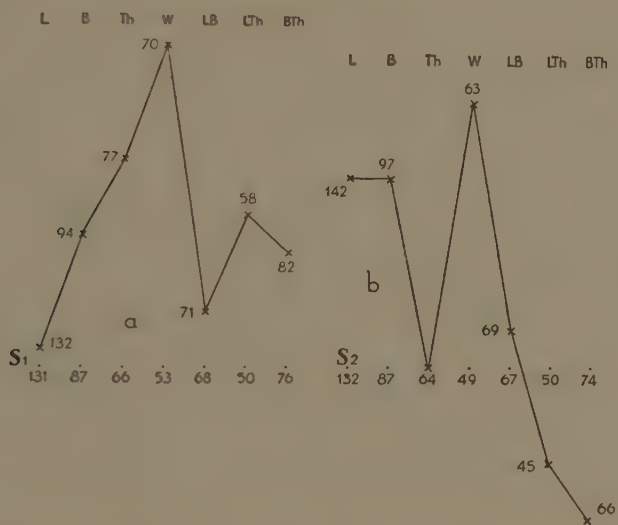

Fig. 4. *a*. Characterogram of 6 p 3 b, initial bean of plant 70, F_2-1934 for pl. 58, F_3-1935.
b. Idem of the averages of the beanyield of pl. 58, F_3-1935.

Van pl. 93 zijn in 1936 3 bonen voortgekweekt. Ze leverden in 1936 de pl. 352, 353 en 354, F_4-1936. Van de uitgangsboon van pl. 93 vcor pl. 352 (tab. 6) behcort de breedte tot de breedte-groep 9.1—9.6 mm, de lengte is niet zeer groot. Alle 6 bonen van de peul van de uitgangsboon hebben een overeenkomstige breedte, b = 9.3—9.4 mm, ook een overeenkomstige lengte, l = 13.0 (dan 13.4) —14.1 mm. De L B-index is hoog; L B = 66—72. Van de bonenopbrengst van pl. 352 van 23 bonen, is de grootste breedte, b = 10.7 mm. Van deze boon is de lengte l = 14.3 mm. Dan volgen 3 bonen met de breedten, b = 9.9 = 9.4 en = 9.3 mm en de lengten l = 14.6, = 14.3 en = 13.5 mm. Deze bonen hebben dus als phaenotype de form. $L_1 l_2 B_1 b_2$; ze zijn alle van eenzelfde peul. Van de overige bonen is de breedte 8.2—8.9 mm en de lengte 13.5—14.3 mm. Dit zijn geen kenmerkende bonen voor de form. $L_1 l_2 B_1 b_2$. De uitgangs-

boon van pl. 93 voor pl. 352 heeft de form. $L_1 l_2 B_1 b_2$ niet in de homozygote of bijna homozygote vorm.

Pl. 353. De uitgangsboon van pl. 93 heeft een grote breedte b = 10.2 mm, de lengte heeft de grenswaarde voor $L_1 L_2$ (l = 15.5 mm). Van de bonenopbrengst van 27 bonen van pl. 353 heeft één boon de grote breedte, b = 9.8 mm, de lengte is l = 15.0 mm, dit is dus geen kenmerkende boon voor de form. $L_1 l_2 B_1 b_2$. Van de overige bonen is de breedte, b = 9.3—7.5 mm en de lengte l = 11.5—13.7 mm. Deze afmetingen van de bonen van de bonenopbrengst van pl. 353 passen weinig bij die van de uitgangsboon van pl. 93, die zelf, vergeleken met de bonenopbrengst van pl. 93, een niet-erfelijke plus-variant is. Ook moeten we er mee rekening houden, dat bonenopbrengsten van op elkaar volgende jaren, slechts ten dele vergelijkbaar zijn. Bij de bonenopbrengst van pl. 353 staat aangetekend „matig, enkele peulen groen" (dus misschien onrijp). Dergelijke aantekeningen zijn er bij veel bonenopbrengsten. Het gewas van 1936 was waarschijnlijk iets minder goed dan dat van 1935. Tab. 2 geeft de gemiddelde lengte en het gemiddelde gewicht van het materiaal van de I- en de II-lijn van 1934, '35, '36 en '37 ter vergelijking. De L B-indices van pl. 353 (en van pl. 352) zijn nog al hoog, ook die van de uitgangsboon van pl. 93 is vrij hoog. Hier blijkt dus verwantschap met de form. $L_1 l_2 B_1 b_2$. Alles tezamen geeft de bonenopbrengst van pl. 353 geen duidelijke aanwijzingen voor de formule van de lengte en de breedte van de uitgangsboon.

Pl. 354. De uitgangsboon van pl. 93 is zeer klein (tab. 6). De 3 andere bonen van de peul komen onderling overeen en zijn veel groter. Er zijn 4 bonen met een grote breedte, b = 9.6—10.1 mm en de lengte 14.9—16.1 mm. De overige bonen hebben de breedte, b = 8.5—9.4 mm en de lengte 13.5—15.1 mm. Er zijn slechts 2 lage L B-indices (L B = 59 en = 60). Ook de bonenopbrengst van pl. 354 is niet kenmerkend voor bonenopbrengsten met de formule $L_1 L_2 B_1 b_2$ of $L_1 l_2 B_1 b_2$ van de uitgangsboon.

Pl. 58 is de 3de bonenopbrengst van F_3-1935, die we hier bespreken, de 2de met een niet zeer grote gemiddelde lengte. Ze heeft een grote gemiddelde breedte en een niet zeer grote gemiddelde lengte; de gemiddelde L B-index is hoog (tab. 5 en 6).

Pl. 58. De uitgangsboon is van pl. 70, F_2-1934 (tab. 6 en fig. 4) en heeft fraai de formule $L_1 l_2 B_1 b_2$ voor de lengte en de breedte. Ook de 2de en de 4de boon van de peul van de uitgangsboon hebben deze formule. In de bonenopbrengst van 51 bonen van pl. 70 zijn 11 bonen met een grote breedte en een niet zeer grote lengte (b = 9.6—10.0; l = 13.3 (dan 13.9)—15.2 mm; L B = 65—74). De bonenopbrengst van 46 bonen van pl. 58, F_3-1935 (tab. 7) heeft 5 bonen met de grote breedten, b = 10.7—11.3 mm. Van 3 van deze bonen is de lengte niet zeer groot, l = 15.1—15.5 mm, van 2 zeer groot, l = 16.0 en = 16.7 mm; L B = 66 en = 68). Van 9 bonen is de breedte, b = 10.1—10.4 mm en de lengte, l = 13.9—15.7 (dan volgt 15.2) mm. De L B-index van de boon met l = 15.7 mm, is L B = 66. Er zijn 12 bonen met de breedte, b = 9.6—10.0 mm; de lengte is l = 13.3 (dan 14.0) —15.2 mm. Al deze bonen hebben dus een niet zeer grote lengte. Er zijn ten slotte 11 bonen met de breedte, b = 9.1—9.6 mm en l = 11.7 (deze is van een boon, die de laatste is in de peul; dan volgt l = 12.8)—14.5 (dan volgt 14.0) mm. Er zijn in de bonenopbrengst van 47 bonen van pl. 58, dus 26 bonen met een grote breedte en deze hebben bijna alle een niet zeer grote lengte. Bij de bonenopbrengst van pl. 58 staat aangetekend: „Alle bizonder brede peulen". Deze bonenopbrengst voldoet zeer goed

aan de eisen van een bonenopbrengst, waarvan de formule van de lengte en de breedte van de uitgangsboon $L_1 l_2 B_1 b_2$ is. Wij zagen, dat ook het phaenotype van de uitgangsboon deze formule heeft.

Van pl. 58 zijn in 1936 2 bonen voortgekweekt. Ze leverden de pl. 259 en 260, F_4-1936 (tab. 6). De uitgangsboon voor pl. 259 heeft de grote breedte, b = 11.3 mm en de niet zeer grote lengte, l = 15.2 mm, L B = 74, (fig. 5). Nog 3 bonen van deze peul hebben eveneens een grote breedte (10.2—10.3 mm); de lengte van deze 3 bonen is l = 14.7, 15.2 en 15.7 mm. Bij de bonenopbrengst van pl. 259 van F_4-1936, staat aangetekend: „slecht, veel schimmel, bonen meest iets aan de rimpelige kant" (blz. 584 en tab. 3). De bonen zijn klein, hebben een klein gewicht; gew. = 30—50 cg (dan volgen 49 en 44 cg. Er zijn slechts 2 bonen met een breedte groter dan 9 mm, nl. b = 9.5 mm. Deze hebben een niet zeer grote en een kleine lengte, l = 13.5 en = 12.8 mm. De L B-index is L B = 70 en = 74. Er zijn slechts 3 bonen met de breedte 8.6—9.0 mm, nl. b = 9.0, 8.9 en 8.7 mm. De kleinste breedte is b = 7.7 mm (l = 11.4 mm). De L B-indices zijn *alle* hoog, (L B = 68—74). Het kan zijn, — het is waarschijnlijk —, dat we hier met kleine bonen als gevolg van slechte milieu-verhoudingen te doen hebben, dus met een achterblijven in de groei. De bonen zijn dan phaenotypisch klein. De hoge L B-indices wijzen daarbij op de mogelijkheid, dat de formule voor de lengte en de breedte genotypisch van deze bonen $L_1 l_2 B_1 b_2$ is.

De 2 bonen met de grootste breedten, beide van dezelfde peul (het is een peul met 2 bonen) zijn in 1937 voortgekweekt en leverden de pl. 206 en 207, F_5-1937 (tab. 6).

Pl. 206. F_5-1937. Er zijn in de bonenopbrengst van 29 bonen van pl. 206 8 bonen met de breedte, b = 9.1—9.5 mm; de lengte is l = 13.0—14.4 (dan nog eens 14.4, dan 13.9) mm. Van één boon is de L B-index = 65; van de overige bonen is L B = 66—71. Er zijn 10 bonen met de grote breedte, b = 8.6—9.0 mm; de lengte is l = 13.0—13.8 mm. De L B-index is 64—68. Van 11 bonen ten slotte is b = 7.5 (dan volgt 8.0) —8.5 mm; de lengte is 10.7 (dan volgt l = 11,2, dan 12.0) —13.6 (dan 13.2) mm. L B-index = 62—72. Ook van pl. 206 is het gewicht der meeste bonen niet groot; w = 29 (dan 38) —70 (dan 65) cg. De bonenopbrengst van pl. 206 voldoet goed aan het phaenotype $L_1 l_2 B_1 b_2$ en de uitgangsboon daarvan aan het genotype $L_1 l_2 B_1 b_2$.

Pl. 207. Het is van belang, om met pl. 206, pl. 207 te vergelijken, waarvan de uitgangsboon van dezelfde peul is. Deze uitgangsboon is de laatste boon van de peul met 2 bonen en is een goed voorbeeld van een boon met de form. $L_1 l_2 B_1 b_2$ (tab. 6 en in Proc. **52**, no. 6, fig. 6). In de bonenopbrengst van pl. 207 zijn 9 bonen met de grote breedte b = 9.2—9.8 mm; de lengte is l = 12.6—14.4 (dan volgen l = 14.2, dan l = 13.7) mm. De L B-index is L B = 68—76. Er zijn 12 bonen met de grote breedte, b = 8.6—8.9 mm; de lengte is l = 11.6—12.8 (dan 12.5) mm. De L B-index is L B = 68—74. Ten slotte zijn er 7 bonen met de breedte, b = 8.1—8.5 mm en de lengte l = 11.3 (dan 11.8)—13.2 (dan 12.7, dan 12.1) mm. De L B-index is L B = 64—72. De bonenopbrengst van pl. 207 heeft een zeer gelijkmatige samenstelling. Ze is een goed voorbeeld van het phaenotype $L_1 l_2 B_1 b_2$. Met het phaenotype van de bonenopbrengst van pl. 207 stemt het phaenotype $L_1 l_2 B_1 b_2$ van de uitgangsboon nog beter overeen, dan dit bij de bonenopbrengst van pl. 206 het geval is. We nemen aan, dat het genotype van de uitgangsboon van pl. 259, F_4-1936 voor pl. 207, F_5-1937, $L_1 l_2 B_1 b_2$ is.

Pl. 260. F_4-1936. De uitgangsboon van pl. 58, F_3-1935 voor pl. 260 heeft, evenals die voor pl. 259, een zeer grote breedte (b = 11.0 mm), doch een zeer grote lengte (l = 16.7 mm). De L B-index is L B = 66. De 2de en laatste boon van de peul met 2 bonen van de uitgangsboon heeft een grote breedte (b = 10.2 mm) en een niet zeer grote lengte (l = 14.7 mm). De L B-index is L B = 69. Van de 23 bonen van de bonenopbrengst van pl. 260 hebben 17 bonen de breedte b = 8.6—9.1 (dan volgt 8.9) mm en de lengte 12.3—13.9 (dan volgt 13.5) mm. Deze 17 bonen hebben een niet zeer grote lengte (L B = 64 (dan 66) —71). Alle bonen van de bonenopbrengst hebben een hoge L B-index.

Daaronder zijn er 6 met een niet grote breedte ($b = 7.7$—8.5 mm). De bonenopbrengst voldoet goed aan het phaenotype $L_1 l_2$ $B_1 b_2$ en de uitgangsboon kan het genotype $L_1 l_2$ $B_1 b_2$ hebben. We moeten daarbij aannemen, dat de zeer grote lengte van de uitgangsboon ($l = 16.7$ mm) een niet-erfelijke variant is van de formule $L_1 l_2$.

Pl. 208. F_5-1937. Van pl. 260, F_4-1936 is in 1937 één boon voortgekweekt; ze leverde pl. 208 (tab. 6). De uitgangsboon van pl. 260 voor pl. 208 is de boon met de grootste lengte ($l = 13.0$ mm, tab. 6 en Proc. **52**, no. 6). Van de overige 4 bonen van de peul met 5 bonen is de lengte $l = 12.9$—13.5 (dan 13.2) mm. De L B-indices zijn L B = 66—67. Er zijn in de bonenopbrengst van 30 bonen van pl. 208, F_5-1937 18 bonen met de grote breedte 8.6—9.2 mm; de lengte is 12.7—14.0 (dan 13.7) mm. De L B-index is 64—69. Van de overige 12 bonen is $b = 8.0$—8.5 mm, $l = 12.0$—13.4 (dan 13.0) mm; L B = 62—69. Er zijn dus 11 bonen met een kleine lengte (d.w.z. $l = 13.0$ mm en kleiner). Het phaenotype van de bonenopbrengst, voor de lengte en de breedte, is $L_1 l_2$ $B_1 b_2$.

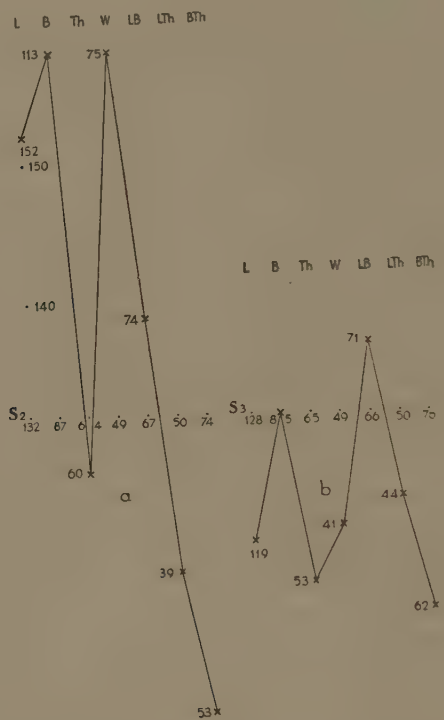

Fig. 5. *a.* Characterogram of 1 p 2 b, initial bean of pl. 58, F_3-1935 for pl. 259, F_4-1936.
b. Idem of the averages of the beanyield of pl. 259, F_4-1936.

De uitgangsbonen voor de pl. 208 en 207, van pl. 260 en 259 verschillen voor de lengte en de breedte beide zeer, daardoor ook de L B-indices. De bonenopbrengsten van de pl. 260 en 259 verschillen in mindere mate (tab. 6). De bonenopbrengst van pl. 260 en haar uitgangsboon beantwoorden in minder raszuivere vorm aan de formule $L_1 l_2$ $B_1 b_2$ van de lengte en de breedte dan de bonenopbrengst van pl. 259 en haar uitgangsboon. Hiermee is in overeenstemming, dat ook de uitgangsboon van pl. 58 voor pl. 260 in dezelfde richting verschilt van de uitgangsboon van pl. 58 voor pl. 259 (tab. 6 en Proc. **52**, no. 6).

Anatomy. — *The digital formula in relation to age, sex and constitutional type.* II. By J. HUIZINGA. (Communicated by Prof. M. W. WOERDEMAN.)

(Communicated at the meeting of March 26, 1949.)

7. *Considerations on the causation of differences in prominence.*

ECKER (1875) believed the problem of prominence differences to be connected with the mobility of the metacarpals. As a measure of this mobility he uses the extent to which the capituli cann be passively displaced in a volo-dorsal direction. The most laterally situated metacarpals (I and V) are movable to the greatest extent and correspond to the least prominent fingers. Metacarpal III is almost immovable and corresponds to the most prominent finger. In the human hand metacarpal IV is movable to a greater extent than II and should, therefore, correspond to a finger shorter than that belonging to II. If mobility and relative length are really correlated in this way, this suggests that Rd. prominence is typical of man, a conclusion which — as we have already pointed out — WOOD JONES (1944) reached by another route. In the Uln. type of the anthropoids, metacarpal II should, according to this reasoning, be more mobile than metacarpal IV, although ECKER admits 'I do not know whether the index finger in apes is more mobile than the ring finger'.

WEISSENBERG (1895) states that BRAUNE was of the opinion that the Uln. type develops as a result of the action of the considerably stronger flexors, whereby the hand undergoes ulnar reflexion so that the apparent length of the ring finger is increased. WEISSENBERG criticises this view remarking, that Rd. types would then be expected to be the rule in cases where 'the hand position in question has not yet had the opportunity of reaching its full development', e.g. in children 'which is, however, not the case'.

But we have already seen that WOLOTZKOI (1924) states that the Rd. type does actually occur with greater frequency in children, a finding that is confirmed by our own investigations (see below).

WECHSLER (1939) also attempted a functional explanation: as a result of the relatively greater use of the radially-situated fingers, a corresponding growth in breadth of the muscles in this region is to be expected. The stronger are these muscles the more the second metacarpo-phalangeal joint will be pushed thumb-wards, producing a bend in the course of II. Through this bending II becomes shortened as regards prominence and the Uln. type develops. 'It would be of interest in this connection to study the degree of correlation between the L/Br index of the hand with the force of pressure.' WOOD JONES (1944) remarks casually, in connection with the development of the elongated index finger:

'Many have dwelt upon some of the separate outcomes of the human dominance of the index finger, and in a rather topsyturvey way the human ability to point out objects has received certain attention, but there is a grave danger of mixing up physical and psychical specialisations, if the act of pointing is made the mainspring of the development'.

III. *Investigation.*

We had the opportunity of studying sexual dimorphism, the variation with age and the connection with constitutional type.

A. *Subjects.*

In 1454 male and 858 female individuals from the age of four years upwards we recorded the age and the mode of prominence of the fingers; in 121 boys and 74 girls aged 7 to 11 years we also determined the constitutional type. (By a child aged 10 years, for instance, we understand one older than 9.6 years and younger than 10.6 etc.).

The groups are shown, together with other data in a table which will be discussed.

In 56 male and 44 females foetuses we made an estimate of the age and determined the prominence type of the right hand.

B. *Method.*

As stated above (see under 6) we used the method described by Wolotzkoi (1924) for determination of the prominence type.

The observations on foetuses were all checked independently by a medical colleague.

C. *Results.*

Arranged according to age (in months) and prominence types, the (right) hands *before birth* show the following picture:

Mnths.	♂♂			♀♀		
	Rd.	Uln.	T.	Rd.	Uln.	T.
3	1	—	—	2	—	—
4	9	—	1	6	—	3
5	6	2	2	6	—	2
6	5	—	1	4	1	—
7	5	3	2	2	1	—
8	6	3	4	5	5	1
9	4	1	1	4	2	—
Total	36	9	11	29	9	6

Although the *ulnar* prominence type occurs in the first six months of gestation, it does not appear in any considerable proportion until the *last three months. Increasing age* is accompanied — at any rate during intrauterine life — by *loss of the radial prominence type* in favour of the

ulnar type. The *mean* frequency of the Rd. type before birth for the two sexes is 65 %.

Our results, thus, differ appreciably from those of MIERZECKI (see remarks above); no other data were available for purposes of comparison. Like WOLOTZKOI, we arranged our (post-natal) data in the age-groups proposed by STRATZ.

Our group aged 1—4 years was too small to be of much significance in itself. The percentages calculated for these children (in brackets) fit reasonably well into the general picture when taken in connection with the other age groups (including the foetal group).

Males.

Age (yrs)	*n*	Rd	Uln.	T.	%% Rd.	%% Uln.	%% T.
1 to 4 incl.	13	9	4	—	(69)	(31)	—
5 „ 7 „	218	111	90	17	51	41	8
8 „ 10 „	405	191	186	28	47	46	7
11 „ 14 „	362	148	192	22	41	53	6
15 „ 20 „	284	108	164	12	38	58	4
21 etc.	172	60	97	15	35	56	9
Total	1454	627	733	94			

Females.

Age (yrs)	*n*	Rd.	Uln.	T.	%% Rd.	%% Uln.	%% T.
1 to 4 incl.	7	6	1	—	(86)	(14)	—
5 „ 7 „	178	102	59	17	57	33	10
8 „ 10 „	331	206	98	27	62	30	8
11 „ 14 „	236	139	78	19	59	33	8
15 „ 20 „	56	23	26	7	41	46	13
21 etc.	50	24	20	6	48	40	12
Total	858	500	281	76			

The frequency of occurrence of the prominence types in the different extrauterine age-groups shows (see also figs. 1 and 2) that our observation on foetuses is not specific for this group. After birth also it appears that increasing age is accompanied by a loss of the Rd. type, but without this type disappearing altogether.

The figures and tables enable us to draw certain conclusions as to sexual dimorphism.

a. Males. In the majority of males the Rd. prominence type is present at birth. The number of such types undergoes a (probably gradual) decrease and corresponds to about 50 % in the first extension period (5—7 years).

The radial types, and probably also the T. types, change into ulnar types.

About the 21st. year the phenomenon referred to WOLOTZKOI is found: The number of ulnar forms shows a slight decrease although not, as stated

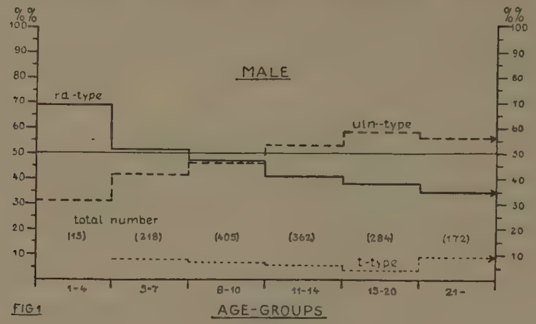

Fig. 1.

by this investigator, in favour of radial types but in favour of the T. types.

If we estimate roughly the percentage of radial forms at birth to be almost 70 %, we see that this falls to 35 % for men over 21 years of age.

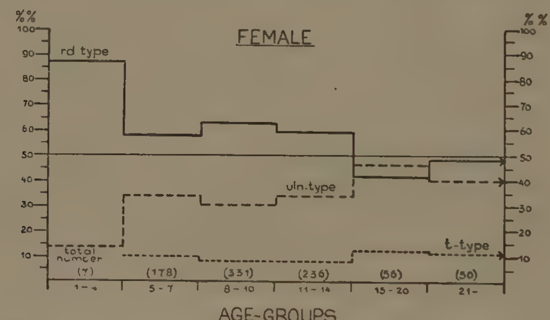

Fig. 2.

b. Females.

In the majority of females also, the radial prominence type is present at birth (probably rather more than 70 %).

This proportion remains high for much longer than is found to be the case in boys, passing the 50 % about the middle of the period of puberty.

This longer stay at the level corresponding to childhood in females than in males has also been repeatedly found — at least for physical characters — in our other investigations (1947, 1948).

We have, of course, no intention of asserting that this is necessarily true of all characters (exceptions are known to exist), nor do we wish at this stage to make any statement other than that given above.

The decrease in the number of radial types is less gradual in females.

In the period of maturation (15 to 20) years, we found in our subjects a large difference in frequency of the radial type between males and females (see also fig. 3), after this period the radial type appears to be more frequent in women than in men.

In women too, we see the phenomenon already described in men to appear about the 21st. year: a decrease in the number of ulnar types which, however, in this case does proceed in favour of the radial type.

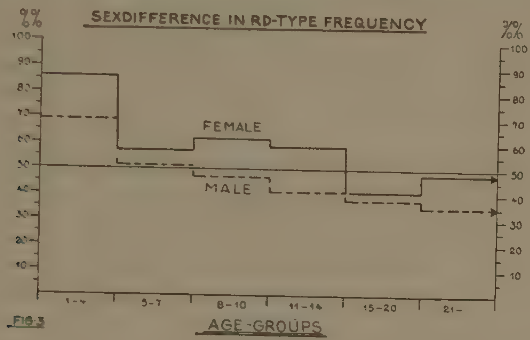

Fig. 3.

If the figures analysed provide us with reliable data, it is presumably the case that the falling-off in the number of radial forms in girls during puberty constitutes a minimum, which is then followed by a rise. In males we have seen that this decrease continues.

Some of the contradictions we have encountered in the literature are undoubtedly to be attributed to age differences in the groups compared.

The possible connection between prominence type and type of physical build has not been sufficiently investigated. Apart from the rather peculiar typology of ROMICH already discussed, we have seen than ECKER was under the impression that he had seen rather more radial types in leptosome individuals.

Using KRETSCHMER's typology with the modern terminology: eurysome (pynic), leptosome and (the intermediate) mesosome, we determined both prominence and physical type in a number of *children*. The results are shown in the following tables.

Boys.

Type	Rd.	Uln.	T.	
Leptos.	31	21	4	56
Mesos.	28	21	—	49
Eurys.	10	5	1	16
Total	69	47	5	121

Girls.

Type	Rd.	Uln.	T.	
Leptos.	15	5	—	20
Mesos.	29	16	1	46
Eurys.	7	1	—	8
Total	51	22	1	74

We find, thus, that in the whole group of *boys* ($n = 121$) the Rd. type appears in **57**% ($n = 69$). In the *leptosome* types among these boys ($n = 56$) the Rd. type is present in **55** % ($n = 31$), in the *mesosome* types ($n = 49$) in **57** % ($n = 28$) and in the *eurysome* types ($n = 16$) in **62** % ($n = 10$).

The Uln. type showed an equal absence of preference for a given bodily build.

For the Rd. type in *girls* the percentages are: all girls, 69 %; leptosome, mesosome and eurysome types, 75 %, 63 % and 7 of 8 respectively.

Our study of children, thus, gives *no* indications of any linking of a given type of physical build to a given type of prominence. We believe, however, that this by no means excludes the possibility that an affinity of this kind may be found to exist when larger groups and older persons with fixed physical type are studied (see below).

We have little to add to our remarks on the causation of prominence differences (II, 7). We should, however, like to draw attention to the possibility that a chronological difference in the formation of the bone centres in the carpus may be *partly* responsible for difference in prominence type in men and women. The available data, however, point only vaguely in this direction.

Another problem is that of prominence type in the light of evolution. We have already seen that the literature does not permit any conclusions as to the occurrence or non-occurrence of Rd. forms in the anthropoids. We ourselves were unable to obtain any suitable anthropoid specimens, still less anthropoid foetuses.

A study of the latter would offer possibilities of examining the problem of prominence from the point of view of L. BOLK's retardation and foetalization theory.

This assumes that the rate of development is retarded in man. This retarded development is believed to have the result that the foetal character of man remains more clearly preserved than that of the other primates. BOLK enumerated a number of characters in which this foetal character is indeed shown (see DE FROE, 1948, p. 306).

It is possible that other workers are in possession of sufficient pre- and postnatal data on anthropoids to (1) establish the occurrence or non-occurrence of Rd. forms and, if these forms are found (2) to ascertain to what extent their occurrence is connected with age.

It would, in our opinion, be well worth while to be able to add further characters to the list given by BOLK or — in the case of a 'negative' result — to study the problem of prominence from different points of view.

We should not omit to remark here that PORTMANN (1944) draws attention to the increasing frequency of leptosomia as a progressive type. In the foregoing we left open the possibility that a connection might exist between, e.g., leptosomia and prominence type. In view of BOLK's theory we might perhaps expect to find a low frequency of the Rd. type among leptosome individuals. It is our opinion that considerations of this kind are sufficient reason for including prominence in the morphological part of the anthropological investigation programme.

REFERENCES.

1. BAKER, F., Anthropological notes on the human hand. American Anthropologist, vol. I, 70 (1888).

2. CASANOVA, Mémoires. T. 6, p. 252, Bruxelles, 1871.
3. ECKER, A., Einige Bemerkungen über einen schwankenden Charakter in der Hand des Menschen. Archiv f. Anthrop., Bnd. 8, 67—75 (1875).
4. FROE, A. DE, Inleiding tot de studie en de beoefening der anthropologie. Amsterdam, 1948.
5. HUIZINGA, J., Structural alterations indicated in the development of the human cranium. Proc. Kon. Ned. Akad. v. Wetensch., Amsterdam, **51**, 76—87 (1948).
6. ————, Cephalometrische verwantschap tusschen verwanten van den eersten graad. Amsterdam (1947).
7. JONES, F. WOOD, Principles of anatomy as seen in the hand, London (1944).
8. MANTEGAZZA, P., Della lunghezza relativa dell'indice e dell'anulare nella mano umana. Arch. per l'Anthrop., p. 22 (1877).
9. MIERZECKI, H., Over de morphologie der hand. Ciba-Tijdschrift, **18**, 573—574 (1946).
10. PFITZNER, W., Anthropologische Beziehungen der Hand- und Fuszmaasse. Morphologische Arbeiten (Schwalbe), Bnd. II, 93—206 (1893).
11. PORTMANN, A., Biologische Fragmente zu einer Lehre vom Menschen. Basel (1944).
12. ROMICH, S., Fingerlängen bei verschiedenen Konstitutionstypen. Anthrop. Anzeiger., IX, 264—267 (1932).
13. RUGGLES, G., Human Finger Types. The Anat. Record. Vol. 46, 199—204 (1930).
14. SCHAAFFHAUSEN, Einige Eigentümlichkeiten der Hand. Corr. Blatt d. dtsch. Gesellsch. f. Anthrop., Ethnol., u. Urgesch. XV Jhrg., p. 94 (1884).
15. SCHULTZ, A. H., Growthstudies on primates bearing upon man's evolution. Am. J. of phys. Anthrop., vol. VII, 149—165 (1924).
16. STRATZ, C. H., Der Körper des Kindes, 1903.
17. WECHSLER, W., Anthropologische Untersuchung der Handform mit einem familienkundlichen Beitrag. Zürich, 1939.
18. WEISSENBERG, S., Ueber die Form der Hand und des Fuszes. Zschr. f. Ethnol., 82—111 (1895).
19. WOLOTZKOI, M., Ueber die zwei Formen der menschlichen Hand, J. Russe d'Anthrop., XIII, 3/4, p. 70—81, (German summary), 1924.

DATE DUE

GAYLORD			PRINTED IN U.S.A.